Molecular and Biological Studies of Novel Treatment for Acute Myeloid Leukemia

Zhou Jianbiao

National University of Singapore

2009

In vitro and *In vivo* study of ABT-869 in treatment acute myeloid leukemia (AML) alone or in combination with chemotherapy or HDAC inhibitors: insight into molecular mechanism and biologic characterization

Zhou Jianbiao
(M.D. Nanjing, M.sc. National University of Singapore)

A THESIS SUBMITTED

FOR THE DEGREE OF DORCTOR OF PHILOSOPHY

DEPARTMENT OF MEDICINE
YONG LOO LIN SCHOOL OF MEDICINE
NATIONAL UNIVERSITY OF SINGAPORE

Singapore 2009

ACKNOWLEDGEMENTS

I would like to express my thanks from my bottom of heart to the following for their support, encouragement, contribution, and help to my study and thesis:

First of all to my supervisor, Dr. Chen Chien-Shing, whom I first worked with when I came back from Boston, USA and for giving your support. I am grateful to the flexible and stimulating work environment you created.

Dr. Hanry Yu, my co-supervisor for your gracious commitments, for supporting my works, especially in the period of transition time in the lab.

Dr. Chng Wee-Joo with your striking passion in cancer research. Thank you for providing me the advice and the opportunity to work with you.

My Ph.D. qualified examination committee-Drs Fred Wong, Goh Boon-Cher, Shazib Pervaiz for the excellent suggestions.

Bi Chonglei for giving me great helps in the works on this thesis.

All present and former colleagues in Drs Chen's and Dr Chng's labs, especially Janaka V. Jasinghe, Pan Mengfei, Liu Shaw-Cheng, Tay Kian Ghee Xie Zhigang, Poon Lai-Fong, Alexis Khng for their helps.

Lim Bee-Choo and Evelyn Neo for their excellent administrative support.

Keith B. Glaser, Daniel H. Albert, Steven K. Davidsen in Abbott Labtoratories for providing ABT-869.

My daughter Nina who is always at the center of my heart and my wife and soul mate Liqin for encouraging me and doing most of housework.

These studies were made possible by Singapore Cancer Syndicate, A*Star, Singapore as well as, Singapore Cancer Society through the Terry Fox Run Fund.

TABLE OF CONTENTS

PUBLICATIONS DERIVED FROM THIS THESIS

1. **Zhou J**, Pan M, Xie Z, Loh SL, Bi C, Tai YC, Lilly M, Lim YP, Han JH, Glaser KB, Albert DH, Davidsen SK, Chen CS. *Synergistic antileukemic effects between ABT-869 and chemotherapy involve downregulation of cell cycle regulated genes and c-Mos-mediated MAPK pathway.* **Leukemia.** 2008; 22(1): 138-146.

2. **Zhou J**, Khng J, Jasinghe VJ, Bi C, Neo CH, Pan M, Poon LF, Xie Z, Yu H, Yeoh AE, Lu Y, Glaser KB, Albert DH, Davidsen SK, Chen CS. *In vivo activity of ABT-869, a multi-target kinase inhibitor, against acute myeloid leukemia with wild-type FLT3 receptor.* **Leukemia Research**. 2008; 32(7): 1091-100.

3. **Zhou J**, Bi C, Jasinghe VJ, Liu SC, Tan KG, Poon LF, Xie Z, Palaniyandi S, Chng WJ, Yu H, Glaser KB, Albert DH, Davidsen SK, Chen CS. *Enhanced activation of STAT pathways and overexpression of survivin confer resistance to FLT3 inhibitors and could be therapeutic targets in AML.* **Blood.** 2009;113(17):4052-62.

4. **Zhou J**, Bi C, Chng WJ, Liu SC, Tan KG, Xie Z, Yu H, Glaser KB, Albert DH, Davidsen SK, Chen CS. *SAHA, a HDAC inhibitor, synergistically potentiates ABT-869 lethality in acute myeloid leukemia cells with FLT3-ITD mutation in association with PRL-3 downregulation*. **Under Review.**

5. **Zhou J**, Goh BC, Albert DH, Chen CS. *ABT-869, a promising multi-targeted tyrosine kinase inhibitor: from bench to bedside.* **J Hematol Oncol.** 2009 Jul 30;2:33.
.

OTHER PUBLICATIONS DURING STUDY PERIOD

1. **Zhou J**, Goldwasser MA, Li A, Dahlberg SE, Neuberg D, Wang H, Dalton V, McBride KD, Sallan SE, Silverman LB, Gribben JG. *Quantitative analysis of minimal residual disease predicts relapse in children with B-lineage acute lymphoblastic leukemia in DFCI ALL consortium protocol 95-01.* **Blood.** 2007;110(5):1607-11.

2. Shen J, Tai YC, **Zhou J**, Stephen Wong CH, Cheang PT, Fred Wong WS, Xie Z, Khan M, Han JH, Chen CS. *Synergistic antileukemia effect of genistein and chemotherapy in mouse xenograft model and potential mechanism through MAPK signaling.* **Experimental Hematology.** 2007;35(1):75-83.

3. Xie Z, Choong PF, Poon LF, **Zhou J**, Khng J, Jasinghe VJ, Palaniyandi S, Chen CS. *Inhibition of CD44 expression in hepatocellular carcinoma cells enhances apoptosis, chemosensitivity, and reduces tumorigenesis and invasion.* **Cancer Chemotherapy Pharmacology.** 2008;62(6):949-57.

4. Jasinghe VJ, Xie Z, **Zhou J**, Khng J, Poon LF , Senthilnathana P, Glaser KB, Albert DH, Davidsen SK, Chen CS. *ABT-869, a multi-targeted tyrosine kinase inhibitor, in combination with rapamycin is effective for hepatocellular carcinoma (HCC) in vivo.* **Journal of Hepatology.** 2008;49(6):985-97.

5. Xie Z, Chng WJ, Tay KG, Liu SC, **Zhou J**, Chen CS. *Therapeutic potential of antisense oligodeoxynucleotides to down-regulate p53 oncogenic mutations in cancers.* **Under review**

SUMMARY

The fate of adult leukemia still remains dismal with 5-year disease free survival (DFS) 2-37% for acute myeloid leukemia (AML). The current treatment approach for AML is chemotherapy, which damages normal cells too and cause severe side effect. The focus of this thesis has been to develop novel therapeutic strategies targeting genetic and epigenetic abnormalities of AML or combination synergies by dissecting the molecular pathways, thus improving clinical outcome of patients with AML.

Internal tandem duplications (ITDs) of fms-like tyrosine kinase 3 (FLT3) receptor play an important role in the pathogenesis of AML and represent an attractive therapeutic target. We first demonstrate ABT-869, a multi-targeted receptor tyrosine kinase inhibitor (TKI) as a potent FLT3 inhibitor. ABT-869 demonstrates significant sequence dependent synergism with cytarabine and doxorubicin. Low density array (LDA) analysis revealed the synergistic interaction involved in down-regulation of cell cycle and MAPK pathway genes. These findings suggest specific pathway genes were further targeted by adding chemotherapy and support the rationale of combination therapy. Thus a clinical trial using sequence-dependent combination therapy with ABT-869 in AML is initiated.

Neoangiogenesis plays an important role in leukemogenesis. We investigated the *in vivo* anti-leukemic effect of ABT-869 against AML with wild-type FLT3 using red fluorescence protein (RFP) transfected HL60 cells with *in vivo* imaging technology in mouse xenograft models. ABT-869 showed a five fold inhibition of tumor growth and decreased p-VEGFR1, Ki-67 labeling index, VEGF and remarkably increased

apoptotic cells in the xenograft models compared to vehicle controls. ABT-869 also reduced the leukemia burden and prolonged survival. Our study supports the rationale for clinically testing an anti-angiogenesis agent in AML with wild type FLT3.

we developed three isogenic resistant cell lines to FLT3 inhibitors. Gene profiling reveals up-regulation of FLT3LG and Survivin, but down-regulation of SOCS genes in MV4-11-R cells. Targeting survivin by shRNA induce apoptosis and augments ABT-869-mediated cytotoxicity. Sub-toxic dose of indirubin derivative (IDR) E804 resensitize MV4-11-R to ABT-869 treatment *in vitro* and *in vivo*. Taken together, these results demonstrate that enhanced activation of STAT pathways and overexpression of survivin are the main mechanism of resistance to ABT-869, suggesting potential targets for reducing resistance developed in patients receiving FLT3 inhibitors. Our findings may indicate a common resistant mechanism in novel therapeutic era.

So far, the FLT3 inhibitors as single agent in clinical trials only induce transient and mild response. Small molecule HDAC inhibitors (HDACi) have proven to be a promising new class of anticancer drugs. We demonstrated that combining ABT-869 with SAHA leaded to synergistic killing of AML cells with FLT3 mutations. To study the molecular mechanism of their interaction, we identified a core gene signature differentially induced more than two-fold by combination therapy in both cell lines. Modulation of PRL-3 expression level using genetic approaches or PRL-3 inhibitor, Pentamidine, demonstrated that PRL-3 played an essential role in the synergism ascribing from the combination with ABT-869 and SAHA. Our results suggest such combination therapies may significantly improve the therapeutic efficacy of FLT3 inhibitors in clinic.

LIST OF TABLES

LIST OF FIGURES

LIST OF ABBREVIATIONS

17-AAG	17-allylamino- 17-demethoxygeldanamycin
acetyl-CoA	acetyl-coenzyme A
ACAT2	Acetyl-CoA Acetyltransferase 2
AML	Acute Myeloid Leukemia
Ara-C	Cytosine Arabinoside
BM	Bone Marrow
BSA	Bovine Serum Albumin
CDK	Cyclin-Dependent Kinase
C/EBPα	CCAAT/enhancer-binding protein α
ChIP	Chromatin Immunoprecipitation
CI	Combination Index
CML	Chronic Myelogenous Leukemia
CRC	Colorectal Carcinomas
Csk	C-terminal Src Kinase
DAPI	4'-6-Diamidino-2-phenylindole
DFS	Disease Free Survival
DMSO	Dimethyl Sulfoxide
Dox	Doxorubicin
E2F1	E2F Transcription Factor 1
FBS	Fetal Bovine Serum
FLT3	FMS-Like Tyrosine Kinase 3
FLT3LG	FLT3 Ligand
G-CSF	Granulocyte Colony-Stimulating Factor
GM-CSF	Granulocyte Macrophage-CSF
HAT	Histone Acetyltransferase
HDAC	Histone Deacetylases
HPF	High Power Field
HSC	Hematopoietic Stem Cell
HSP90	Heat Shock Protein 90
IDR	Indirubin Derivative
IFI16	Interferon gamma-inducible gene 16
IHC	Immunohistochemistry
IP	Intraperitoneally
ITD	Internal Tandem Duplication
JNK	c-Jun N-terminal Kinase
KDR	Kinase Insert Domain Receptor
LDA	Low density Array
LRP	Lung-Resistance Protein
MAPK	Aitogen-Activated Protein Kinase
MDS	Myelodysplastic Syndromes
MDR	Multi-Drug Resistance Protein
MM	Multiple Myeloma
MVD	Microvessel Density
NOD/SCID	Non-diabetics/Severe Combined Immunodeficiency
OD	Optical Density
ORC	Origin Recognition Complex
ORC1L	ORC, subunit 1-like (yeast)
PBS	Phosphate Buffered Saline

PCR	Polymerase Chain Reaction
PDGFR	Platelet-Derived Growth Factor Receptor
PFA	Paraformaldehyde
PI	Propidium Iodide
PI3K	Phosphoinositide 3-kinase
PLZF	Promyelocytic Leukemia Zinc Finger protein
PRL-3	Phosphatase of Regenerating Liver 3
Rb	Retinoblastoma Protein
RFP	Red Fluorescence Protein
RNAi	RNA interference
RTK	Receptor Tyrosine Kinase
SD	Standard Deviation
SAHA	Suberoylanilide Hydroxamic Acid
SOCS	Suppressor Of Cytokine Signaling
STAT	Signal Transducers and Activators of Transcription
TKI	Tyrosine Kinase Inhibitor
TPO	Thrombopoietin
TUNEL	TdT-mediated dUTP Nick-End Labeling
VEGF	Vascular Endothelial Growth Factor
VPA	Valproic Acid
vWF	von Willibrand Factor

Chapter 1. Synergistic antileukemic effects between ABT-869 and chemotherapy involve downregulation of cell cycle regulated genes and c-Mos-mediated MAPK pathway

1.1. Introduction

Internal tandem duplications (ITDs) of the fms-like tyrosine kinase 3 (FLT3), varying from 3 to≥400 base pairs in the juxtamembrane d omain, are found in 20-25% of adult AML cases.[1-3] In addition, activating point mutations in the second kinase domain occur in about 7% of adult AML patients.[4] FLT3 mutations therefore are the most common genetic alteration in AML. Clinically, FLT3-ITD is associated with poor outcome, but the prognosis of FLT3 activating point mutation remains inconclusive.[5-7]

FLT3-ITD mutations trigger strong autophosphorylation of the FLT3 kinase domain, and constitutively activate several downstream effectors such as the PI3K-AKT pathway, RAS-MEK-MAPK pathway, and the STAT5 pathway.[8,9] FLT3-ITD mutations also suppress transcription factors associated with myeloid differentiation and apoptosis, including PU.1, CCAAT/enhancer-binding protein α (C/EBPα),[10] promyelocytic leukemia zinc finger (PLZF) protein,[11] RUNX1/AML1,[12] RSG2[13] and Foxo3a.[14-16] On the other hand, FLT3-ITDs up-regulate proliferation associated genes like PIM1.[17] Taken together, FLT3-ITDs simultaneously bring on several hallmarks of leukemogenesis[18] by blocking myeloid differentiation, inducing signaling for uncontrolled proliferation, and producing resistance to apoptosis.

The mainstream chemotherapy regime for AML is a combination of cytosine arabinoside (Ara-C) and anthracyclines such as doxorubicin (Dox). Despite initial responses to chemotherapy, most adult AML eventually relapse. Long-term disease

free survival is only 20-30%. Thus, the development of novel therapeutic agents that target critical genetic aberrations holds promise for improving outcomes in patients with AML.

ABT-869, a novel ATP-competitive tyrosine kinase inhibitor (TKI), is active against FLT3 kinase (IC_{50} = 4 nM) and other platelet-derived growth factor receptor (PDGFR) family members, as well as vascular endothelial growth factor (VEGF) receptors (IC_{50} = 4, 66 and 4 nM for KDR, PDGFRβ and CSF-1R respectively), but less active against unrelated RTKs.[19,20] Cellular assays and tumor xenograft models demonstrated that ABT-869 was effective in a broad range of cancers including small cell lung carcinoma, colon carcinoma, breast carcinoma, and MV4-11 tumors *in vitro* and *in vivo.*[19,21] However, considering the complexity of the disease, monotherapy with ABT-869 is unlikely to deliver complete or lasting responses in AML. Furthermore, resistance to TKIs has been well described in patients treated with imatinib mesylate monotherapy for chronic myelogenous leukemia (CML).[22] Combination regimens including ABT-869 and conventional chemotherapy may potentially reduce resistance and achieve better outcomes for AML patients.

A combination approach has also been pursued with other TKIs. It has been reported that combination of SU11248 with Ara-C or Dox exerted synergistic effects[23] and CEP-701 showed *in vitro* sequence-dependent synergistic cytotoxic effects on FLT3-ITD leukemia cells when combined with chemotherapy.[24] In this study, the sequence-dependent synergism was attributed to CEP-701 induced cell cycle arrest and it was speculated that the sequential treatment first induced pro-apoptotic signals, then withdrew pro-survival signals.[25] Studies of the molecular mechanisms on synergistic interactions are needed for better understanding the full potential of

combination therapy. The chemical structure of ABT-869 (*N*-[4-(3-amino-1*H*-indazol-4-yl)phenyl]-*N*1-(2-fluoro-5-methylphenyl) urea) is different from SU11248 (3-Substituted indolinoneindolinone) and CEP-701 (Indolocarbazole)[19] suggesting that the therapeutic efficacy of ABT-869 can not be extrapolated from the experience of related compounds. Hence, the clinical applications of ABT-869 will greatly benefit from better understanding of the molecular mechanism of the compound in sole or combination therapies both *in vitro* and *in vivo*.

We here, for the first time, present further characterization of molecular mechanism of G_1-phase cell cycle arrest and apoptosis caused by ABT-869 as a single agent and the potential mechanism of synergism with the cytotoxic agents Ara-C and Dox *in vitro* and *in vivo*.

1. 2. Materials and methods

1.2.1. Cell lines and primary patient samples

MV4-11 and MOLM-14 cells were cultured with RPMI1640 (Invitrogen, Carlsbad, CA) supplemented with the addition of 10% of fetal bovine serum (FBS, JRH Bioscience Inc, Lenexa, KS) at density of 2 to 10 x 10^5 cells/ml in a humid incubator with 5% CO_2 at 37ºC.

Bone marrow (BM) blast cells (>90%) from newly diagnosed AML patients were obtained at National University Hospital (NUH) in Singapore with informed consent. Three samples were confirmed to harbor a 36, 60/78 (two duplicated fragments detected), 62 bp ITDs of FLT3 gene respectively and one had D835Y (GAT -> TAT at codon 835) point mutation. Thawed cells were cultured in EGM™-2 medium (Cambrex, Walkersville, MD) supplemented with SingleQuots® (Cambrex) growth

factors, cytokines (hFGF, hEGF, Hydrocortisone, GA-1000 , VEGF, R^3-IGF-1) with or in absence of drug incubation.

1.2.2. ABT-869 and chemotherapy reagents

ABT-869 was kindly provided by Abbott Laboratories (Chicago, IL). For *in vitro* and *in vivo* experiments, ABT-869 was prepared as published before.[21] Clinical grade Ara-C (100 mg/mL, Pharmacia, WA, Australia) and Dox (2 mg/mL, Pharmacia) were diluted just before use. The MEK inhibitor U0126 was purchased from Promega and dissolved in DMSO at concentration of 10 mM as stock. It was further diluted before use.

1.2.3. Cell viability assays

Leukemic cells were seeded in 96-well culture plates at a density of 2×10^4 viable cells/100 µl/well in triplicates, and were treated with ABT-869, chemotherapeutic agents or combination therapy. Colorimetric CellTiter 96 AQ_{ueous} One Solution Cell Proliferation Assay (MTS assay, Promega, Madison, WI) was used to determine the cytotoxicity. The absorbance of each well was recorded at 490 nm using an Ultramark® 96-well plate reader (Bio-Rad, Hercules, CA). The percentage of viable cell was reported as the mean of optical density (OD) of the treated wells divided by the mean of OD of DMSO control wells after normalization to the signal from wells without cells. IC_{50} was determined by MTS assay and calculated with CalcuSyn software (Biosoft, Cambridge, UK). Each experiment was triplicated.

1.2.4. Combination index and isobologram analysis

The calculation of combination index (CI) and isobolograms with the CalcuSyn software was described previously.[26] Briefly, the CI values were calculated

according to the levels of growth inhibition (Fraction affected, Fa) by each agent individually and combination of ABT-869 with Ara-C or Dox or U0126. Isobolograms, which indicate the equipotent combinations of different dose ($ED_{50,}$ ED_{75} and ED_{90}, etc), were used to illustrate synergism (CI <1), antagonism (CI >1) and additivity (CI = 1). Constant ratio combinations of the two drugs at 0.25x, 0.5x, 1x, 2x and 4x of their ED_{50} was used. Three independent studies were conducted for each combination.

1.2.5. Immunoblot analysis

Preparation of the cell lysate and immunoblotting were performed as previously described.[26] Antibodies used were as follows: anti-cyclins D and E, anti-Bcl-xL, anti-Bcl2, anti-BAD, anti-BAX, anti-BAK, anti-poly (ADP-ribose) polymerase (PARP), anti-cleaved PARP, anti-caspase-3, anti-cleaved caspase-3, anti-caspase-7, and anti-cleaved caspase-7 from Cell Signaling Technology (CST, Danvers, MA); anti-Actin, anti-p21, anti-p27, anti-p53, anti-CDK2, and anti-CDK4 from Santa Cruz Biotechnology (Santa Cruz, CA). Rabbit anti-human c-Mos oncoprotein polyclonal antibody was purchased from Chemicon (Temecula, CA).

1.2.6. Low density Array (LDA)

Gene expression profiling was investigated with custom PCR-based analysis using TaqMan® Low Density Arrays (LDA; Applied Biosystems, Foster City, CA).[27] RNA was extracted from cells using Purescript RNA isolation kit (Genetra systems, Minneapolis, MN). First strand cDNA was synthesized with SuperScript® III First-Strand Synthesis SuperMix (Invitrogen). PCR amplification was performed in the 7900HT Fast Real-time System (Applied Biosystems). The LDA array was custom made with TaqMan® Gene Expression Assays, which allows the simultaneous

measurement of expression of 384 genes in a single sample. Each sample was duplicated. The target genes include anti- and pro-apoptotic genes, cell cycle regulated genes, DNA damage genes, stress gene, PI3K/AKT pathway, MAPK pathway, JAK/STAT pathway, mTOR pathway, VEGF pathway, NOTCH pathway, WNT pathway, NFκB pathway, invasion and metastasis related genes, oncogenes, as well as housekeeping genes. Sequence Detection System (SDS) 2.2.1 software (Applied Biosystems) was used to perform relative quantitation (RQ) of target genes using the comparative C_T ($\Delta\Delta C_T$) method.

1.2.7. shRNA studies

Expression Arrest™ Human retroviral pSM2 shRNAmir individual constructs CCND1 (clone ID: V2HS_88365) and c-Mos (clone ID: V2HS_36817) shRNA, as well as non-silencing shRNA control (RHS1707) were purchased from Open Biosystems (Huntsville, AL). The Expression Arrest™ Human retroviral shRNAmir individual constructs are form the laboratory of Dr. Greg Hannon at Cold Spring Harbor Laboratory (CSHL) which created an RNAi Library comprised of multiple short-hairpin RNAs (shRNAs) specifically targeting annotated human genes. RetroPack PT67 cells (Clontech, Mountain View, CA) were seeded into a 6-well plate at 60-80% confluence (4×10^5 cells/well) 24 hours before transfection, 5 µg of each shRNA vector and 10 µl of Lipofectamine 2000 (Invitrogen) were used for transfection. PT67 cells were diluted and plated after transfection 24 hours in culture medium with 2 µg/ml puromycin (Clontech). After 1 week selection, the large, healthy colonies were isolated and transferred into individual plates. Filtered medium containing viral particles together with 6 µg/ml polybrene were used for infecting MV4-11 cells (2 x

10^6) respectively. Cultures were replaced with fresh medium postinfection 24 hours, and then subjected to immunoblot and cell viability assay.

1.2.8. Xenograft mouse model

Female severe combined immunodeficiency (SCID) mice (17-20 g, 4-6 weeks old) were purchased from Animal Resources Centre (Canning Vale, Australia). Exponentially growing MV4-11 cells (5×10^6) were subcutaneously injected into loose skin between the shoulder blades and left front leg of recipient mice. All treatment was started 25 days after the injection, when the mice had palpable tumor of 300-400 mm^3 average size, Ara-C was intraperitoneally (I.P.) injected at 10 mg/kg/day for consecutive 4 days. ABT-869 was administrated at 15 mg/kg/day by oral gavage daily. In the combination group. Ara-C was given 4 days, followed by ABT-869 daily for 26 days. Each group comprised of 10 mice.

The length (L) and width (W) of the tumor were measured with callipers, and tumor volume (TV) was calculated as $TV = (L\times W^2)/2$. The protocol was reviewed and approved by Institutional Animal Care and Use Committee in compliance to the guidelines on the care and use of animals for scientific purpose.

1.2.9. Immunohistochemistry (IHC)

Tissue fixation and procedure of Hematoxylin and eosin staining were processed as described previously.[26] The sources and conditions of the primary antibodies were as following: p-STAT5 (Tyr694, 1:50, Epitomics, Burlingame, CA), p-AKT (Ser473, 1:200, CST), p-ERK1/2 (Tyr204, 1:50, Santa Cruz), VEGF (1:100, Lab Vision, CA), cleaved PARP (1:50, CST). The anti-PIM1 antibody (clone 19F7) has been previously described.[28] The slides were counterstained in hematoxylin for 30

seconds and mounted with cover slides. The images were analyzed by a Zeiss Axioplan 2 imaging system with AxioVision 4 software (Zeiss, Germany).

1.2.10. Statistical analysis

Number of viable cells, tumor volume, and survival time were expressed in mean ± standard deviation (SD). Tumour volume reduction of the treatment groups was compared to the untreated control group by Student's *t*-test, and *P* values of < 0.05 were considered to be significant. Survival analysis was performed by Kaplan-Meier analysis (SPSS, ver.12). Survival curves of the treatment groups were compared to the untreated control group, and statistical significance were given in log-rank test ($P < 0.05$).

1.3. Results

1.3.1. Molecular signaling pathways of cell cycle arrest and apoptosis induced by ABT-869 treatment

ABT-869 profoundly inhibited FTL3-ITD AML cell proliferation (MV4-11, MOLM-14 and TF1-ITD), but minimally inhibit growth of FLT3 wide type cells, including HEL (M5), KG-1 (M1), NB4 (M3), NOMO-1 (M5), HL60 (M2) and U937 (M5) (Figure 1.1). ABT-869 induced G_1 cell cycle arrest and apoptosis in both MV4-11 and MOLM-14 (Figure 1.2). We further analysed the molecular mechanisms of ABT-869 induced cell cycle arrest and apoptosis. Key cell cycle-regulated proteins were analyzed by immunoblotting. In MV4-11 and MOLM-14 cells, ABT-869 modulated the G_1/S transition regulators in a time-dependent fashion as it entirely down-regulated cyclins D and E by 16h and induced the expression of $p21^{waf1/Cip}$ progressively. The increasing expression of cyclin E in MV4-11 cells at 4h, in MOLM-14 cells at 1h and cyclin D in MOLM-14 cells at 8h after drug exposure could be due to the fact that

cells intended to progress to S phase at the early time points.[29] The expression of cyclin-dependent kinase (CDK) 2 and 4 was relatively stable. $p27^{kip1}$ was increased and maximal in MV4-11 at 16h and in MOLM-14 at 8h after treatment (Figure 1.3A). These data suggested that simultaneous terminal reduction of cyclins D and E, the key G1/S cyclins, and progressive increases in cyclin dependent kinase inhibitors (CDKIs) $p21^{waf1/Cip}$, $p27^{kip1}$ contributed to the blockage of G_1/S progression induced by ABT-869.

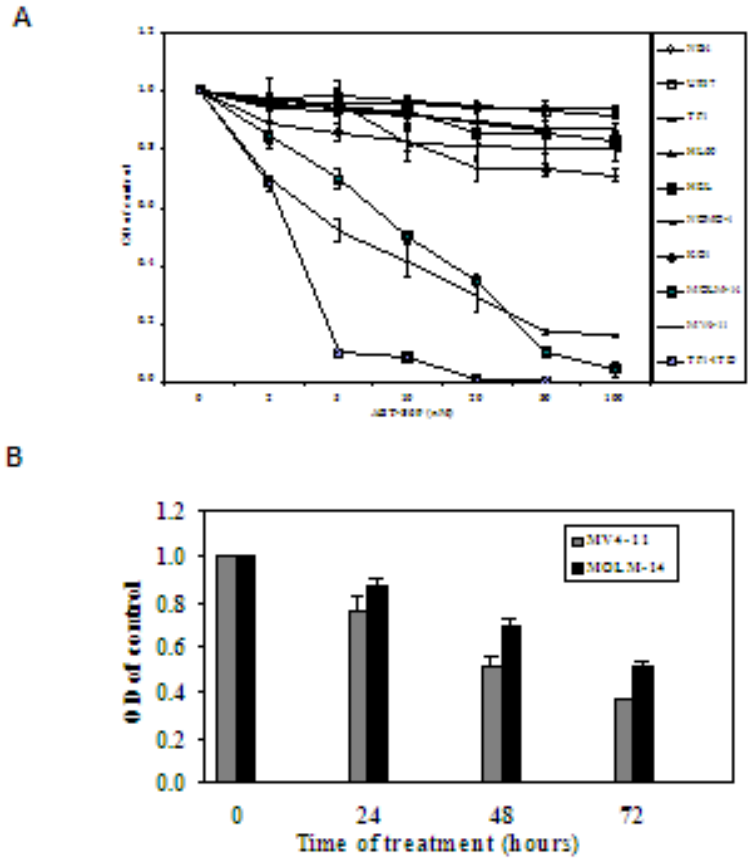

Figure 1.1. ABT-869 showed different effects on a spectrum of AML cell lines. Values are presented as the mean +/- SD (n = 3). (A) Effect of ABT-869 on proliferation determined by MTS assay of numerous leukemia cell lines after a 48 hour exposure. ABT-869 showed impressive inhibition on TF1-ITD, MV4-11 and MOLM-14 cells compared to other non-FLT3 mutated cell lines. (B) MV4-11 and MOLM-14 cells were exposed to ABT-869 at a concentration of 5 nM for 0, 24 and 48 hours. ABT-869 displayed inhibition on MV4-11 and MOLM-14 cell proliferation in a time-dependent manner.

To elucidate the mechanisms of ABT-869 induced apoptosis of FLT3-ITD-AML cells, the expression of several apoptosis associated proteins was examined. Proapoptotic BAD was gradually increased in MV4-11 cells and intensively increased after exposure to ABT-869 for 8h in MOLM-14 cells. In both cell lines, ABT-869 augmented the expression of proapoptotic proteins BAK and BID, and decreased the expression of anti-apoptotic Bcl-xL protein in a time-dependent manner. Cleaved BID could be visualized as early as 1 hour after ABT-869 treatment. Another anti-apoptotic protein Bcl2 was not altered. ABT-869 also transiently induced the expression of p53 immediately after 1h drug exposure. The protein level of BAX was increased in only in MV4-11 cells at 16h post treatment, not in MOLM-14 cells (Figure 1.3B). After incubation with ABT-869, cleavage of effector caspase 7 was detected in MV4-11 at 1h and in MOLM-14 at 4h and increased in a time-dependent fashion thereafter. However, cleaved caspase 3 was more prominently observed in MV4-11 cells than in MOLM-14 cells. Cleavage of PARP was also observed in both cells (Figure 1.3B).

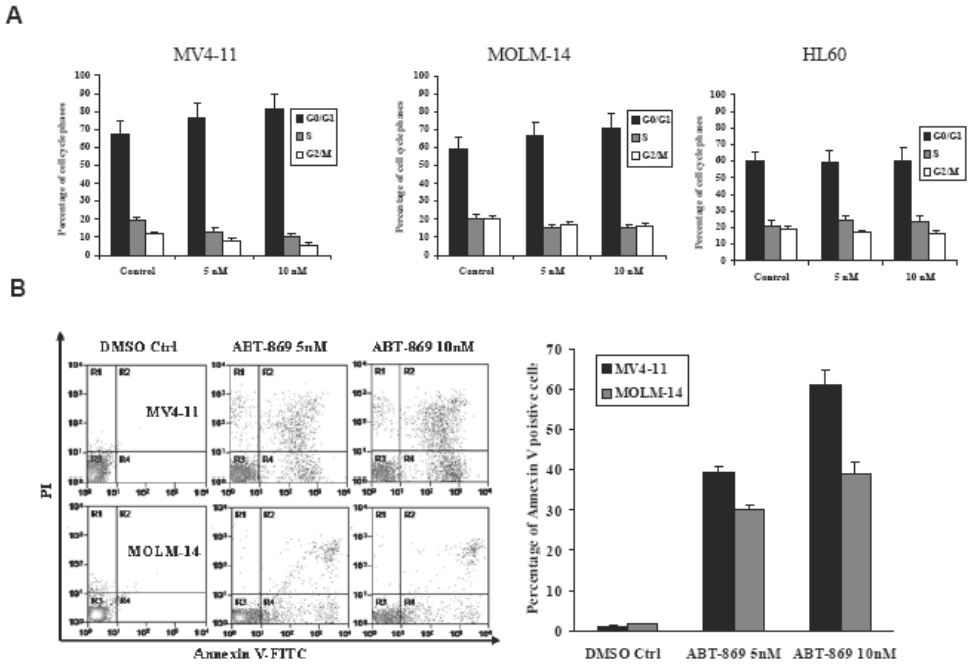

Figure 1.2. ABT-869 induced G0/G1 cell cycle arrest and apoptosis of MV4-11 and MOLM-14 cells. (A) FACS analysis of cell cycle distributions after MV4-11, MOLM-14 and HL60 treated with ABT-869 at concentration of 0, 5, and 10 nM for 24 hours. The bar graph indicated the percentage of cell number in each cell cycle phase. This experiment was triplicated. HL60 cell line was used as control. In MV4-11 and MOLM-14 cells, the percentage of G0/G1 cells were significantly increased after ABT-869 treatment ($p < 0.05$). (B) Flow cytometric analysis of apoptosis by Annexin V-FITC/PI double staining in MV4-11 and MOLM-14 cells treated with ABT-869 at concentration of 0, 5, and 10 nM for 48 hours. The quadrants-R1, R2, R3 and R4 demonstrated the cells were in the condition of viable (double negative), early apoptosis (Annexin V+, PI-), late apoptosis (Annexin V+, PI+) and death (double positive) respectively. The percentage of Annexin V positive cell number are in the right bar figure.

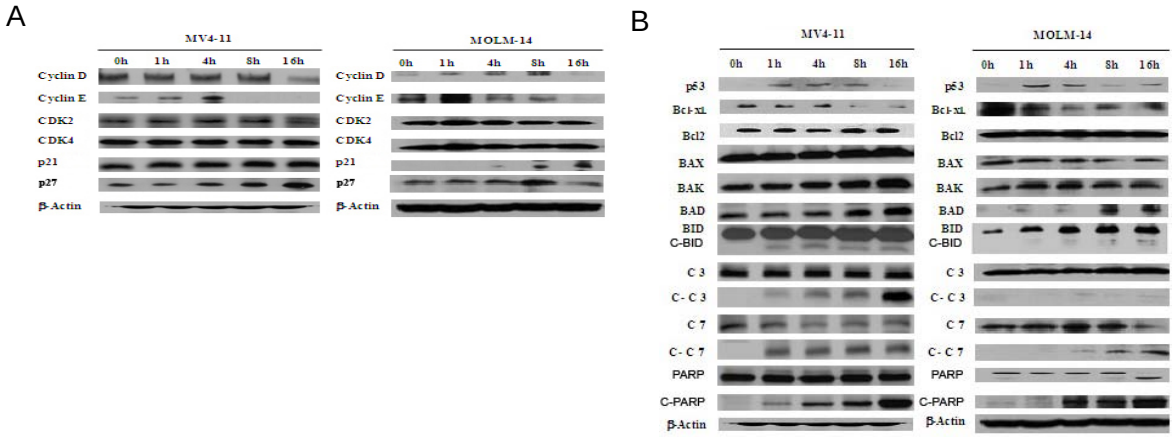

Figure 1.3. The molecular mechanisms of cycle arrest and apoptosis induced by ABT-869 treatment in MV4-11 and MOLM-14 cells. MV4-11 and MOLM-14 cells were exposed with ABT-869 6 nM and 9 nM respectively for 0, 1, 4, 8 and 16 hours, then washed, lysed and subjected to 12% SDS-PAGE. Western blots were detected with indicated antibodies for the assessment of the expression level changes in (A) cell cycle regulated proteins and (B) apoptosis regulated proteins. -Actin was used to confirm equal loading protein of each sample. C-BID and C-PARP referred to cleaved-BID and cleaved-PARP respectively.

1.3.2. Simultaneous treatment with ABT-869 and chemotherapeutic agents

Prior to studying the combination effect, the efficacy of Ara-C and Dox as single agent was first confirmed. The IC_{50} of Ara-C on MV4-11 and MOLM-14 cells at 48 h were 450 and 250 nM respectively, and the IC_{50} of Dox for these two cell lines were 350 and180 nM respectively. MV4-11 and MOLM-14 cells were treated with ABT-869 and in combination with either Dox or Ara-C, then assayed for cell survival by MTS

assay. As shown in the Figure 1.4A, the effect of combining ABT-869 and Ara-C at their ED_{50} or ED_{75} approximated the respective theoretic additive values indicated by the diagonals. In contrast, combining ABT-869 and Ara-C at their ED_{90} concentrations resulted in a value that fell far to the right of the diagonal in MV4-11 cells, but not in MOLM-14 cells. These data suggest that at lower doses there is an additive or mildly synergistic interaction, while at higher doses the two agents might interact in an antagonistic manner.[26] All of the combination results of ABT-869 and Dox were to the lower left of the diagonals, indicating synergistic effects (Figure 1.4B).

1.3.3. Sequence-dependent interactions between ABT-869 and chemotherapy

We next employed a sequence-dependent method as described by Levis et al.[24] MV4-11 and MOLM-14 cells were treated with ABT-869 at various doses for 24h, and after washing then followed by addition of Ara-C or Dox incubation for 48h. Isobologram analysis for both cell lines showed that the combination values were located on the diagonal (ED_{50}) and far right of the diagonals (ED_{75} and ED_{90}) (Figure 1.4C). This indicated that pretreatment with ABT-869 antagonized the cytotoxicity of Ara-C. But, pretreatment with ABT-869 followed by Dox appeared to have both antagonistic (ED_{50}) and synergistic (ED_{75} and ED_{90}) effects in MV4-11 cells (Figure 1.4D, left isobologram) and have essentially antagonism in MOLM-14 cells (Figure 1.4D, right isobologram).

Lastly, chemotherapy followed by ABT-869. MV4-11 and MOLM-14 cells were exposed to Ara-C or Dox for 24h, and washed out then transferred into medium containing ABT-869 for an additional 48h. Synergistic effect of pretreatment with Ara-C or Dox, followed by ABT-869 were consistently identified at ED_{50}, ED_{75} and ED_{90}

points (Figure 1.4E and 1.4F). The CI values obtained for ABT-869 in combination with Ara-C and Dox employing three sequences are shown in Table 1. To determine whether the combination therapy produce synergism in induction of apoptosis, the Annexin-V/PI double staining was used to assess MV4-11 cells treated with Ara-C followed by ABT-869. The CI values at ED_{50}, ED_{75} and ED_{90} were 0.56, 0.50, and 0.38 respectively which indicated synergism. These data illustrated that pretreatment with chemotherapy followed by ABT-869 produced synergistic effects on inhibition of proliferation and induction of apoptosis.

To further validate findings in cell lines, patient samples with either FLT3-ITD (Pt#1, 2, 3), FLT3-D835Y point mutation (Pt#4) or wild-type FLT3 (Pt#5, 6, 7) were treated with Ara-C 24h first, followed by ABT-869. Primary cells were incubated with either ABT-869 (20, 40, 80, 160, 320 nM), or Ara-C (100, 200, 400, 800, 1600 nM) alone and in combination. The CI values of these patient samples with FLT-ITD and D835Y mutations ranged from 0.67 to 0.08, indicative of synergism between the two agents on a primary AML specimen with FLT3-ITD or D835Y point mutation. In contrast, the combination of Ara-C and ABT-869 on 3 patient samples with wild-type FLT3 didn't produce a synergistic effect (CI values between 0.9 to 1.2).

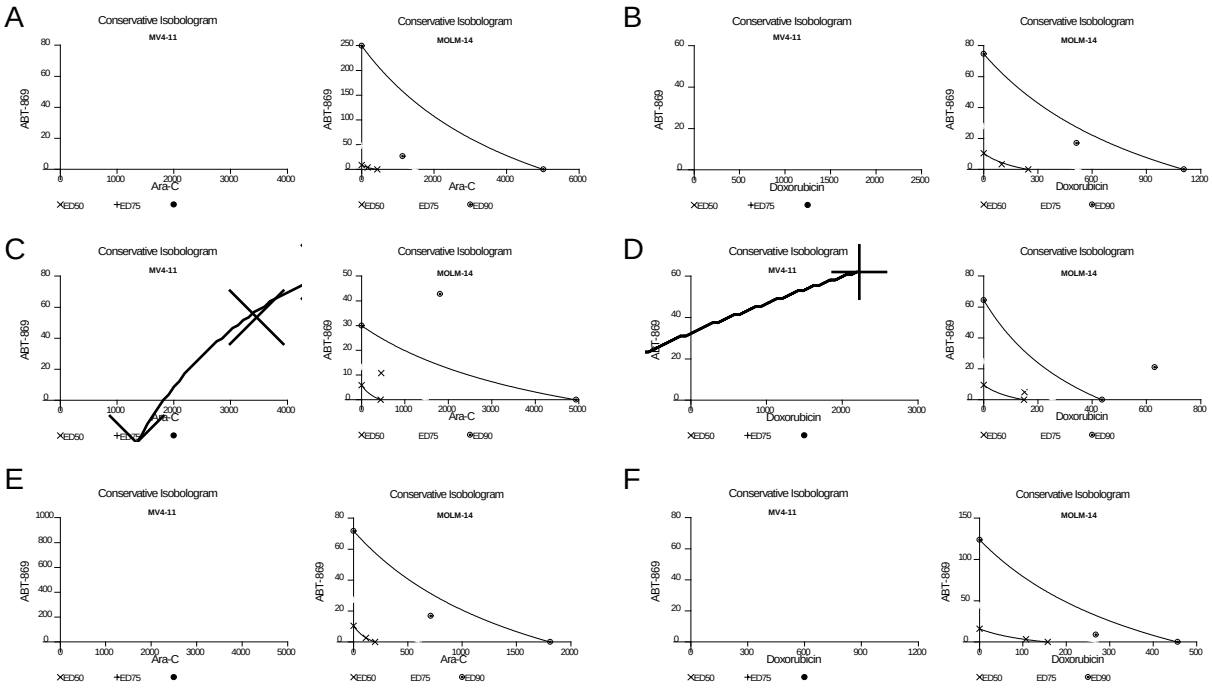

Figure 1.4. Conservative isobolograms showing the interactions among three different models of combination with ABT-869 and chemotherapeutic agents on the proliferation of MV4-11 and MOLM-14 cells. The drug concentration unit is nM. The diagonal lines linking up the ED_{50}, ED_{75} and ED_{90} values of two drugs represent the theoretic additive lines. Synergism is indicated by the ED points located on the lower left of the diagonal. Antagonism is implied by ED points located on the upper right above the diagonal. Additive effects are indicated by when the ED points fall on the diagonal. These results were generated by CalcuSyn software for (A) simultaneous combination of ABT-869 with Ara-C, (B) simultaneous combination of ABT-869 and Dox , (C) pretreatment with ABT-869 first followed by Ara-C, (D) pretreatment with ABT-868 first followed by Dox, (E) pretreatment with Ara-C first in addition of ABT-869, (F) pretreatment with Dox first in addition of ABT-869. The results are from 3 representative independent experiments.

Table 1.1. Combination index (CI) values in three models of ABT-869 and chemotherapeutic agents. Chemotherapy first followed by ABT-869 produced best synergistic interaction among the 3 different combinations.

		Simultaneous			ABT-869 first			Chemotherapy first		
		CIs at			CIs at			CIs at		
		ED_{50}	ED_{75}	ED_{90}	ED_{50}	ED_{75}	ED_{90}	ED_{50}	ED_{75}	ED_{90}
ABT-869 + Ara-C	MV4-11	0.75	0.92	1.14	0.90	1.20	1.65	0.62	0.41	0.27
	MOLM-14	0.93	0.80	0.69	2.00	1.70	1.60	0.82	0.72	0.62
ABT-869 + Dox	MV4-11	0.59	0.64	0.70	1.13	0.85	0.64	0.69	0.67	0.65
	MOLM-14	0.73	0.70	0.69	1.53	1.62	1.76	0.80	0.75	0.65

The CI values were calculated based on the combination wide range of dose with ABT-869 and chemotherapeutic agents. Only the values for the combination of their typical dose of ED_{50}, ED_{75} and ED_{90} were showed. The results represented the means of 3 different experiments.

1.3.4. Inhibition of cell cycle related genes and MAPK pathway played an important role in the synergistic mechanism

To address the underlying molecular mechanism of the synergism between ABT-869 and chemotherapy, we utilized a real-time PCR-based approach to profile the gene expression between MV4-11 cells treated with combination therapy (Ara-C followed by ABT-869) and single agent therapy. The significantly down-regulated gene clusters in combination therapy contained probes for genes involved in cell cycle regulation and the MAPK pathway as compared to Ara-C or to ABT-869 treatment alone (Table 1.2). Among all the affected genes, CCND1 and Moloney murine sarcoma viral oncogene homolog (c-Mos) were the two most significantly downregulated. To examine their functional roles in the synergistic manifestation, Western blot analysis confirmed that combination treatment also significantly decreased CCND1 and c-Mos at the protein level, as well as blockage of the MAPK pathways, indicated by reduced phosphorylation of ERK protein (Figure 1.5A). Specific inhibition of CCND1 (approximately 80% reduction) and c-Mos (approximately 60%) by shRNAs was confirmed by immunoblot analysis (Figure 3B, right panel). Essentially, silencing either CCND1 or c-Mos remarkably potentiated ABT-869 induced inhibition to a similar degree as combination therapy (Ara-C 100 nM followed by ABT-869) when compared to control shRNA treatment ($p<0.01$) (Figure 1.5B). To further validate the importance of MAPK pathway, we used a ERK inhibitor U0126 in combination of ABT-869 in 3 different sequences. The IC_{50} of U0126 on MV4-11 is 14 μM. Both sequence-dependent combinations (ABT-869 first

or U0126 first) produced synergism (Figure 1.5C, middle and right isobolograms). When the two drugs given simultaneously, it achieved synergistic effect at IC_{50} and IC_{75} and additive effect at IC_{90} (Figure 1.5C, left isobologram). These data provide further evidences that MAPK signaling transduction pathway, specifically via MEK/ERK pathway, is critical for the synergism.

In addition, we investigated whether PI3K/AKT, another important pro-survival signaling pathway was involved in combination therapy or not. Western blot revealed that the reduction of p-AKT was more obvious in ABT-869 alone than the combination, suggesting this pathway is not the mechanism for the synergistic effect in combination studies.

Table 1.2. LDA analysis revealed that combination therapy further down-regulated genes involved in cell cycle regulation and MAPK pathway.

	Fold Changes			
Genes and ID	**Comb vs ABT-869**	**ABT-869 vs Ctrl**	**Comb vs Ara-C**	**Ara-C vs Ctrl**
Cell cycle				
ATM-Hs00175892_m1	-1.6 ± 0.1	1.1 ± 0.1	-1.5 ± 0.1	1.1 ± 0.1
RB1-Hs00153108_m1	-1.5 ± 0.1	-1.1 ± 0.1	-1.5 ± 0.1	1.0 ± 0.1
CCND1-Hs00277039_m1	-37 ± 4.2	-2.2 ± 0.1	-12.2 ± 3	-3.3 ± 0.4
CCND2-Hs00277041_m1	-1.8 ± 0.1	-1.4 ± 0.1	-1.9 ± 0.1	-1.3 ± 0.1
FOXO3A-Hs00818121_m1	-2.2 ± 0.1	1.5 ± 0.1	-1.5 ± 0.1	-1.1 ± 0.1
MAD1L1-Hs00269119_m1	-1.5 ± 0.1	1.0 ± 0.1	-1.6 ± 0.1	1.1 ± 0.1
PRKDC-Hs00179161_m1	-1.9 ± 0.2	-1.1 ± 0.1	-2.1 ± 0.1	1.0 ± 0.1
CDK7-Hs00361486_m1	-1.5 ± 0.1	-2.4 ± 0.1	-1.5 ± 0.1	-2.3 ± 0.1
MAPK pathway				
FGFR4-Hs00242558_m1	-2.0 ± 0.1	-2.3 ± 0.1	-1.5 ± 0.1	-2.0 ± 0.1
MOS-Hs00271264_s1	-4.6 ± 0.4	-2.1 ± 0.1	-71.4 ± 9.2	17 ± 3.7
NRAS-Hs00180035_m1	-1.5 ± 0.1	1.1 ± 0.1	-1.5 ± 0.1	1.1 ± 0.1
KRAS-Hs00270666_m1	-1.6 ± 0.1	1.1 ± 0.1	-1.5 ± 0.1	1.0 ± 0.1
SRC-Hs00178494_m1	-2.1 ± 01.	-1.2 ± 0.1	-1.5 ± 0.1	-1.3 ± 0.1
MAPK1-Hs00177066_m1	-2.3 ± 0.1	-2.0 ± 0.2	-2.1 ± 0.1	-1.7 ± 0.1
MAPK8-Hs00177083_m1	-2.0 ± 0.1	1.7 ± 0.1	-1.5 ± 0.1	1.4 ± 0.1
MAP4K1-Hs00179345_m1	-1.5 ± 0.1	1.3 ± 0.1	-1.7 ± 0.1	1.3 ± 0.1
FOS-Hs00170630_m1	-1.5 ± 0.1	-2.3 ± 0.1	-1.5 ± 0.1	-2.2 ± 0.1

*IDs denote the TaqMan® Gene Expression Assays. Comb: Combination therapy (Ara-C followed by ABT-869). Ctrl: DMSO Control. Minus numbers indicated decreased fold of expression.

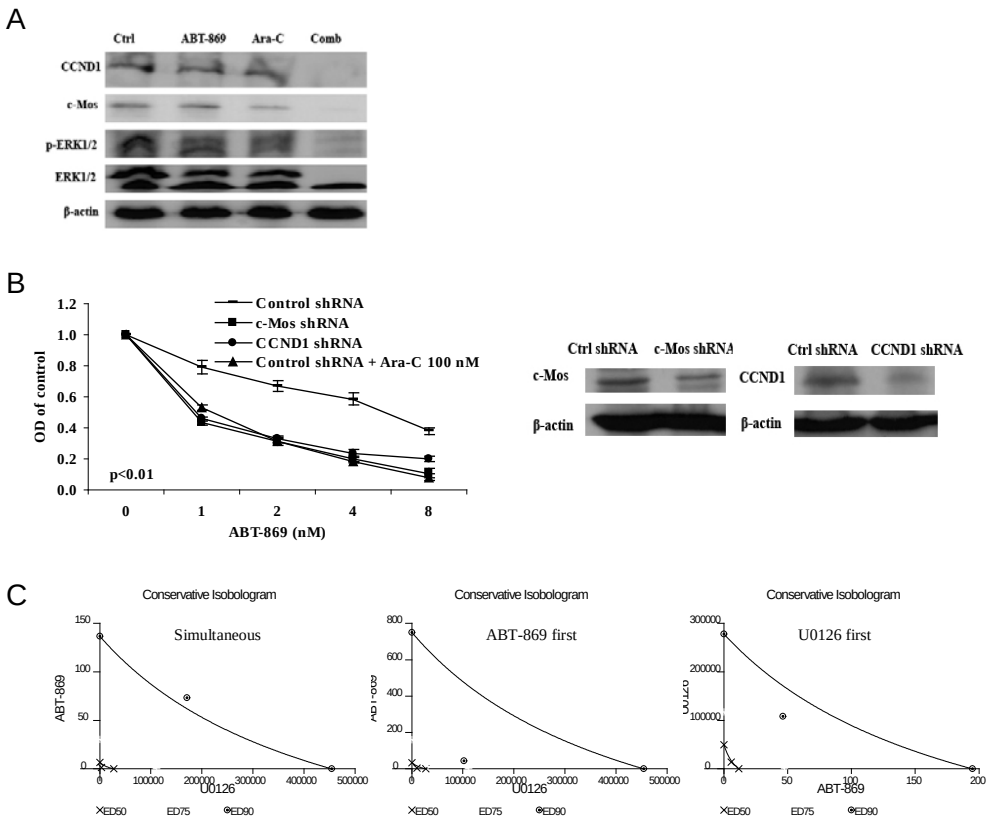

	Simultaneous	ABT-869 frist	U0126 first
CI at ED_{50}	0.33	0.49	0.77
CI at ED_{75}	0.55	0.37	0.67
CI at ED_{90}	0.91	0.28	0.62

Figure 1.5. CCND1 and c-Mos played important roles in the molecular mechanisms of synergistic effect by combination therapy. (A) MV4-11 cells were treated with DMSO control, ABT-869, Ara-C and combination therapy (Ara-C followed by ABT-869), then subjected to immunoblot analysis. (B) Silencing either c-Mos or CCND1 by shRNA augment the cell proliferation inhibition with ABT-869. MV4-11 cells treated with control, c-Mos or CCND1 shRNA separately, then exposured to ABT-869 at various dosage or Ara-C 100 nM followed by ABT-869. MTS assay was used to assess the growth inhibition. (C) Conservative isobologrames of ABT-869 in combination with U0126 in 3 different sequences. MV4-11 cells were treated with ATB-869 at concentration of 1.5, 3, 6, 12, 24 nM or U0126 at concentration of 3.5, 7, 14, 28, 56 μM simultaneously or sequentially (ABT-869 first or U0126 first) in a same fashion as ABT-869 in combination with chemotherapy. CalcuSyn software was used to generated the isobologram for simultaneous treatment (left panel), ABT-869 first followed by U0126 (middle panel) and U0126 first followed by ABT-869 (right panel). All CI values at IC50, IC75 and IC90 of the 3 combinations were shown in the table at bottom. The results are from 3 representative independent experiments.

1.3.5. In Vivo Efficacy of ABT-869, alone or in combination with cytotoxic drugs, for treatment in MV4-11 mice xenografts

Based on the *in vitro* results, the optimal combination sequence (chemotherapy followed by ABT-869) was studied *in vivo*. Tumors in mice treated with Ara-C alone showed an initial growth delay during chemotherapy treatment, then grew at the same rate as those in the vehicle control group (Figure 1.6). In the ABT-869 monotherapy group, a complete response (no palpable tumor) was observed in 2/10 mice by day 35 and in all mice by day 39. In the combination group, a complete response was observed in 6/10 mice at day 35 and in all mice by day 39. All treatments were stopped at day 54. The anti-tumor effects of ABT-869 or the combination were significantly better when compared to Ara-C alone or control ($p<0.001$). The combination therapy resulted in faster reduction of tumor burden compared to ABT-869 treatment alone ($p=0.03$) and more complete responders as compared to ABT-869 treatment alone. We did not observe any adverse side effects in the treatment groups in terms of behavior or body weight changes.

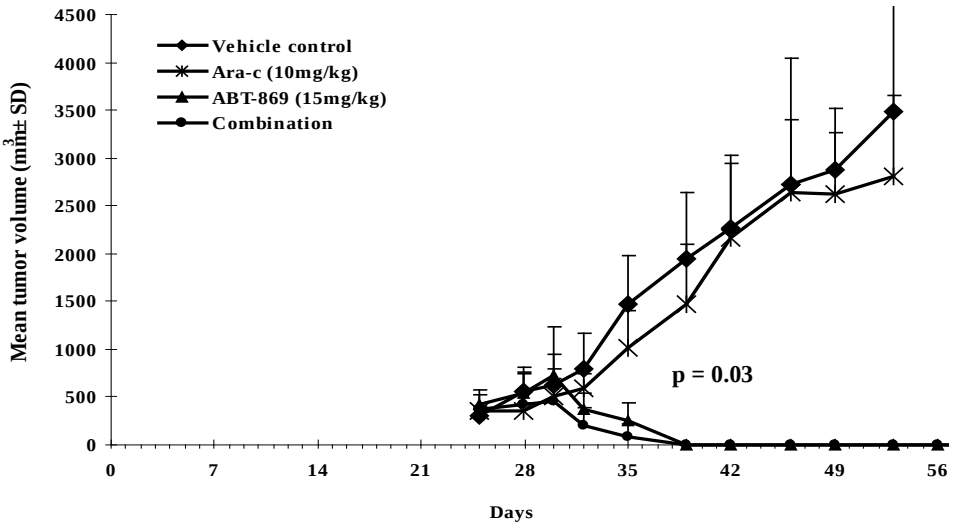

Figure 1.6. Combination therapy achieved a faster reduction of established tumor volume than ABT-869 single agent or Ara-C treatment.

1.3.6. Molecular events following in vivo treatment of MV4-11 tumors with ABT-869

In addition to a reduction of tumor volume, ABT-689 demonstrated significant biochemical effects on MV4-11 xenografts tumor. Histological examination of tumor specimens showed treated samples to be less cellular, compared to samples from mice treated with vehicle only (Figure 1.7A). A 15 mg/kg/day dose of ABT-869 effectively reduced p-STAT5 (Figure 1.7B), p-AKT (Figure 1.7C), p-ERK1/2 (Figure 1.7D), and PIM1 (Figure 1.7E), all of which are reported to be important FLT3 downstream effectors. In addition, the expression of VEGF was profoundly reduced in the treated tissue (Figure 1.7F). Cleavage of PARP was increased after the treatment (Figure 1.7G). Together, these data supported that the *in vivo* biological effect of ABT-869 is associated with the inhibition of multiple pathways including FLT3, STAT5, AKT, MAPK, and angiogenesis.

1.4. Discussion

Multi-targeted TKIs including FLT3 inhibitors are promising targeted therapeutics for leukemia harboring FLT3 mutations. In this study, we further dissected the molecular mechanisms for ABT-869 on proliferation and apoptosis. We then demonstrated the importance of sequence specific synergistic effect in combining targeted therapy such as ABT-869 with chemotherapy in cell lines and primary AML cells containing either FLT3-ITD or FLT3-D835Y. Our findings highlighted the “sequence specific” feature of TKIs which has been suggested with other TKIs.[24] The greatest synergism occurs when the cytotoxic agents were administered first, followed by ABT-869.

We observed cleaved caspase 3 mainly in MV4-11 cells. It has recently been reported that caspase 3 is responsible for DNA fragmentation and morphologic

changes, while caspase 7 is responsible for the loss of cellular viability.[30] MV4-11 which has both alleles with mutated FLT3, is more sensitive to ABT-869 than MOLM-14 which has one allele with FLT3-ITD and the other allele with wild type.

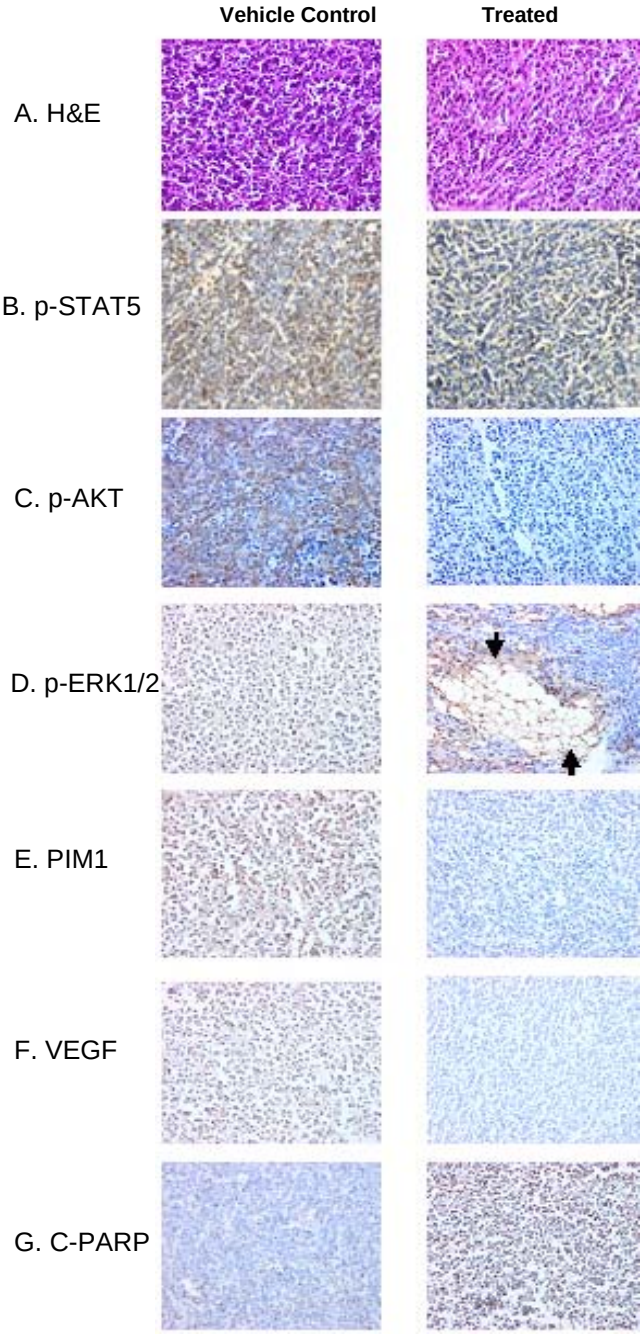

Figure 1.7. *In vivo* effect of ABT-869 on MV4-11 tumor xenograft model. SCID mice with established MV4-11 xenograft were treated with vehicle or ABT-869.

Excised tumor pieces were embedded in paraffin and stained with either (A) H & E or immunostained with (B) p-STAT5, (C) p-AKT, (D) p-ERK1/2, (E) PIM-1, (F)VEGF and (G) cleaved (C)-PARP. The magnification of all pictures is 400x. Arrows indicate that necrosis with fat replacement in this area.

Furthermore, this current study, for the first time, demonstrates that the synergism of combination therapy is due to down regulation of cell cycle regulated genes and genes in MAPK pathway. Combination treatment not only completely inhibits phosphor-ERK1/2, but also results in decreased expression of wild type ERK1, which likely also contributes to inhibition of MAPK pathway. In addition to its well-described function in G_1 to S phase progression, CCND1 overexpression has been found in a variety of cancers including B-cell lymphoma, multiple myeloma and breast cancer, thus CCND1 is also regarded as an oncogene.[31] The c-Mos proto-oncogene product, a serine/threonine kinase, is a strong activator of the MAPK pathway, which is important for oocyte maturation.[32,33] In somatic cells, constitutive expression of c-Mos in mouse fibroblasts leads to neoplastic transformation.[34] Deregulated expression of c-Mos has been discovered in various human cancer cell lines and primary patient samples, including neuroblastoma,[35] thyroid medullary carcinoma[36] and non-small lung carcinomas.[37] It is noteworthy that increased levels of CCND1 is found in both c-Mos transformed cells and c-Mos transgenic mice.[34] The MAPK pathway is a major regulator of cell survival and proliferation and its activation is well documented in leukemia.[38] These observations are in line with our results with LDA, immunoblot and shRNA analysis and U0126 inhibitor. Most interestingly, our data suggest that targeting cell cycle genes, notably CCND1 and c-Mos mediated MAPK/MEK/ERK pathway could be the main mechanism of the synergistic interactions between chemotherapy and ABT-869.

For simultaneous combinations, ABT-869 and Ara-C together only achieved an additive effect, while ABT-869 and Dox together produced synergism. SU11248, another FLT3 inhibitor, also was found to synergistically interact with Ara-C or Dox *in vitro* when given concurrently[23]. In contrast, pretreatment with ABT-869 followed by chemotherapy yielded an undesirable antagonistic effect. The antagonism observed could result from G_1-phase cell cycle arrest and the removal of cells in the S-G_2/M boundary by ABT-869, resulting in more cells under quiescent condition. Ara-C is a phase-specific agent that is most active against cells in S-phase. In contrast, Dox is active against cells during multiple phases of the cell cycle.[39] Collectively, pretreatment with ABT-869 would make subsequent chemotherapy less efficacious. In agreement with our data, antagonism has been reported with pretreatment with CEP-701, another FLT3 inhibitor, followed by Ara-C or etoposide.[24]

The animal experiment provided further evidence to support that chemotherapy followed by ABT-869 is the sequence of choice for combination. The *in vivo* IHC study showed that ABT-869 has vigorous biological activities against FLT3 signaling pathways, demonstrated by the pronounced inhibition of several main FLT3 downstream targets. ABT-869 also reduced the expression of VEGF in the MV4-11 tumors. VEGF specifically promotes the proliferation of endothelial cells and is a major regulator of tumor angiogenesis *in vivo*. Because ABT-869 is a multi-target kinase inhibitor, the inhibitory effect of non-FLT3 targets such as VEGF could also contribute to the reduction of MV4-11 tumor *in vivo*. These findings highlight the critical role of *in vivo* animal models in the preclinical development of TKIs.

Our data demonstrates the ability of ABT-869 to interact synergistically with chemotherapy in a sequence-dependent manner and reveals the mechanism of

synergy as further suppression of cell cycle regulated genes and the c-Mos mediated MAPK/MEK/ERK pathway. These observations will help to define the optimal combination therapy for future clinical trials in AML.

1.5. References

1. Nakao M, Yokota S, Iwai T, Kaneko H, Horiike S, Kashima K *et al.* Internal tandem duplication of the flt3 gene found in acute myeloid leukemia. *Leukemia* 1996; **10**: 1911-1918.
2. Schnittger S, Schoch C, Dugas M, Kern W, Staib P, Wuchter C *et al.* Analysis of FLT3 length mutations in 1003 patients with acute myeloid leukemia: correlation to cytogenetics, FAB subtype, and prognosis in the AMLCG study and usefulness as a marker for the detection of minimal residual disease. *Blood* 2002; **100**: 59-66.
3. Thiede C, Steudel C, Mohr B, Schaich M, Schakel U, Platzbecker U *et al.* Analysis of FLT3-activating mutations in 979 patients with acute myelogenous leukemia: association with FAB subtypes and identification of subgroups with poor prognosis. *Blood* 2002; **99**: 4326-4335.
4. Yamamoto Y, Kiyoi H, Nakano Y, Suzuki R, Kodera Y, Miyawaki S *et al.* Activating mutation of D835 within the activation loop of FLT3 in human hematologic malignancies. *Blood* 2001; **97**: 2434-2439.
5. Gilliland DG, Griffin JD. The roles of FLT3 in hematopoiesis and leukemia. *Blood* 2002; **100**: 1532-1542.
6. Levis M, Small D. FLT3: ITDoes matter in leukemia. *Leukemia* 2003; **17**: 1738-1752.
7. Stirewalt DL, Radich JP. The role of FLT3 in haematopoietic malignancies. *Nat Rev Cancer* 2003; **3**: 650-665.
8. Hayakawa F, Towatari M, Kiyoi H, Tanimoto M, Kitamura T, Saito H *et al.* Tandem-duplicated Flt3 constitutively activates STAT5 and MAP kinase and introduces autonomous cell growth in IL-3-dependent cell lines. *Oncogene* 2000; **19**: 624-631.
9. Mizuki M, Fenski R, Halfter H, Matsumura I, Schmidt R, Muller C *et al.* Flt3 mutations from patients with acute myeloid leukemia induce transformation of 32D cells mediated by the Ras and STAT5 pathways. *Blood* 2000; **96**: 3907-3914.
10. Zheng R, Friedman AD, Levis M, Li L, Weir EG, Small D. Internal tandem duplication mutation of FLT3 blocks myeloid differentiation through suppression of C/EBPalpha expression. *Blood* 2004; **103**: 1883-1890.
11. Takahashi S, McConnell MJ, Harigae H, Kaku M, Sasaki T, Melnick AM *et al.* The Flt3 internal tandem duplication mutant inhibits the function of transcriptional repressors by blocking interactions with SMRT. *Blood* 2004; **103**: 4650-4658.
12. Takahashi S, Harigae H, Kameoka J, Sasaki T, Kaku M. AML1B transcriptional repressor function is impaired by the Flt3-internal tandem duplication. *Br J Haematol* 2005; **130**: 428-436.
13. Schwable J, Choudhary C, Thiede C, Tickenbrock L, Sargin B, Steur C *et al.* RGS2 is an important target gene of Flt3-ITD mutations in AML and functions in myeloid differentiation and leukemic transformation. *Blood* 2005; **105**: 2107-2114.
14. Brandts CH, Sargin B, Rode M, Biermann C, Lindtner B, Schwable J *et al.* Constitutive activation of Akt by Flt3 internal tandem duplications is necessary for

increased survival, proliferation, and myeloid transformation. *Cancer Res* 2005; **65**: 9643-9650.
15. Scheijen B, Ngo HT, Kang H, Griffin JD. FLT3 receptors with internal tandem duplications promote cell viability and proliferation by signaling through Foxo proteins. *Oncogene* 2004; **23**: 3338-3349.
16. Zeng Z, Samudio IJ, Zhang W, Estrov Z, Pelicano H, Harris D *et al.* Simultaneous inhibition of PDK1/AKT and Fms-like tyrosine kinase 3 signaling by a small-molecule KP372-1 induces mitochondrial dysfunction and apoptosis in acute myelogenous leukemia. *Cancer Res* 2006; **66**: 3737-3746.
17. Kim KT, Baird K, Ahn JY, Meltzer P, Lilly M, Levis M *et al.* Pim-1 is up-regulated by constitutively activated FLT3 and plays a role in FLT3-mediated cell survival. *Blood* 2005; **105**: 1759-1767.
18. Hanahan D, Weinberg RA. The hallmarks of cancer. *Cell* 2000; **100**: 57-70.
19. Albert DH, Tapang P, Magoc TJ, Pease LJ, Reuter DR, Wei RQ *et al.* Preclinical activity of ABT-869, a multitargeted receptor tyrosine kinase inhibitor. *Mol Cancer Ther* 2006; **5**: 995-1006.
20. Guo J, Marcotte PA, McCall JO, Dai Y, Pease LJ, Michaelides MR *et al.* Inhibition of phosphorylation of the colony-stimulating factor-1 receptor (c-Fms) tyrosine kinase in transfected cells by ABT-869 and other tyrosine kinase inhibitors. *Mol Cancer Ther* 2006; **5**: 1007-1013.
21. Shankar DB, Li J, Tapang P, Owen McCall J, Pease LJ, Dai Y *et al.* ABT-869, a multitargeted receptor tyrosine kinase inhibitor: inhibition of FLT3 phosphorylation and signaling in acute myeloid leukemia. *Blood* 2007; **109**: 3400-3408.
22. Druker BJ, Sawyers CL, Capdeville R, Ford JM, Baccarani M, Goldman JM. Chronic myelogenous leukemia. *Hematology (Am Soc Hematol Educ Program)* 2001: 87-112.
23. Yee KW, Schittenhelm M, O'Farrell AM, Town AR, McGreevey L, Bainbridge T *et al.* Synergistic effect of SU11248 with cytarabine or daunorubicin on FLT3 ITD-positive leukemic cells. *Blood* 2004; **104**: 4202-4209.
24. Levis M, Pham R, Smith BD, Small D. In vitro studies of a FLT3 inhibitor combined with chemotherapy: sequence of administration is important to achieve synergistic cytotoxic effects. *Blood* 2004; **104**: 1145-1150.
25. Brown P, Levis M, McIntyre E, Griesemer M, Small D. Combinations of the FLT3 inhibitor CEP-701 and chemotherapy synergistically kill infant and childhood MLL-rearranged ALL cells in a sequence-dependent manner. *Leukemia* 2006; **20**: 1368-1376.
26. Shen J, Tai YC, Zhou J, Stephen Wong CH, Cheang PT, Fred Wong WS *et al.* Synergistic antileukemia effect of genistein and chemotherapy in mouse xenograft model and potential mechanism through MAPK signaling. *Exp Hematol* 2007; **35**: 75-83.
27. Abruzzo LV, Lee KY, Fuller A, Silverman A, Keating MJ, Medeiros LJ *et al.* Validation of oligonucleotide microarray data using microfluidic low-density arrays: a new statistical method to normalize real-time RT-PCR data. *Biotechniques* 2005; **38**: 785-792.
28. Ionov Y, Le X, Tunquist BJ, Sweetenham J, Sachs T, Ryder J *et al.* Pim-1 protein kinase is nuclear in Burkitt's lymphoma: nuclear localization is necessary for its biologic effects. *Anticancer Res* 2003; **23**: 167-178.
29. Gong J, Traganos F, Darzynkiewicz Z. Staurosporine blocks cell progression through G1 between the cyclin D and cyclin E restriction points. *Cancer Res* 1994; **54**: 3136-3139.

30. Lakhani SA, Masud A, Kuida K, Porter GA, Jr., Booth CJ, Mehal WZ *et al.* Caspases 3 and 7: key mediators of mitochondrial events of apoptosis. *Science* 2006; **311**: 847-851.
31. Musgrove EA. Cyclins: roles in mitogenic signaling and oncogenic transformation. *Growth Factors* 2006; **24**: 13-19.
32. Mansour SJ, Matten WT, Hermann AS, Candia JM, Rong S, Fukasawa K *et al.* Transformation of mammalian cells by constitutively active MAP kinase kinase. *Science* 1994; **265**: 966-970.
33. Sagata N. What does Mos do in oocytes and somatic cells? *Bioessays* 1997; **19**: 13-21.
34. Yang Y, Pham CD, Arlinghaus RB, Khillan JS, Singh B. Elevated level of cyclin D1 in mos-transformed cells. *Int J Oncol* 1998; **12**: 1199-1202.
35. Li CC, Chen E, O'Connell CD, Longo DL. Detection of c-mos proto-oncogene expression in human cells. *Oncogene* 1993; **8**: 1685-1691.
36. Parkar MH, Seid JM, Stringer BM, Ingemansson S, Woodhouse N, Goyns MH. Abnormal expression of the MOS proto-oncogene in human thyroid medullary carcinoma. *Cancer Lett* 1988; **43**: 185-189.
37. Gorgoulis VG, Zacharatos P, Mariatos G, Liloglou T, Kokotas S, Kastrinakis N *et al.* Deregulated expression of c-mos in non-small cell lung carcinomas: relationship with p53 status, genomic instability, and tumor kinetics. *Cancer Res* 2001; **61**: 538-549.
38. Lee JT, Jr., McCubrey JA. The Raf/MEK/ERK signal transduction cascade as a target for chemotherapeutic intervention in leukemia. *Leukemia* 2002; **16**: 486-507.
39. Grzanka A, Zuryn A, Styczynski J, Grzanka AA, Wisniewska H. The effect of doxorubicin on the expression of cyclin A in K-562 leukemia cell line. *Neoplasma* 2005; **52**: 489-493.

Chapter 2. In vivo activity of ABT-869, a multi-target kinase inhibitor, against acute myeloid leukemia with wild-type FLT3 receptor

2.1. Introduction

Neoangiogenesis plays an important role in tumorigenesis, as well as leukemogenesis.[1] Vascular endothelial growth factor (VEGF)-A is a major angiogenesis regulator, promoting hematopoietic stem cell (HSC) survival and repopulation by an internal autocrine loop manner.[2] It binds and activates two receptor tyrosine kinases, VEGFR1 (FLT1) and VEGFR2 (KDR, FLK1). The binding affinity of VEGFR1 is about 4 to 6 times higher that of VEGFR2,[3,4] but this receptor has only weak tyrosine kinase activity.[5] The expression of VEGF and its receptors are detected in a variety of hematological malignancies, including acute lymphoblastic leukemia,[6] acute myeloid leukemia,[7,8] myelodysplastic syndromes (MDS),[9] chronic leukemias,[10,11] lymphoma[12,13] and multiple myeloma (MM).[12,14] In AML, a number of studies have suggested a possible autocrine/paracrine pathway between VEGF and its receptors, which contributes to poor survival of a subset of leukemias and to progression of the disease.[7,15-18] It has been documented that this binding subsequently activates multiple pathways, including PI3K/AKT,[16,17] MAPK,[17] NFκB.[17] The expression of VEGFR1 is found to be more common in hematological malignancies than VEGFR2.[14,19] Furthermore, based upon data from a mouse xenograft model, VEGFR1 is responsible for the homing and survival of ALL cells in bone marrow and for the onset of extramedullary disease. [19] It also has been demonstrated that VEGFR1+ hematopoietic stem cells (HSCs), but not VEGFR2+, are responsible for differentiation, mobilization and reconstitution of hematopoiesis.[20] Recently, a novel concept of “premetastatic niche” was proposed based upon the observation that VEGFR1+ bone marrow HPC is an initiator of a cluster of cells in

the tissue at common sites of metastasis before the metastatic tumor cell arrives.[21] So VEGFR1 could possess broader function in normal hematopoiesis and leukemogenesis than VEGFR2.

Targeting VEGF/VEGFR receptors appears to be an alternative approach for treating AML. Several small molecular inhibitors are under clinical development. SU11248, a multi-target inhibitor against FLT3, c-kit, PDGFR and VEGFR1 and 2, is reported to induce clinical response with short duration in AML patients with FLT3 mutant or wild type in two phase I studies.[22,23] PTK787/ZK 222584, targeting VEGFR1/2/3, the platelet-derived growth factor receptor (PDGFR) and c-kit, induces complete remission in about 30% of patients with AML when combined with chemotherapy.[24] The early clinical trial data, although preliminary, demonstrates that disrupting VEGF/VEGFRs signaling pathways is potential clinically efficacious.

ABT-869, a novel ATP-competitive tyrosine kinase inhibitor (TKI), is active against vascular endothelial growth factor VEGFRs, as well as PDGFR family members (FLT3, c-kit, CSF-1R) and others, but less active against unrelated RTKs.[25,26] Cellular assays and tumor xenograft models demonstrated that ABT-869 was effective in a broad range of cancers including small cell lung carcinoma, colon carcinoma, breast carcinoma, and MV4-11 tumors *in vitro* and *in vivo*. [25,26] We have reported that ABT-869 induced significant apoptosis in cells with FLT3 mutation *in vitro* (IC_{50} value of 4nM) and profound antileukemic effect in a mouse xenograft model.[27] However, *in vitro* ABT-869 only shows minimal cytotoxic effect on AML cells with wild type FLT3. [27] Based on the preclinical studies suggesting the role of VEGF pathways in leukemogenesis, it is likely that the antileukemic effect of ABT-869 will

be best evaluated *in vivo*. In this report, we specifically test the *in vivo* therapeutic benefit of ABT-869 in a wild type FLT3 and VEGFR1+ AML cell line, HL60.

2.2. Materials and methods

2.2.1. Cell culture and establishment of a fluorescent protein labeled leukemia cell line

HL60, a wild type FLT3 AML cell line, was cultured in 90% RPMI1640 (Invitrogen, Carlsbad, CA) with 10% of fetal bovine serum (FBS, JRH Bioscience Inc, Lenexa, KS). Cells were maintained in density of 2 x 10^5 to 10x10^5 cells/ml in a humid incubator with 5% CO_2 at 37ºC. HL60 cells were transfected with pDsRed2-C1 vector (Clontech, Mountain View, CA) using Nucelofector device (Amaxa AG, Germany) according to the manufacturer's protocol. Briefly, 5 x 10^6 cells were mixed with 5 µg of pDsRed2-C1 vector and 100 µl of Solution-V, transferred to a cuvette. The program T-019 was used to transfect the cells in the Nucelofector device. After transfection, cells were immediately transferred into a 6-well plate containing prewarmed (37ºC) complete medium. After 24 hours post-transfection, the cells were spun into pellets and resuspended in new medium containing 1 µg/ml G418 (Invitrogen) for positive clone selection. The positive cells were monitored with Nikon fluorescent microscope. The antibiotic selection lasted for 3 weeks and was followed by the serial dilution method over a one month period to establish a long term stable clone with red fluorescence protein (RFP), designated as HL60-RFP.

2.2.2. Drug preparation

ABT-869 was prepared weekly prior to *in vivo* study as details in method in part I.[28]

2.2.3. Xenograft leukemia models

2.2.3.1. Subcutaneous model: Female Balc/c nude mice were purchased from Animal Resources Centre (ARC, Canning Vale, Australia). Exponentially growing HL60-RFP cells (5×10^6) with >95% viability were washed in 1 x PBS twice and subcutaneously injected into loose skin between the shoulder blades and left front leg of recipient mice from both control and ABT-869 treated groups. The treatment was initiated 15 days after tumor cell implantation, when the mice had palpable tumor of 100-200 mm^3 average size. ABT-869 was administrated at 15 mg/kg/day by oral gavage daily for consecutive 21 days for the study group. Mice in control group were given oral gavage with the diluents of the study drug as vehicle control. The measurements of tumors were taken by conventional callipers method, as well as monitored by using OV100 imaging system every other day. There were 10 mice for each group.

2.2.3.2. Bone marrow transplantation model: Female non-obese diabetic-severe combined immunodeficiency (NOD/SCID) mice (4-6 weeks old) were purchased from ARC. As a standard procedure to improve the engraftment efficiency, mice were given Endoxan® (Cyclophosphamide, Baxter Oncology GmbH, Germany) 150 mg/kg/day for two day followed by one rest day before leukaemia cells were injected. Ten million of HL60-RFP cells were washed in 1 x PBS twice and inoculated into mice via tail vein injection for both control and treatment groups. ABT-869 was administrated at 15 mg/kg/day by oral gavage daily for consecutive 22 days. There were 10 mice for each group. Three mice of each group were sacrificed for sampling

blood for FACS analysis after 1 week of treatment. The remaining 7 mice of each group were used for long term survival analysis.

Mice were closely monitored for weight, loose fur, hatch back, paralysis of hind legs and tumor size was measured serially. For tumor size measurements, the length (L) and width (W) of the tumor were measured with callipers, and tumor volume (TV) was calculated as $TV = (L \times W^2)/2$. The mice were sacrificed at the onset of weakness or paralysis of back limbs, fur erection, incapacitating macroscopic tumors, sluggish behaviour or curved disfiguration of the spine. The protocol was reviewed and approved by Institutional Animal Care and Use Committee in compliance to the guidelines on the care and use of animals for scientific purpose. For statistical comparisons *P* value was calculated using a 2-tailed t test.

2.2.4. Visualization of treatment efficacy in living mice

The Olympus Small Animal Imaging System OV100 (Olympus Corp., Tokyo, Japan) was used to monitor tumor development and treatment efficacy in living mice.[29] The imaging was captured with a CCD camera and directly processed with Cell software (Olympus Biosystems, Tokyo, Japan).

2.2.5. Cell staining, antibodies, and flow cytometry

For flow cytometry, cells extracted from mouse bone marrow (BM) were washed in 1 x PBS with 1% bovine serum albumin (BSA), filtered through 0.45 µm BD Cell Strainer (BD Biosciences, San Jose, CA) and blocked with 2% human AB serum for 10 minutes on ice, and stained with monoclonal antibodies in PBS + 1% BSA for 20 minutes on ice. Antibodies used were anti-human CD45-FITC and isoptype control IgG2a-FITC (BD Biosciences). Red blood cells were lysed with BD lysis buffer. Flow

cytometric analysis was performed on a FACS Calibur instrument (BD Biosciences) and analyzed with CellQuest software (BD Biosciences). For each experiment, a total of 10,000 events were analyzed.

2.2.6. Immunohistochemistry (IHC)

Tissue preparation and antigen retrieveal was performed as decrscribed in Part I, Section 1.2.9. Slides were then incubated with a panel of primary antibodies. The sources and conditions of the primary antibodies were as following: VEGFR1 (1:50, Chemicon, Temecula, CA) p-VEGFR1 (Tyr1213, 1:50, Calbiochem, San Diego, CA), Ki-67 (1:50, Neomarkers, Fremont, CA), VEGF (1:100, Lab Vision, Fremont, CA). The slides were counterstained in hematoxylin for 30 seconds and mounted with cover slides. For microvessel density (MVD) analysis, paraffin embedded tumor sections were stained with von Willibrand factor (vWF) endothelial cell marker (1:100, Chemicon) Measurement of microvessel density was performed as previously described [30]. Briefly, tissue sections were screened under the microscope, randomly selected six hotspots of microvessel dense fields were evaluated under high power field (hpf, x200). Mean microvessels count in six fields was taken as microvessel density which was expressed as microvessels / hpf. The images were analyzed by a Nikon fluorescence microscopy TE2000-S (Nikon Corp., Japan)

2.2.7. TUNEL assay

DeadEnd™ FLuorometric TUNEL System (Promega, Madison, WI) was used to detect apoptosis in tissue samples based on the manufacturer's protocol. Briefly, pretreated paraffin-embedded tissues were fixed with 4% PFA for 15 minutes, washed in 1xPBS twice. The tissues then permeabilized with 20 µg/ml Proteinase K solution, repeated fixative and wash steps. After equilibration, nucleotide mix and rTdT enzyme were added and DAPI nuclear staining dye was applied as counterstaining. The slides were mounted with cover slides. Green fluorescence of apoptotic cells (fluorescein-12-dUTP) in a blue background was detected by a Nikon fluorescence microscopy TE2000-S.

2.2.8. Statistical analysis

Tumor volume reduction of the treatment groups was compared to the untreated control group by Student's *t*-test, and *P* values of < 0.05 were considered to be significant. Survival analysis was performed by Kaplan-Meier analysis (SPSS, ver.14.0). Survival curves of the treatment groups were compared to the untreated control group, and statistical significance were given in log-rank test ($P < 0.05$).

2.3. Results

2.3.1. Establishment of stable HL60-RFP cell line

The pDsRed2-C1 transfected HL60 cells were serially diluted and seeded in 96-well plates with 1 µg/ml G418. The selected HL60-RFP cells have a stable, noticeably bright FRP fluorescence after numerous passages without the selective antibiotics (Figure 2.1). The excitation/emission wave length of DsRed2 is 558 nm/583 nm. To compare the characteristic of the transfected clone with the parental line, HL60-RFP and HL-60 were then subjected to in vitro cytotoxic (MTS) assay[31] and xenograft

model study. There was no significant difference between the IC_{50} values for doxorubicin (360 vs. 357 nM) and cytosine arabinoside (560 vs. 557 nM). Furthermore, in the xenograft model, there is no significant difference in tumor growth rate and capacity of bone marrow engraftment between these two cell lines. These tests suggest that HL60-RFP is characteristically representing its parental line.

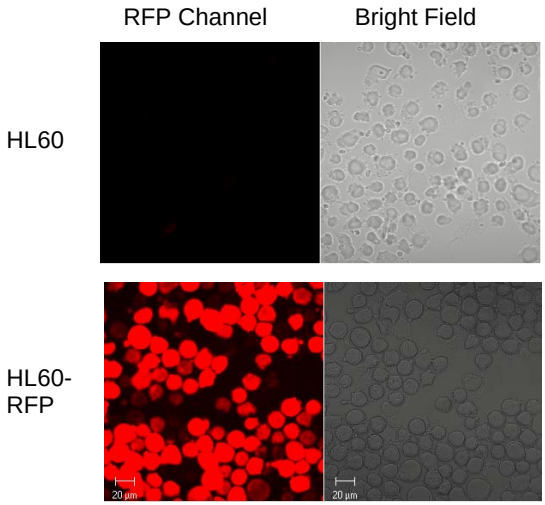

Figure 2.1. Stable human leukemia HL60 clone with high expression of RFP *in vitro*. Stable HL60-RFP cells and the parental HL60 cells were spun down onto a glass slid using a Shandon Cytospin4 (Thermo Scientific, Inc., Waltham, MA) at 1,000 rpm for 5 minutes, then fixed with 4% paraformaldehyde (PFA). Pictures were taken with Olympus FV300 confocal microscopy (Olympus Corp.). Bar = 20 µm.

2.3.2. ABT-869 inhibited the HL60-RFP xenograft tumor progression

Tumors in mice treated with vehicle control continued to grow to an average of 4231.2 ± 430 mm^3 at day 38 (Figure 2.2A).In contrast to *in vitro* findings, *in vivo* ABT-869 therapy significantly reduced the progression of tumor to 829.5 ± 210 mm^3 ($p<0.001$ compared to the control group).

Using OV100 imaging system, tumor volume was constructed from the primary tumor imaging in two dimensions (mm^2) as shown in Figure 2.2B. The average

tumor volume was 435 ± 39 mm^2 in the control group and 195.7 ± 27 mm^2 in the ABT-869 treated group. The two sets of measurement obtained by calipers and OV100 imaging system showed a good correlation coefficient between these two measurements (R=0.97). Subsequent consecutive whole body imaging of HL60-RFP tumors in living mice were taken and the tumor growth and progression were quantified with imaging analysis. Figure 2.3A and 2.3B shows the consecutive images acquired from one mouse in each group at different time points.

Under high magnification (x0.8), we observed that ABT-869 treated mice showed paleness of tumor surface as compared to control group after 2 weeks' treatment, suggesting reduced vascular structure. The retardation of tumor progression is accompanied with a decrease in neoangiogenesis, which was visually apparent. To validate this observation by OV100 imaging system, IHC analysis of intratumor MVD was performed, which is widely used method for quantification of angiogenesis and neovascularization. As shown in Figure 2.3C, the "hotspots" MVD was significantly lower in ABT-869 treated tumor than in vehicle tumor (mean MVD 31.2 ± 9 vs 114.7 ± 12, $p < 0.001$).

A

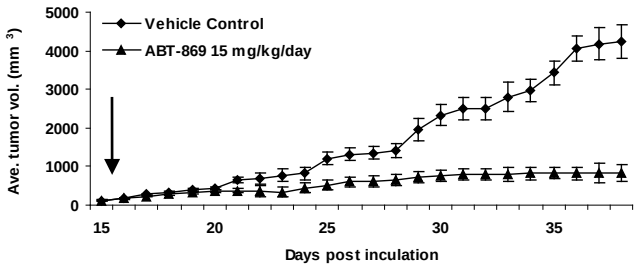

B

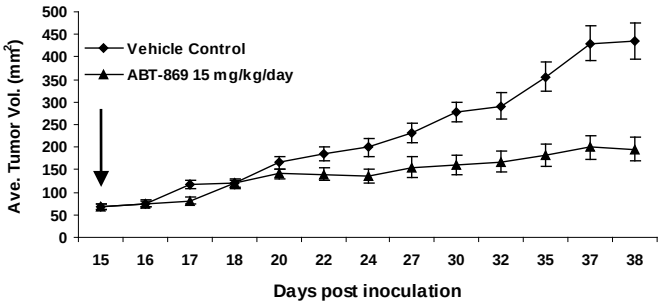

Figure 2.2. The effects of ABT-869 on HL60-RFP tumor growth *in vivo*. (A) Tumor volume curves were constructed with measurements taken by conventional calliper. (B) Tumor volume curves were plotted with measurements taken by OV100 Small Animal Imaging System determined by the fluorescent direct-view images. Arrows indicate treatment start.

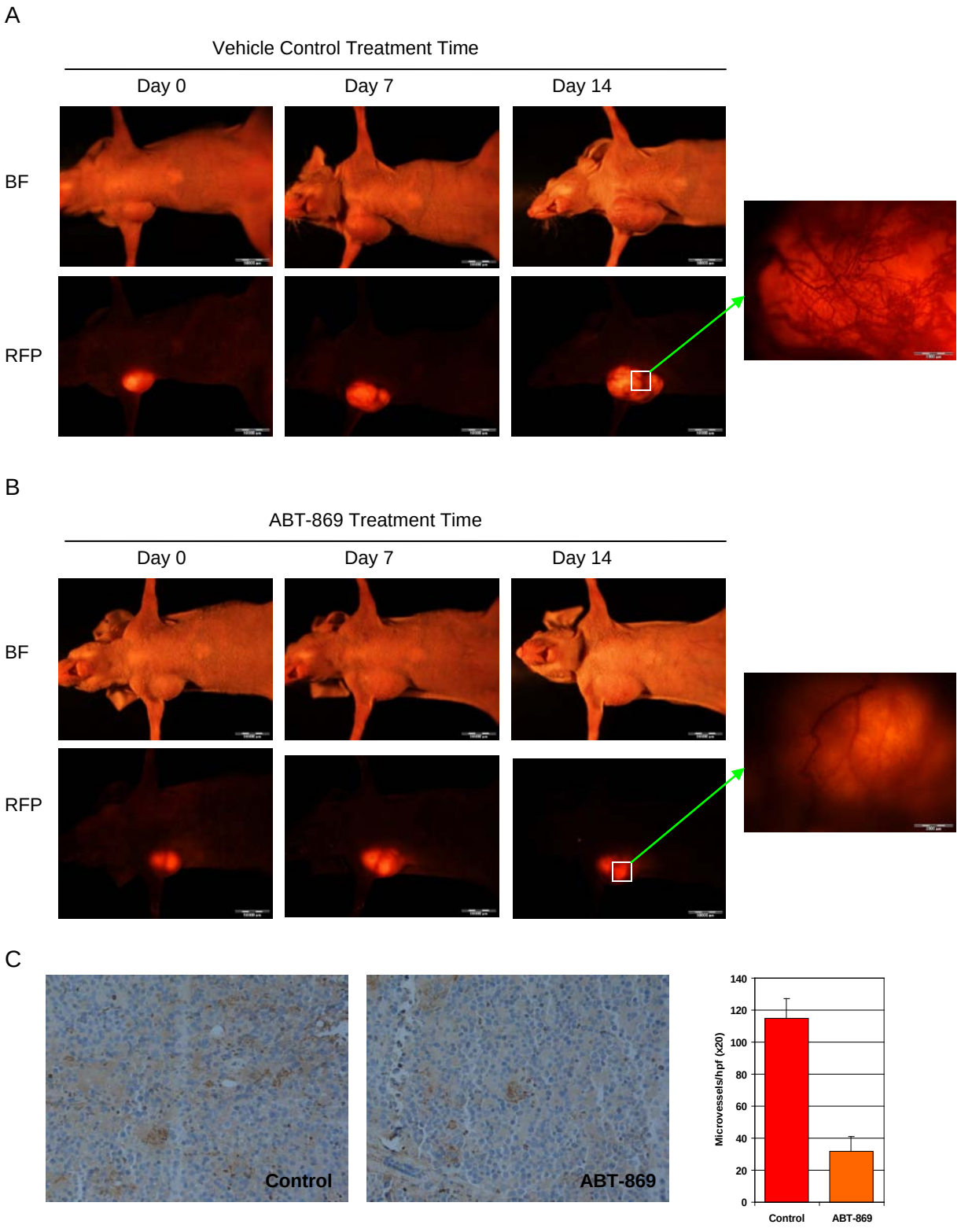

Figure 2.3. Sequential real-time whole-body fluorescence imaging of HL60-RFP tumor growth in living mice. (A) Mice were treated with vehicle control. (B) Mice treated with ABT-869 (15 mg/kg/day). Arrow-pointed pictures show the direct view of distribution of blood vessel network on the tumor surface in the two representative

mice. There is less of a tumor vessel network in ABT-869 treated mice. BF: bright field channel. RFP: RFP channel. (C) Staining of microvessels (hotspots, brownish staining) in vehicle control and ABT-869 treated tumor samples by anti-vWF immunostaining (original magnification x200). The right bar figure represents mean MVD of six hotspots in vehicle control and ABT-869 treated tumor samples.

2.3.3. ABT-869 prolonged survival in the HL60-RFP murine bone marrow transplantation model

The effect of ABT-869 was further evaluated in a systemic leukemia model. Treatment was started 3 weeks after tail vein injection of HL60 cells. FACS analysis of mouse bone marrow samples demonstrated that human CD45 positive cells were significantly reduced in the ABT-869 treated group (Figure 2.4A-B). The results showed that the average numbers of CD45 positive cells were 55 ± 23% and 13 ± 6% respectively ($p=0.03$). ABT-869 treatment also prolonged the survival of mice with HL60 tumors. Kaplan-Meier analysis revealed that the survival time was significantly prolonged in the ABT-869-treated group when compared to the control group (Median survival, 39 vs. 29 days; $p<0.001$, Figure2. 4).

A

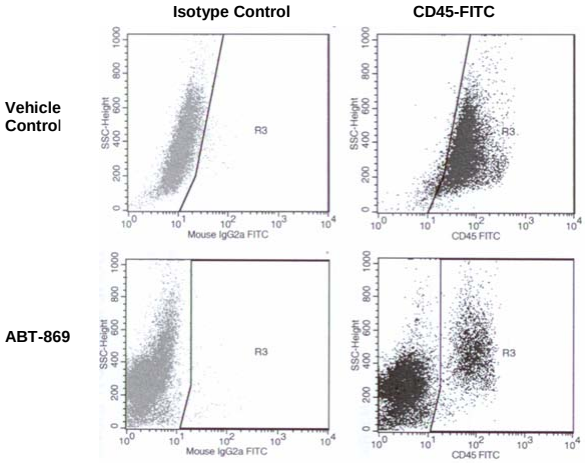

B

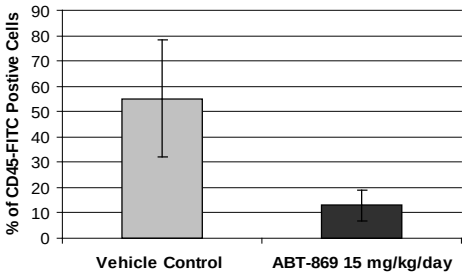

C

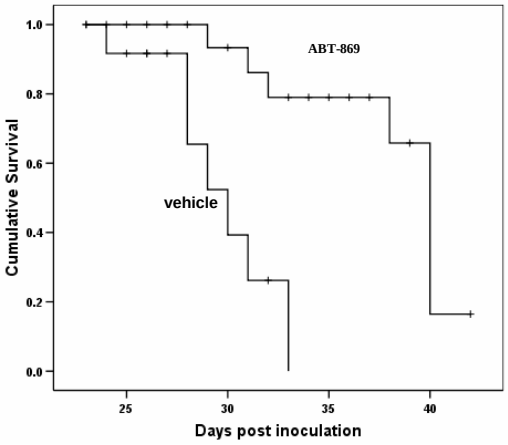

Figure 2.4. The effects of ABT-869 on NOD/SCID mice with systemic leukemia. See "Materials and Methods" for intravenous cell injection and treatment details. (A) Representative FACS profiles from vehicle control and ABT-869 treated mice. (B) Bar graph of average percentage of human CD45 positive cells in bone marrows from 3 vehicle controls and ABT-869 treated mice at 1 week's time point. (C) Seven mice in each group were used for the construction of the survival curves.

2.3.4. *In vivo* biological efficacy of ABT-869

To further study the observed different sizes of tumors between treated and control groups, we performed histological examination of tumor specimens. Figure 2.5A shows treated samples to be less cellular, compared to samples from mice treated with vehicle only. A 15 mg/kg/day dose of ABT-869 effectively inhibited the expression of p-VEGFR1 (Figure 2.5C) and Ki-67 (Figure 2.5D), a common proliferative marker. The level of VEGFR1 was not varied significantly between control and treated samples (Figure 2.5B). The Ki-67 labeling index, calculated as the percentage of positive staining cells of total nucleated cells in a x400 field (average of 5 x400 fields) was 95 ± 1.8 vs 58 ± 1.7 ($p < 0.001$) for vehicle control and ABT-869 treated samples respectively. In addition, the expression of VEGF was significantly reduced in the treated specimens (Figure 2.5E). Furthermore, tunnel assay revealed induction of cellular apoptosis in the treated tumor samples (Figure 2.6). Together, these data support that the *in vivo* biological effect of ABT-869 is associated with the inhibition of neoangiogenesis.

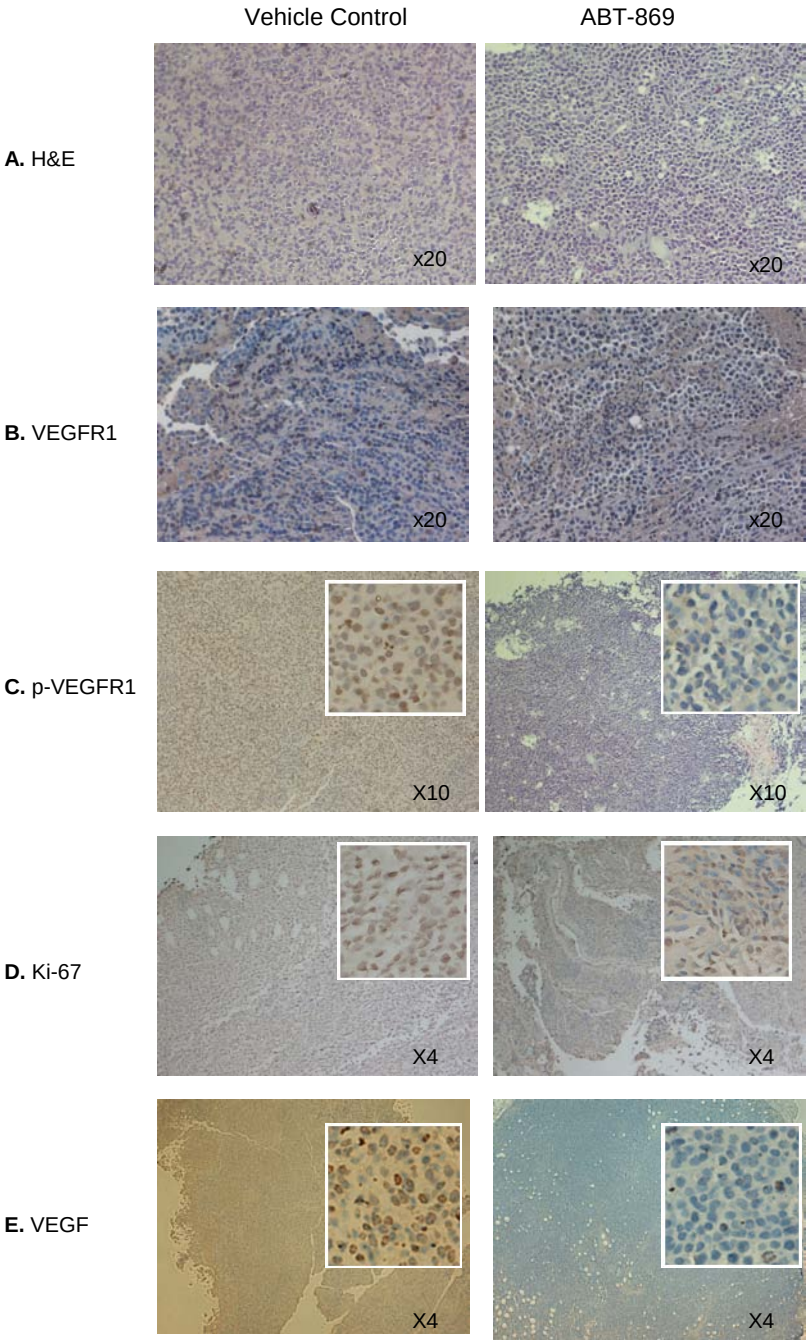

Figure 2.5. *In vivo* effect of ABT-869 on HL60-RFP tumor xenograft model. Nude mice with established HL60-RFP xenograft were maintained with vehicle or ABT-869. Excised tumor pieces were embedded in paraffin and stained with either (A) H & E or immunostained with (B) VEGFR1, (C) p-VEGFR1, (D) Ki-67, or (E) VEGF. The original magnification of all inserted pictures is 400x.

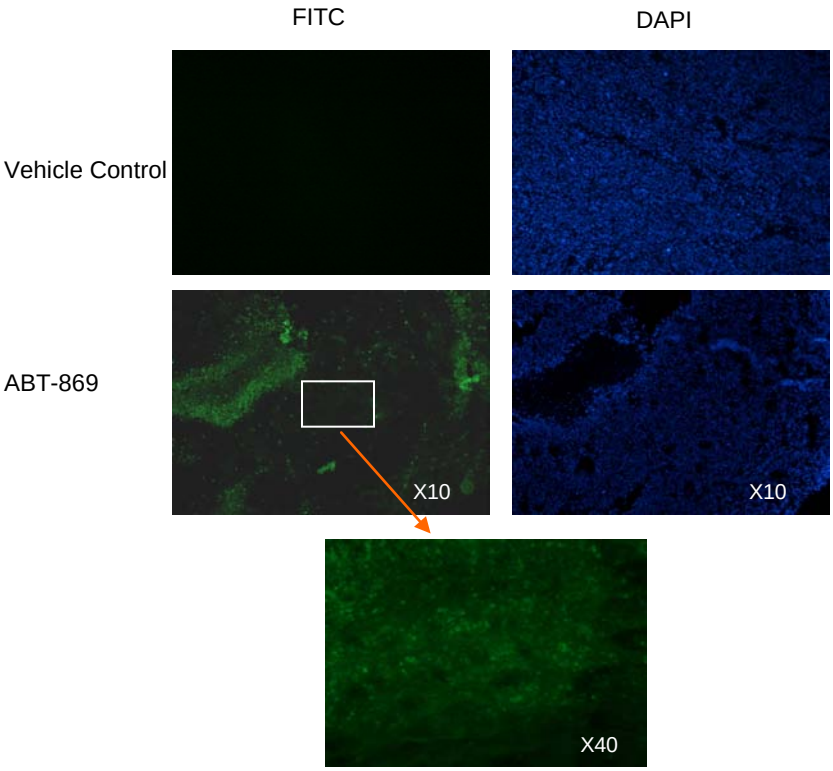

Figure 2.6. ABT-869 treatment induced apoptosis in the *in vivo* tumor samples. Apoptosis was measured by TUNEL assay and analyzed by a Nikon fluorescence microscopy TE2000-S. Apoptotic cells were catalytically incorporated with fluorescein-12-dUTP and DAPI dye was used as nuclear counterstaining. Green staining represents apoptotic cells.

2.4. Discussion

AML, a rapid porgressive disease, remains an arduous task for oncologists. A large body of evidences indicates bone marrow neoangiogenesis, orchestrated by different angiogenic growth factors, implicates the pathogeneisis of AML. VEGF and its receptors are major regulators in neogangiogenesis in AML.[1,14,32,33] In this report, we demonstrate that ABT-869 is effective *in vivo* against HL60-RFP in subcutaneous implant and bone marrow transplantation xenograft models. The molecular mechanism of the antileukemic effect of ABT-869 may involve the blockage of the

VEGF/VEGFR1 activation loop, and the induction of apoptosis resulting in inhibition of neoangiogenesis in leukemia.

The imbalance of pro-angiogenic molecules and anti-angiogenic molecules (angiogenic switch) is a classic model for tumor development and metastasis.[32,33] Angiogenesis inhibitors have been extensively investigating for the treatment of "angiogenesis-dependent" diseases, most demonstrated in solid tumors and more recently including hematological malignancies.[14,34] VEGF/VEGFR loops are the key modulators regulating physiological and pathological angiogenesis. So dysregulation of these signaling pathways therefore play a pivotal role in the leukemogenesis and therapeutic failure. A study of Fragoso *et al*. revealed VEGFR1 activation promotes leukemic cells migration to an extramedullary site by actin polymerization and lipid raft formation, and increases cell proliferation *in vitro* and in a murine model.[19] VEGFR1 is the most common and abundant VEGF receptor expressed in leukemia cell lines and primary patient samples including CML, ALL and AML.[19,35] The preferable expression pattern highlights the important role of VEGFR1/VEGF loop in the pathogenesis of leukemia. It is worthy of note that prior studies have shown VEGFR1[19] and VEGF production[36] play a crucial role in bone marrow homing and engraftment of leukemia cells in NOD/SCID mice. Since ABT-869 inhibits VEGFR1 and VEGF *in vivo*, this also could potentially contribute to its antileukemic effect, although the treatment was started 3 weeks after inoculation of leukemia cells, Taken together, as a consequence of blockage of this activation by ABT-869, the results obtained from our *in vivo* studies support the concept that the therapeutic potential of multi-target kinase inhibitors like ABT-869 is not limited to patients with FLT3 mutations, but potentially can be expanded to those with activation of a VEGFR/VEGF loop.

Besides the VEGFR1/VEGF pathway, intervening with the VEGFR2 and VEGFR3 receptors has also shown efficacy in AML. A report from Santos et al demonstrates the existence of internal (private) and external VEGF/VEGFR2 (KDR) in a subset of AML. Blocking both pathways simultaneously produces a synergistic effect by decreasing cell viability.[17] It has also been reported that interaction between VEGF/VEGFR3 (FLT4) induces leukemia cell proliferation, survival and resistance to chemotherapy by switching the Bcl-2/Bax ratio, whose balance precisely determines whether cells undergoing survival or apoptosis.[37] On the other hand, a VEGF antagonist soluble (NRP-1) has been shown to inhibit angiogenesis and growth in a localized murine model and prolongs survival rate in a systemic leukemia model as compared to mice treated with control vector.[37] Exposure of AML cells to VEGF induces cells resistant to chemotherapy by upregulation of Mcl-1, an anti-apoptotic protein.[38] Furthermore, we can not exclude the possibility of additional targets such as PDGFR family by ABT-869, contributing to its biological activity, as observed in BIBF1120, a indolinone derivative multi-targeted compound.[39]

In addition to conventional measurement with caliper, our study employed a real-time whole-body imaging technology[40,41] to monitor RFP labeled tumor growth, as well as neoangiogenesis consecutively in the living mouse. Measurements obtained by caliper are subjective and may be affected by the operator, which causes increased variances. In contrast, the significant advantage of using live imaging system is to obtain quantitative measurements objectively. It offers a valuable opportunity to directly visualize the neoangiogenesis on the tumor surface and observe the drug response measured by inhibition of tumor growth and reducing of blood vessel network continuously without sacrifice mice, as exemplified in this study. The

approach described here may be useful to test the activities of novel anti-cancer compound, as well as chemotherapy drugs.

Collectively, using both implanted tumor model and systemic leukemia model, we have demonstrated that ABT-869 inhibits tumor growth and prolongs survival of mice bearing HL60 cells. Our results suggest ABT-869 might represent a promising novel agent to the current therapy approaches or combination with conventional cytotoxic drugs for the treatment of wild type FLT3-AML.

2.5. References:

1. Zhou J, Mauerer K, Farina L, Gribben JG. The role of the tumor microenvironment in hematological malignancies and implication for therapy. Front Biosci 2005;10:1581-96.
2. Gerber HP, Malik AK, Solar GP, Sherman D, Liang XH, Meng G, et al. VEGF regulates haematopoietic stem cell survival by an internal autocrine loop mechanism. Nature 2002;417:954-8.
3. Millauer B, Wizigmann-Voos S, Schnurch H, Martinez R, Moller NP, Risau W, et al. High affinity VEGF binding and developmental expression suggest Flk-1 as a major regulator of vasculogenesis and angiogenesis. Cell 1993;72:835-46.
4. Terman BI, Dougher-Vermazen M, Carrion ME, Dimitrov D, Armellino DC, Gospodarowicz D, et al. Identification of the KDR tyrosine kinase as a receptor for vascular endothelial cell growth factor. Biochem Biophys Res Commun 1992;187:1579-86.
5. Waltenberger J, Claesson-Welsh L, Siegbahn A, Shibuya M, Heldin CH. Different signal transduction properties of KDR and Flt1, two receptors for vascular endothelial growth factor. J Biol Chem 1994;269:26988-95.
6. Koomagi R, Zintl F, Sauerbrey A, Volm M. Vascular endothelial growth factor in newly diagnosed and recurrent childhood acute lymphoblastic leukemia as measured by real-time quantitative polymerase chain reaction. Clin Cancer Res 2001;7:3381-4.
7. Fiedler W, Graeven U, Ergun S, Verago S, Kilic N, Stockschlader M, et al. Vascular endothelial growth factor, a possible paracrine growth factor in human acute myeloid leukemia. Blood 1997;89:1870-5.
8. Hussong JW, Rodgers GM, Shami PJ. Evidence of increased angiogenesis in patients with acute myeloid leukemia. Blood 2000;95:309-13.
9. Bellamy WT, Richter L, Sirjani D, Roxas C, Glinsmann-Gibson B, Frutiger Y, et al. Vascular endothelial cell growth factor is an autocrine promoter of abnormal localized immature myeloid precursors and leukemia progenitor formation in myelodysplastic syndromes. Blood 2001;97:1427-34.
10. Aguayo A, Manshouri T, O'Brien S, Keating M, Beran M, Koller C, et al. Clinical relevance of Flt1 and Tie1 angiogenesis receptors expression in B-cell chronic lymphocytic leukemia (CLL). Leuk Res 2001;25:279-85.

11. Verstovsek S, Lunin S, Kantarjian H, Manshouri T, Faderl S, Cortes J, et al. Clinical relevance of VEGF receptors 1 and 2 in patients with chronic myelogenous leukemia. Leuk Res 2003;27:661-9.
12. Bellamy WT, Richter L, Frutiger Y, Grogan TM. Expression of vascular endothelial growth factor and its receptors in hematopoietic malignancies. Cancer Res 1999;59:728-33.
13. Nagy JA, Vasile E, Feng D, Sundberg C, Brown LF, Detmar MJ, et al. Vascular permeability factor/vascular endothelial growth factor induces lymphangiogenesis as well as angiogenesis. J Exp Med 2002;196:1497-506.
14. Podar K, Anderson KC. The pathophysiologic role of VEGF in hematologic malignancies: therapeutic implications. Blood 2005;105:1383-95.
15. Dias S, Hattori K, Zhu Z, Heissig B, Choy M, Lane W, et al. Autocrine stimulation of VEGFR-2 activates human leukemic cell growth and migration. J Clin Invest 2000;106:511-21.
16. List AF, Glinsmann-Gibson B, Stadheim C, Meuillet EJ, Bellamy W, Powis G. Vascular endothelial growth factor receptor-1 and receptor-2 initiate a phosphatidylinositide 3-kinase-dependent clonogenic response in acute myeloid leukemia cells. Exp Hematol 2004;32:526-35.
17. Santos SC, Dias S. Internal and external autocrine VEGF/KDR loops regulate survival of subsets of acute leukemia through distinct signaling pathways. Blood 2004;103:3883-9.
18. Schuch G, Machluf M, Bartsch G, Jr., Nomi M, Richard H, Atala A, et al. In vivo administration of vascular endothelial growth factor (VEGF) and its antagonist, soluble neuropilin-1, predicts a role of VEGF in the progression of acute myeloid leukemia in vivo. Blood 2002;100:4622-8.
19. Fragoso R, Pereira T, Wu Y, Zhu Z, Cabecadas J, Dias S. VEGFR-1 (FLT-1) activation modulates acute lymphoblastic leukemia localization and survival within the bone marrow, determining the onset of extramedullary disease. Blood 2006;107:1608-16.
20. Hattori K, Heissig B, Wu Y, Dias S, Tejada R, Ferris B, et al. Placental growth factor reconstitutes hematopoiesis by recruiting VEGFR1(+) stem cells from bone-marrow microenvironment. Nat Med 2002;8:841-9.
21. Kaplan RN, Riba RD, Zacharoulis S, Bramley AH, Vincent L, Costa C, et al. VEGFR1-positive haematopoietic bone marrow progenitors initiate the pre-metastatic niche. Nature 2005;438:820-7.
22. Fiedler W, Serve H, Dohner H, Schwittay M, Ottmann OG, O'Farrell AM, et al. A phase 1 study of SU11248 in the treatment of patients with refractory or resistant acute myeloid leukemia (AML) or not amenable to conventional therapy for the disease. Blood 2005;105:986-93.
23. O'Farrell AM, Foran JM, Fiedler W, Serve H, Paquette RL, Cooper MA, et al. An innovative phase I clinical study demonstrates inhibition of FLT3 phosphorylation by SU11248 in acute myeloid leukemia patients. Clin Cancer Res 2003;9:5465-76.
24. Roboz GJ, Giles FJ, List AF, Cortes JE, Carlin R, Kowalski M, et al. Phase 1 study of PTK787/ZK 222584, a small molecule tyrosine kinase receptor inhibitor, for the treatment of acute myeloid leukemia and myelodysplastic syndrome. Leukemia 2006;20:952-7.
25. Albert DH, Tapang P, Magoc TJ, Pease LJ, Reuter DR, Wei RQ, et al. Preclinical activity of ABT-869, a multitargeted receptor tyrosine kinase inhibitor. Mol Cancer Ther 2006;5:995-1006.
26. Guo J, Marcotte PA, McCall JO, Dai Y, Pease LJ, Michaelides MR, et al. Inhibition of phosphorylation of the colony-stimulating factor-1 receptor (c-Fms)

tyrosine kinase in transfected cells by ABT-869 and other tyrosine kinase inhibitors. Mol Cancer Ther 2006;5:1007-13.
27. Shankar DB, Li J, Tapang P, Owen McCall J, Pease LJ, Dai Y, et al. ABT-869, a multitargeted receptor tyrosine kinase inhibitor: inhibition of FLT3 phosphorylation and signaling in acute myeloid leukemia. Blood 2007;109:3400-8.
28. Zhou J, Pan M, Xie Z, Loh SL, Bi C, Tai YC, et al. Synergistic antileukemic effects between ABT-869 and chemotherapy involve downregulation of cell cycle-regulated genes and c-Mos-mediated MAPK pathway. Leukemia 2007 Oct 18; [Epub ahead of print].
29. Yamauchi K, Yang M, Jiang P, Xu M, Yamamoto N, Tsuchiya H, et al. Development of real-time subcellular dynamic multicolor imaging of cancer-cell trafficking in live mice with a variable-magnification whole-mouse imaging system. Cancer Res 2006;66:4208-14.
30. Poon RT, Ng IO, Lau C, Yu WC, Yang ZF, Fan ST, et al. Tumor microvessel density as a predictor of recurrence after resection of hepatocellular carcinoma: a prospective study. J Clin Oncol 2002;20:1775-85.
31. Shen J, Tai YC, Zhou J, Stephen Wong CH, Cheang PT, Fred Wong WS, et al. Synergistic antileukemia effect of genistein and chemotherapy in mouse xenograft model and potential mechanism through MAPK signaling. Exp Hematol 2007;35:75-83.
32. Bergers G, Benjamin LE. Tumorigenesis and the angiogenic switch. Nat Rev Cancer 2003;3:401-10.
33. Ferrara N, Gerber HP, LeCouter J. The biology of VEGF and its receptors. Nat Med 2003;9:669-76.
34. Folkman J. Angiogenesis: an organizing principle for drug discovery? Nat Rev Drug Discov 2007;6:273-86.
35. Gerber HP, Ferrara N. The role of VEGF in normal and neoplastic hematopoiesis. J Mol Med 2003;81:20-31.
36. Fusetti L, Pruneri G, Gobbi A, Rabascio C, Carboni N, Peccatori F, et al. Human myeloid and lymphoid malignancies in the non-obese diabetic/severe combined immunodeficiency mouse model: frequency of apoptotic cells in solid tumors and efficiency and speed of engraftment correlate with vascular endothelial growth factor production. Cancer Res 2000;60:2527-34.
37. Dias S, Choy M, Alitalo K, Rafii S. Vascular endothelial growth factor (VEGF)-C signaling through FLT-4 (VEGFR-3) mediates leukemic cell proliferation, survival, and resistance to chemotherapy. Blood 2002;99:2179-84.
38. Katoh O, Takahashi T, Oguri T, Kuramoto K, Mihara K, Kobayashi M, et al. Vascular endothelial growth factor inhibits apoptotic death in hematopoietic cells after exposure to chemotherapeutic drugs by inducing MCL1 acting as an antiapoptotic factor. Cancer Res 1998;58:5565-9.
39. Kulimova E, Oelmann E, Bisping G, Kienast J, Mesters RM, Schwable J, et al. Growth inhibition and induction of apoptosis in acute myeloid leukemia cells by new indolinone derivatives targeting fibroblast growth factor, platelet-derived growth factor, and vascular endothelial growth factor receptors. Mol Cancer Ther 2006;5:3105-12.
40. Hoffman RM. The multiple uses of fluorescent proteins to visualize cancer in vivo. Nat Rev Cancer 2005;5:796-806.
41. Yang M, Baranov E, Wang JW, Jiang P, Wang X, Sun FX, et al. Direct external imaging of nascent cancer, tumor progression, angiogenesis, and metastasis on internal organs in the fluorescent orthotopic model. Proc Natl Acad Sci U S A 2002;99:3824-9.

Chapter 3. Enhanced activation of STAT pathways and overexpression of survivin confer resistance to FLT3 inhibitors and could be therapeutic targets in AML

3.1. Introduction

Internal tandem duplication (ITD) in juxtamembrane (JM) and point mutation PM in the kinase domain (KD) of fms-like tyrosine kinase 3 (FLT3) are common genetic lesions in acute myeloid leukemia (AML).[1-5] Recently, additional point mutations were identified in the extracellular domain and JM domain by high-throughput DNA sequencing.[6]

FLT3 mutations induce receptor dimerization and autophosphorylation of the KD, in turn, resulting in constitutive activation of phosphoinositide 3-kinase (PI3K-AKT), RAS-MEK-mitogen-activated protein kinase (MAPK), and signal transducers and activators of transcription (STAT) 5 pathways.[1-5] On the biological level, it leads to uncontrolled cell proliferation, blockage of differentiation and cell survival. Therefore, FLT3 mutations play an important role in leukemogenesis, and represent attractive therapeutic targets. [1,2,4,5] A number of small molecule tyrosine kinase inhibitors (TKIs) are currently undergoing different phases of clinical development.[7] Although most FLT3 inhibitors show potent efficacy *in vitro* with IC_{50} values in the nanomole range, the majority of patients only have moderate and transient responses.[8] Furthermore, under prolonged therapy with TKIs, leukemic cells could develop resistance to FLT3 inhibitors when used as monotherapy. This is exemplified by the resistance phenomenon to imatinib mesylate (Gleevec), the first small molecule kinase inhibitor for the treatment of chronic myeloid leukemia (CML) harboring the BCR-ABL fusion oncogene. The identification of point mutations in the ATP binding site or gene

amplification of BCR-ABL from imatinib-resistant CML patients[9] promoted researchers to investigate the role of acquired mutations in resistance to FLT3 inhibitors.

Mutations in the ATP-binding pocket have been identified through PCR-based mutagenesis screening in murine Ba/F3-FLT3-ITD cells and selected for growth in the presence of PKC412,[10] or in a resistant Ba/F3-FLT3-ITD cell line developed by coculture with SU5416.[11] Resistance to PKC412 resulting from the N676K point mutation in the FLT3 kinase domain has been described in a clinical trial patient.[12] Human leukemia cell lines are valuable disease models. Piloto O *et al*. used long-term exposure of human leukemia cell lines, including MOLM-14 (AML-M5, one allele wild-type and the other FLT3-ITD allele), Hb1119 (ALL, FLT3-D836H) and SEM-K2 (overexpression of wild-type FLT3), to FLT3 inhibitors, CEP-5214 and CEP-701, to generate 6 resistance human cell lines.[13] Selection of activating Ras mutations has been found in 2 out of 6 FLT3 inhibitor resistant cell lines, but no point mutation in the FLT3 kinase domain was found in all 6 resistant cell lines.[13]

To further investigate other potential mechanisms of resistance to multi-targeted TKIs, we developed three resistant cell lines (designated as MV4-11-R1, -R2, -R3) by long-term coculture of the human leukemia cell line, MV4-11 (AML, both allele FLT-ITD), with ABT-869, a multi-targeted TKI with activity against FLT3.[14] We also explored the combination of ABT-869 with other small molecule inhibitors to overcome resistance and thereby potentially provide novel treatments *in vitro* and *in vivo*.

3.2. Materials and Methods

3.2.1. Small molecular inhibitors and reagents

ABT-869, a multi-targeted TKI with activity against FLT3, was kindly provided by Abbott Laboratories (Chicago, IL). For *in vitro* and *in vivo* experiments, the preparation for ABT-869 was previously published.[15] Indirubin derivative (IDR) E804, Tyrene CR4, AG490, AG1296, JAK3 Inhibitor II, NU6140 and FLT3 inhibitor III were purchased form Calbiochem (Gibbstown, NJ) and dissolved in dimethyl sulfoxide (DMSO) before use. SU5416 and 5-aza-deoxycytidine (5-aza) were purchased from Sigma-Aldrich (St. Louis, MO). Human FLT3 ligand was obtained from Pepro Tech Inc. (Rocky Hill, NJ).

3.2.2. Cell lines and development of resistant cell lines

Human MV4-11 cells were cultured with RPMI1640 (Invitrogen) supplemented with10% of fetal bovine serum (FBS, JRH Bioscience Inc, Lenexa, KS) at density of 2 to 10 x 10^5 cells/ml in a humid incubator with 5% CO_2 at 37ºC. Log phase growing MV4-11 cells were cocultured with increasing concentration of ABT-869 for 3 months. Three parallel experiments were performed in parallel for selection of resistant lines. These resistant lines were grown in normal medium without ABT-869 for at least 48 hours before experiments.

3.2.3. Cell viability assays

Leukemic cells were seeded in 96-well culture plates at a density of 2 × 10^4 viable cells/100 µl/well in triplicates, and were treated with small molecular inhibitors. Colorimetric CellTiter 96 AQ_{ueous} One Solution Cell Proliferation Assay (MTS assay, Promega, Madison, WI) was used to determine the cytotoxicity as described

previously[15]. IC_{50} values were determined by MTS assay and calculated with CalcuSyn software (Biosoft, Cambridge, UK). Each experiment was in triplicate.

3.2.4. Flow cytometric analysis

For analysis of MRP1 and MDR expression, two million cells were fixed and stained according to the manufacture's instruction and analyzed with a Dako Cytomation Cyan LX (DakoCytomation Denmark A/S, Denmark) flow cytometer, using Summit (v4.3) software. For apoptosis assays, annexin V-FITC binding assay (BD Pharmingen, San Diego, CA) was used as recommended by the manufacturer. For cell cycle analysis, one million cells were fixed, stained with Propidium Iodide (PI, BD Pharmingen) and analysed by flow cytometry.

3.2.5. Western blot analysis

Preparation of the cell lysate and immunoblotting were performed as previously described.[16] Antibodies used were as follows: anti-FLT3, anti-p-FLT3, anti-p-STAT1 (Tyr701), anti-p-STAT3 (Tyr705, clone 3E2), anti-p-STAT5 (Tyr694), anti-STAT1, anti-STAT3, anti-STAT5, anti-Survivin, anti-poly (ADP-ribose) polymerase (PARP), anti-cleaved PARP, from Cell Signaling Technology (CST, Danvers, MA) and anti-Actin, anti-LRP, anti-MRP1, anti-MDR, IgG Isotype control from Santa Cruz Biotechnology (Santa Cruz, CA).

3.2.6. Low density Array (LDA)

Gene expression profiling was investigated with custom real-time PCR-based analysis using TaqMan Low Density Arrays (LDA; Applied Biosystems, Foster City, CA) as described in the Chapter 1.[15]

3.2.7. Reverse transcription (RT)-PCR and Real-time quantitative (RQ)-PCR

The primers and RT-PCR conditions for survivin analysis were adopted from Mahotka *et al*.[17] Sequences of primers for survivin RQ-PCR were described before.[18] The sequences of primers of STAT3 for RQ-PCR were as follows: STAT3-RQ forward: 5'-CCTGAAGCTGACCCAGGTAGC-3'; STAT3-RQ reverse: 5'- forward: 5'-CACCTTCACCATTATTTCCAAACTG-3'. Sequences of primers of SOCS1, SOCS2 and SOCS3 for RQ-PCR were published before.[19] Power SYBR® Green PCR Master Mix was used as recommendation by the manufacturer (Applied Biosystems). GAPDH was used as internal control. SDS 2.2.1 software (Applied Biosystems) was used to perform relative quantitation (RQ) of target genes using the comparative C_T ($\Delta\Delta C_T$) method.

3.2.8. Transfection

Human STAT3 cDNA was purchased from Open Biosystems (Huntsville, AL) and cloned into pEGFP vector (Clontech, Mountain View, CA). MV4-11 cells were transfected with pEGFP control vector, and pEGFP-STAT3 separately using Nucelofector device (Amaxa AG, Germany) according to the manufacturer's protocol. Briefly, 3 x 10^6 cells were mixed with 2 µg of vector and 100 µl of Solution-L, transferred to a cuvette. The program Q-001 was used to transfect the cells in the Nucelofector device. After transfection, cells were immediately transferred into a 6-well plate containing prewarmed (37ºC) complete medium. After 48 hours post-transfection, the cells were spun into pellets and followed by RNA extraction, cDNA synthesis and RQ-PCR analysis for gene expression.

Human full-length of survivin cDNA was obtained from Open Biosystems and cloned into lentivirus pLVX-puro vector (Clontech) within *Eco*RI/*Bam*HI site. The construct

was validated by sequencing. The production and harvest of high titer lentivirus was performed using Lenti-X™ HT Packaging System (Clontech) as recommended by the manufacturer. MV4-11 cells were infected with pLVX-puro-Survivin lentivirus particulars and selected in culture medium containing gradually incrementally increased concentration of puromycin ranging from 400 ng/ml to 2 μg/ml for three weeks. The stable transfectant cell line was designated as "MV4-11-Survivin..

3.2.9. Short-hairpin (shRNA) studies

A pool of survivin (RHS4529-NM_001168) shRNA, as well as non-silencing shRNA control (RHS1707) was purchased from Open Biosystems. RetroPack PT67 cells (Clontech) were seeded into a 6-well plate at 60-80% confluence (4×10^5 cells/well) 24 hours before transfection, 5 μg of each shRNA vector and 10 μl of Lipofectamine 2000 (Invitrogen) were used for transfection. PT67 cells were diluted and plated after transfection for 24 hours in culture medium with 2 μg/ml puromycin (Clontech). After 1 week selection, the large, healthy colonies were isolated and transferred into individual plates. Filtered medium containing viral particles together with 6 μg/ml polybrene were used for infecting cells (2×10^6) respectively. Twenty-four hours postinfection, cultures were replaced with fresh medium and subjected to immunoblot and cell viability assay.

3.2.10. Chromatin immunoprecipitation (ChIP) assay

ChIP assays were done by using CHIP-IT™ Express Kit from Active Motif (Carlsbad, CA). Briefly, log-phase growing MV4-11-R cells were incubated with 37% formaldehyde to cross-link protein-DNA complexes. The cross-linked chromatin was then extracted, diluted with lysis buffer and sheared with Enzymatic Shearing

Cocktail (Active Motif). Ten μL of total sheared chromatin was used as positive control in PCR analysis. The remaining chromatin was divided into equal amount for immunoprecipitation with either anti-Stat3 or anti-IgG (negative control) polyclonal antibody (Santa Cruz Biotechnology) on magnetic beads. The immunoprecipitates were eluted, reversed cross-linked and treated with Proteinase K. Purified DNA was subjected to PCR with primers specific for a region (nucleotides 1821-2912) in human the *Survivin* promoter (GenBank™ accession number U75285). The sequences of the PCR primers used are as follows: pSurvivin forward primer, 5'-CTGGCCATAGAACCAGAGAAGTGA-3'; pSurvivin reverse primer, 5'-CCACCTCTGCCAACGGGTCCCGCG-3'.

3.2.11. Xenograft mouse model

Female Blab/C nude mice (17-20 g, 4-6 weeks old) were purchased from Animal Resources Centre (Canning Vale, Australia). Exponentially growing MV4-11-R cells (5×10^6) were subcutaneously injected into loose skin between the shoulder blades and left front leg of recipient mice. All treatments were started 10 days after the injection, when the mice had palpable tumors of an average size of approximately 200 mm^3. ABT-869 was administrated at 15 mg/kg/day by oral gavage daily.[15,20] IDR E804 was prepared and given the same as ABT-869, but at dose of 10 mg/kg/day. In the combination group, mice were treated with both compounds at the same dose as monotherapy. Treatments lasted for 14 days. Each group was comprised of 10 mice.

The length (L) and width (W) of the tumor were measured with callipers, and tumor volume (TV) was calculated as $TV = (L\times W^2)/2$. The protocol was reviewed and

approved by Institutional Animal Care and Use Committee in compliance to the guidelines on the care and use of animals for scientific purpose.

3.2.12. Immunohistochemistry (IHC)

Tissue fixation followed by Hematoxylin and eosin staining were done as described previously.[16] Sources and incubation conditions for the primary antibodies were as follows: anti-Survivin (clone 71G4, CST), anti-Ki-67 (Neomarkers, Fremont, CA) and anti-cleaved PARP (CST). The slides were counterstained in hematoxylin for 30 seconds and mounted with cover slides. The images were analyzed by a Zeiss Axioplan 2 imaging system with AxioVision 4 software (Zeiss, Germany).

3.2.13. Statistical analysis

Number of viable cells, tumor volume, and survival time were expressed in mean ± standard deviation (SD). Tumour volume reduction of the treatment groups was compared to the untreated control group by Student's *t*-test, and *P* values of < 0.05 were considered to be significant.

3. 3. Results

3.3.1. Long term coculture of MV4-11 cells with ABT-869 resulted in cross-resistance to other FLT3 inhibitors

Human leukemia MV4-11 cells with both alleles FLT-ITD were cocultured with gradually increasing concentration of ABT-869 for 3 months. Three separate cultures were performed in parallel, resulting in 3 resistant lines, designated as MV4-11-R1, MV4-11-R2 and MV4-11-R3. In addition, MV4-11-R represents a pool of MV4-11-R1, -R2, and –R3.

The MTS assay and CalcuSyn software were used to determine the cytotoxic effects of ABT-869, FLT3 inhibitor III, AG1296 and SU5416 on resistant lines and the parent MV4-11 cell line. The IC_{50} values of ABT-869 on resistant lines was about 9 times higher than parent MV4-11 cells. Furthermore, the resistant lines were cross-resistance to structurally unrelated FLT3 inhibitors (Table 3.1). Similarly, annexin V binding assay revealed that the resistant lines were also resistant to ABT-869-, FLT3 inhibitor III-, AG1296- and SU5416-induced apoptosis as compared to the parent MV4-11 cells.

Table 3.1. Comparison the potency (IC_{50} values) of ABT-869 and other structurally unrelated FLT3 inhibitors for inhibiting the proliferation of MV4-11, MV4-11-R, MV4-11+FLT3 ligand and MV4-11-Survivin cells.

		IC_{50} (nM)			
Drugs	Structure	MV4-11	MV4-11-R	MV4-11+FLT3 ligand*	MV4-11-Survivin
ABT-869	3-aminoindazole	6	52	40	> 200
FLT3 Inhibitor III	5-phenyl-2-thiazolamine	26	83	1300	713
AG 1296	tyrphostin	1657	> 7,000	> 7,000	> 10,000
SU5416	3-substitued indolinone	270	3039	3076	> 10,000

Notes: Cells were seeded in 96-well culture plates at a density of 2×10^4 viable cells/100 µl/well in triplicates, and were treated with each compound for 48h. Colorimetric MTS assay was used to determine the cytotoxicity. IC_{50} was determined by MTS assay and calculated with CalcuSyn software (Biosoft, Cambridge, UK). Each experiment was in triplicate. *FLT3 ligand 50 ng/ml.

3.3.2. Overexpression of FLT3, p-FLT3 receptor or multi-drug resistant related proteins, or mutations in KD were not responsible for resistance to FLT3 inhibitors in MV4-11-R

To investigate the mechanisms of drug resistance, immunoprecipitation and Western blot analysis were performed to compare the expression of the wild type FLT3 and p-FLT3 receptor in resistant lines with parent MV4-11 cells. This analysis demonstrated that their expression level were similar (Figure 3.1A). Western blot and flow cytometric analysis were used to determine the expression of multi-drug resistant related proteins. Lung-resistance protein (LRP, Figure 3.1B) was not upregulated in MV4-11-R cells. Multi-drug resistance protein (MDR, Figure 3.1B) was expressed 10-folds higher in both MV4-11-R and parental MV4-11 as compared to isotype controls. MDR-related protein (MRP1, Figure 3.1B) was not detected in MV4-11 and the resistant lines.

Treatment of MV4-11-R cells with ABT-869 still lead to inhibition of FLT3 phosphorylation (Figure 3.1C), but it was not completely abolished as in MV4-11 parental cells under the same treatment condition.

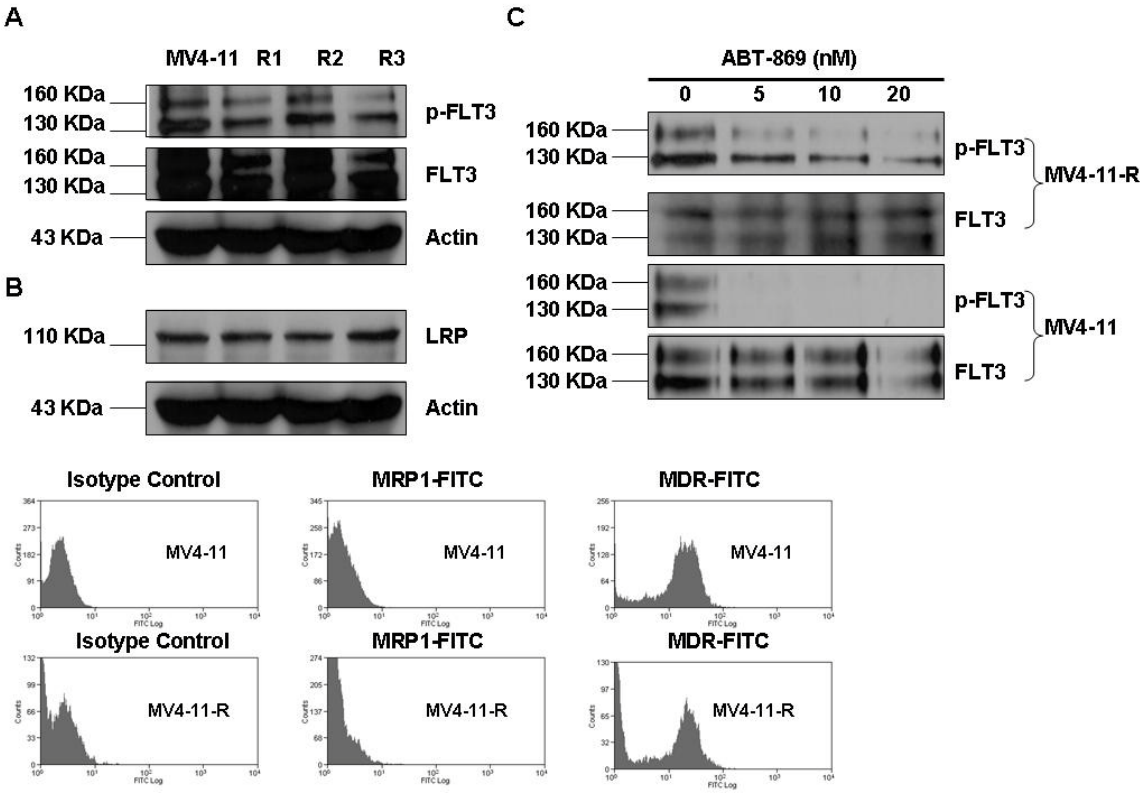

Figure 3.1. Comparison of the expression of phosphorylated FLT3 receptor, total FLT3 receptor and multi-drug resistant related proteins (LRP, MRP1 and MDR) among the parental MV-11 and resistant lines. R1, R2 and R3 induicate MV4-11-R1, MV4-11-R2 and MV4-11-R3 respectively. (A) Immunoprecipitation (IP) and immunoblot analysis reveals that there is no significant difference in the expression of p-FLT3 and FLT3 receptor among MV4-11 and MV4-11-R1, -R2 and –R3. IP was performed using anti-FLT3 antibody, followed by Western blot with anti-p-Tyrosine antibody. The same blot was then stripped and reprobed with anti-FLT3 antibody. (B) Western blot and FACS analysis found the expression of LRP, MRP1 and MDR was not varied significantly among MV4-11 and MV4-11-R1, -R2 and –R3. (C) MV4-11 and MV4-11-R cells were treated with ABT-869 at dose of 0, 5, 10, 20 nM for 1 hour. IP and Western blot were performed as the same way as described above.

3.3.3. Identification of enhanced activation of STAT pathways and overexpression of survivin in the resistant lines

To explore possible novel mechanisms of resistance, we utilized a real-time PCR-based approach to profile and compare the gene expression among MV4-11 cells and the 3 resistant lines. The list of all differentially expressed genes more than 2-fold among them was shown in Table 3.2. Based upon low density array analysis, FLT3 ligand (FLT3LG) and BIRC5 (Survivin) were up-regulated about 2-fold, while suppressor of cytokine signaling (SOCS) family (SOCS-1, -2, -3) were down-regulated 2-fold (Table 2). Consistent with the transcriptional changes, FLT3LG and survivin also were elevated and SOCS1 and SOCS2 were reduced at the protein level by Western blot analysis (Figure 3.2A). The level of decrease reduction in SOCS1 and SOCS2 expression was quantified by densitometry analysis.

Table 3.2. Differentially expressed genes in MV4-11-R vs MV4-11

Gene - ID*	RefSeq	Fold Change
Upregulation list		
BIRC5-Hs00153353_m1	NM_001012271.1	2.05
FLT3LG-Hs00181740_m1	NM_001459.2	2.38
ABL2-Hs00270858_m1	NM_005158.3	4.17
ADK-Hs00417073_m1	NM_001123.2	2.22
AMOT-Hs00611096_m1	NM_133265.2	41.67
AQP3-Hs00185020_m1	NM_004925.3	2.75
ATF3-Hs00231069_m1	NM_001030287.2	2.40
AXL-Hs00242357_m1	NM_001699.3	3.97
CCNA1-Hs00171105_m1	NM_001111045.1	2.33
CCNB1-Hs00259126_m1	NM_031966.2	3.52
CCNB2-Hs00270424_m1	NM_004701.2	2.02
CDC25C-Hs00156411_m1	NM_022809.1	2.01
CDC2-Hs00176469_m1	NM_001786.2	2.11
CRISPLD2-Hs00230322_m1	NM_031476.1	2.06
CXCL12-Hs00171022_m1	NM_199168.2	27.00
EGF-Hs00153181_m1	NM_001963.3	10.33
FIGF-Hs00189521_m1	NM_004469.2	4.67
GATA1-Hs00231112_m1	NM_002049.2	2.29
GTSE1-Hs00212681_m1	NM_016426.4	2.12
MAF-Hs00193519_m1	NM_005360.3	35.00

MKI67-Hs00606991_m1	NM_002417.3	2.17
PDGFC-Hs00211916_m1	NM_016205.1	2.07
PGF-Hs00182176_m1	NM_002632.4	4.54
PLK1-Hs00153444_m1	NM_005030.3	2.35
TNFRSF12A-Hs00171993_m1	NM_016639.1	2.84
VEGFC-Hs00153458_m1	NM_005429.2	11.33
WT1-Hs00240913_m1	NM_024424.2	3.27
ZNF331-Hs00218578_m1	NM_018555.4	2.96
Downregulation list		
SOCS1-Hs00705164_s1	NM_003745.1	-2.01
SOCS2-Hs00374416_m1	NM_003877.3	-2.43
SOCS3-Hs00269575_s1	NM_003955.3	-2.38
AES-Hs00171280_m1	NM_198970.1	-2.04
AFF1-Hs00610550_m1	NM_005935.1	-6.57
ANG;RNASE4-Hs00265741_s1	NM_001145.2	-2.31
BAMBI-Hs00180818_m1	NM_012342.2	-4.09
BBC3-Hs00248075_m1	NM_014417.2	-3.17
DUSP1-Hs00610256_g1	NM_004417.2	-2.67
EGR1-Hs00152928_m1	NM_001964.2	-2.22
EGR2-Hs00166165_m1	NM_000399.2	-2.26
ETS1-Hs00428287_m1	NM_005238.2	-3.05
FER-Hs00245497_m1	NM_005246.1	-2.32
FGF7;FLJ30435-Hs00173565_m1	NM_002009.2	-16.15
FGFR4-Hs00242558_m1	NM_213647.1	-2.61
FOS-Hs00170630_m1	NM_005252.2	-4.45
HLA-DPA1-Hs00410276_m1	NM_033554.2	-19.08
HLA-DRA-Hs00219578_m1	NM_019111.3	-12.98
ICAM1-Hs00277001_m1	NM_000201.1	-2.27
ICAM2-Hs00609563_m1	NM_000873.2	-2.22
IRF1-Hs00233698_m1	NM_002198.1	-2.56
KLF4-Hs00358836_m1	NM_004235.3	-2.97
MLL;GAS7-Hs00245902_m1	NM_201432.1	-2.56
NCOR2-Hs00196955_m1	NM_001077261.1	-2.40
NGFRAP1-Hs00276273_s1	NM_206915.1	-3.81
NOTCH1-Hs00413187_m1	NM_017617.2	-3.42
NTRK3-Hs00176797_m1	NM_001007156.1	-235.85
PTEN-Hs00829813_s1	NM_000314.4	-2.04
RGS2-Hs00180054_m1	NM_002923.1	-2.01
SMAD1-Hs00195432_m1	NM_001003688.1	-409.84
TGFA-Hs00177401_m1	NM_003236.1	-7.31
TP53I3-Hs00153280_m1	NM_147184.1	-2.19

*ID denotes the TaqMan Gene Expression Assays

Since the SOCS family is a negative regulator of STAT pathway,[21] we hypothesize that that STAT pathways would be up activated in the resistant lines. Indeed, Western blot analysis confirmed the overexpression of p-STAT1, p-STAT3 and p-STAT5 in the resistant lines compared to the parent MV4-11 (Figure 3.2B), which suggest that STAT activity is constitutively enhanced in the resistant lines. It is interesting to note that wild type STAT1, but not wild type STAT3 and STAT5, was also increased in the resistant lines, which likely resulted from intensified STAT1 activity (p-STAT1), since STAT1 itself has been identified as one of the STAT1 target genes (Figure 3.2B). In addition to the STAT pathways, PI3K/AKT and MAPK signaling pathways also play an important role in promoting cell survival and proliferation; however, p-AKT and p-ERK1/ERK2 were not overexpressed in the resistant lines (Figure 3.2B).

Aberrant methylation of SOCS genes have been reported in AML and solid tumors, [19,22] so we further determined whether this epigenetic changes caused downregulation of SOCS genes in MV4-11-R cells. The expression of SOCS1, 2, and 3 genes was restored by the demethylating agent 5-aza treatment in MV4-11-R cells, but essentially not changed in MV4-11 parental cells, suggesting SOCS promoters in MV4-11 parental cells are not sensitive to demethylating therapy (Figure 3.2C).

We have looked at the 3 most widely studied survivin splice variants,[17] and RT-PCR analysis showed that all 3 transcripts appeared to be upregulated with the normal transcript (431 bp) as the dominant transcript in the resistant lines (Figure 3.2D), however, the expression of other variants is unknown in our resistant lines.[23]

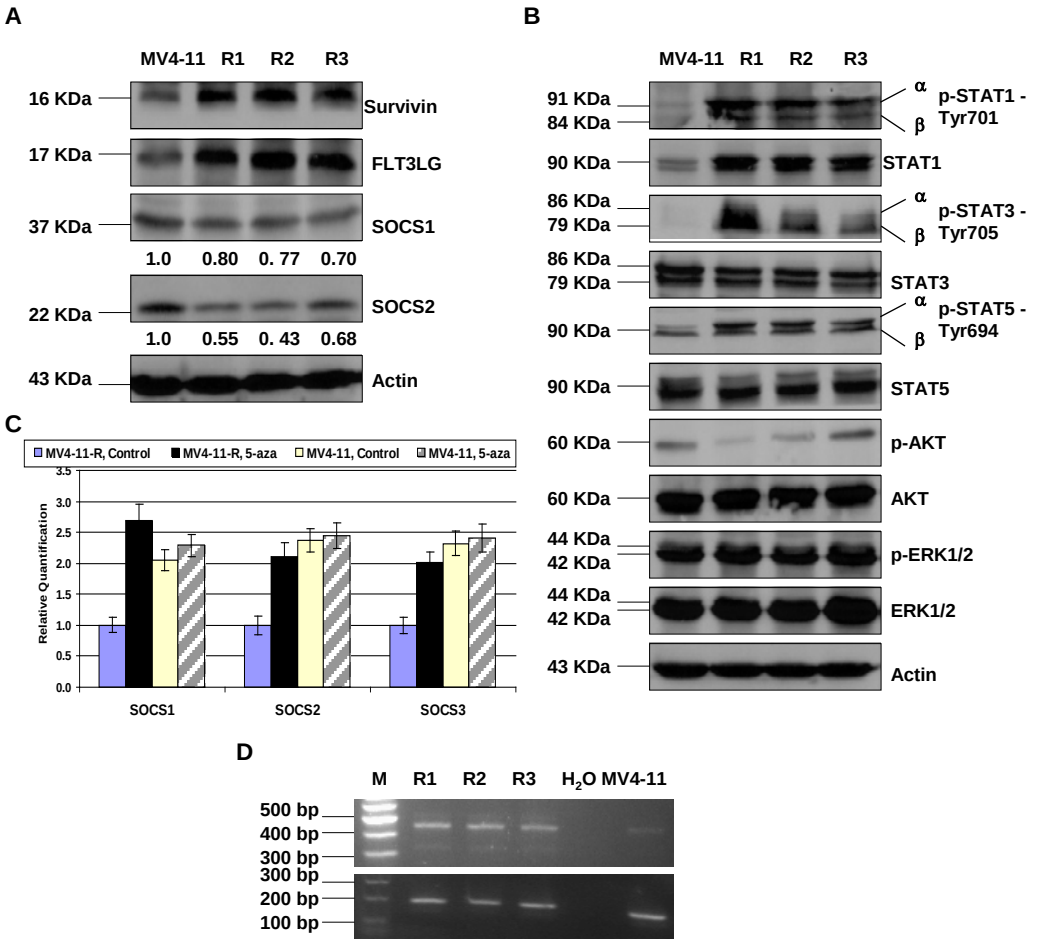

Figure 3.2. Validation of FLT3LG, survivin and SOCS1 and SOCS2 expression and STAT pathway overactivation at the translational level, RQ-PCR quantification of SOCS gene family and confirmation of normal transcript of *Survivin* in MV4-11-R cells. MV4-11 and MV4-11-R cells were washed, then lysed and subjected to 10% to 12% SDS-PAGE. Western blots were detected with the indicated antibodies for the assessment of expression level changes in (A) FLT3LG, survivin, SOCS1, and SOCS2. Densitometric analysis was performed using Amersham Image Scanner with LabScan ImageQuant TL Software (Amersham Biosciences, Piscataway, NJ). The protein levels of SOCS1 and SOCS2 were normalized with each respective actin level. (B) Western blot analysis of STAT, AKT and MAPK pathway molecules. (C) MV4-11 parental and MV4-11-R cells were seed at density of 2 x 10^5/ml in 10 ml culture medium and treated with PBS control and 3 μM (final concentration) of 5-aza. Fresh medium was changed and new drug was added everyday. After 3 days, cells were harvested, washed with 1 x PBS twice. Then the pellets were lysed, followed by RNA extraction and RQ-PCR. (D) RT-PCR confirmed the overexpression of *Survivin* transcripts in resistant lines. The size of normal transcript is 431 bp and two other transcript variants-*Survivin-2B* and *Survivin-ΔEx3* are 500 bp and 329 bp respectively (upper panel). GAPDH was used as internal control (lower panel).

3.3.4 Upregulation of survivin in MV4-11-R cells resulted in changes in cell cycle and apoptosis

Survivin has dual roles in suppressing apoptosis and modulating cell cycle.[24] We sought to investigate the influence of upregulated survivin on cell cycle and apoptosis in MV4-11-R cells. After serum deprived for 48 hours, MV4-11 parental cells and MV4-11-R cells were transferred into complete medium for additional 24 hours. Flow cytometric analysis revealed that MV4-11 parental cells had a significantly decreased S phase population (6.5% vs 17.8%, $p < 0.01$), but a dramatically increased G_2/M phase population (49.6% vs 20.3%, $p < 0.01$) as compared to MV4-11-R cells.

Furthermore, there were 4.5 times more dead cells in MV4-11 cells than in MV4-11-R cells as determined by the trypan blue dye exclusion method at the end of serum depletion 48 hours. Taken together, these results suggest that overexpression of survivin in MV4-11-R cells leads to accelerated S phase shift and resistance to apoptosis.

3.3.5. FLT3 ligand mediated STAT activities and survivin expression

To mimic the overexpression of FLT3LG in the resistant cells, we cultured the parent MV4-11 cells with increasing concentration of FLT3 ligand in the cell culture for 48 hours. Additional FLT3 ligand stimulation fairly elevated the expression level of p-STAT1, p-STAT3 and p-STAT5 (Figure 3.3A). The expression of survivin was also increased in a concentration-dependent manner in response to FLT3 ligand stimulation (Figure 3.3A). To test if leukemia cells can be protected by FLT3 ligand, we treated MV4-11 cells with the same panel of FLT3 inhibitors in the presence of 50 ng/ml of FLT3 ligand in culture medium for 48 hours. Adding FLT3 ligand rendered

MV4-11 cells resistance to all the FLT3 inhibitors tested, though the degree of IC_{50} increment varied (Table 3.1).

The FLT3 ligand exists in membrane-bound and soluble forms, which are both biologically active. To test whether secreted soluble form of FLT3 ligand by MV4-11-R cells contributes to resistance, we first harvested conditioned medium from MV4-11-R cells incubated in complete medium for 12 hours, Then, MV4-11 cells were washed twice with 1xPBS and cultured in conditioned medium for 2, 4 and 6 hours, followed by Western blot analysis. As shown in Figure 3.3B, incubation in conditioned medium resulted in elevated expression of p-FLT3, p-STATs and survivin.

To investigate the effect of downregulation of FLT3 ligand, MV4-11-R cells were treated with a FLT3 ligand neutralizing antibody for 48 hours, and cell viability was analyzed. Figure 3.3C showed the viable cell number was significantly decreased and apoptotic cell number was significantly increased in FLT3 ligand neutralizing antibody treated samples as compared to untreated or isotype control treated samples. As expected, in neutralizing antibody treated samples, the expression of p-FLT3, p-STATs and survivin was reduced (Figure 3.3D).

These data suggest that FLT3 ligand plays an important role in mediating the resistance to FLT3 inhibitors.

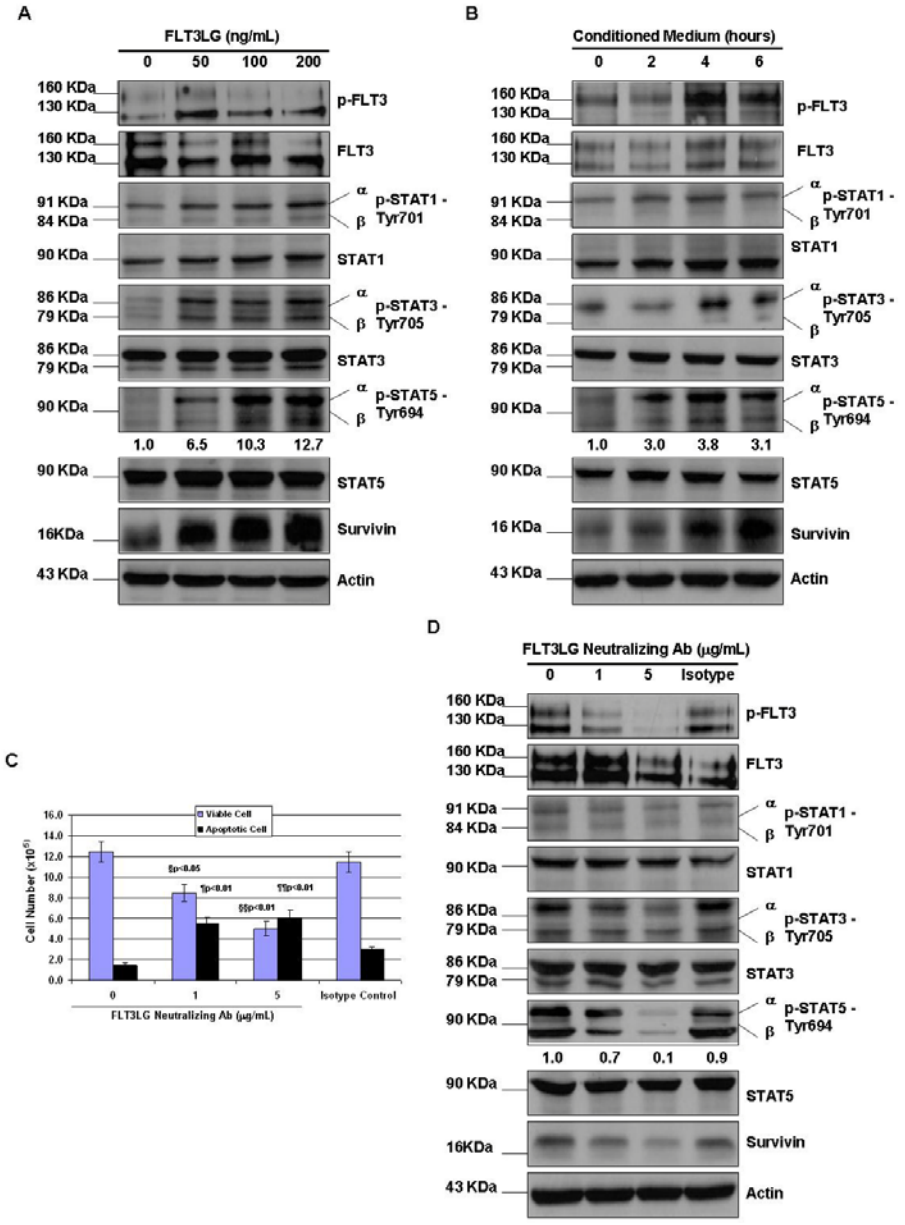

Figure 3.3. The effect of FLT3LG on activity of STAT signaling pathway and the expression of survivin. (A) MV4-11 cells were cultured with FLT3 ligand for 48h, then were washed, lysed and subjected to either IP of p-FLT3 receptor as described in Figure 1 or 10% to 12% SDS-PAGE. (B) MV4-11 cells were cultured in conditioned medium for 0, 2, 4, and 6 hours. Cells were then washed, lysed and followed by IP and immunoblot analysis. (C) MV4-11-R cells were treated with FLT3LG neutralizing antibody and isotype control antibody for 48 hours. Viable cells and apoptotic cells were counted by by the trypan blue dye exclusion method. (D) After counting, cells were then washed, lysed and followed by IP and immunoblot analysis. Densitometric analysis was performed for p-STAT5 using Amersham Image Scanner with LabScan ImageQuant TL Software.

3.3.6. Modulation of survivin expression influenced drug sensitivity

To demonstrate the critical role of survivin in the regulation of resistance, we used a pool of shRNA to specially target survivin. Western blot analysis confirmed specific inhibition of survivin by approximately 80% with the pool of survivin-shRNAs (Figure 3.4A,). Silencing survivin remarkably potentiated ABT-869-induced apoptosis in MV4-11-R cells when compared to control shRNA treatment ($p < 0.001$). On the contrary, MV4-11 parental cells, in the presence of IC_{50} dose of ABT-869, are not sensitive to Survivin-shRNA ($p > 0.05$) (Figure 3.4B).

To further confirm the role of survivin in drug resistance, we evaluated the effect of overexpression of survivin in transfected MV4-11 parental cells. The stable transfectants (MV4-11-Survivin) showed overexpression of survivin protein (Figure 3.4C). MTS assays revealed an exceptional increase in resistance to the panel of FLT3 inhibitors in MV4-11-Survivin cells (Table 3.1).

Taken together, these data unequivocally demonstrated that survivin is crucial in mediating resistance to FLT3 inhibitors.

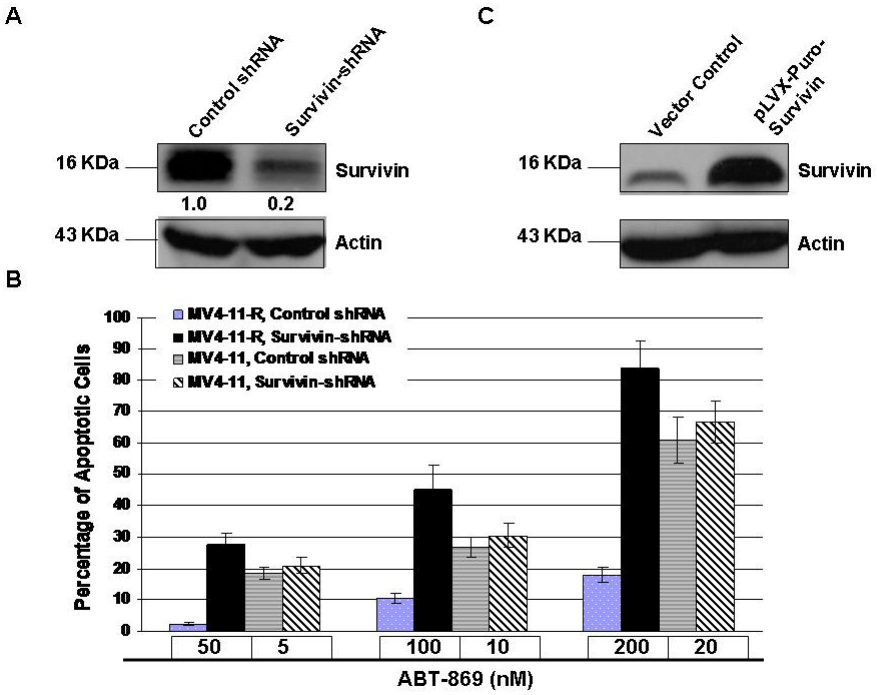

Figure 3.4. Knockdown of Survivin potentiated ABT-869 induced apoptosis in MV4-11-R cells. (A) MV4-11-R cells were treated with non-target control shRNA or Survivin shRNA pools for 48h, and then harvested for Western blot analysis. Actin level served as loading controls. Densitometric analysis was performed using Amersham Image Scanner with LabScan ImageQuant TL Software. The level of survivin was normalized with each actin level. (B) Following knockdown, MV4-11-R cells were treated with ABT-869 at dose of 50, 100, 200 nM and MV4-11 parental cells were treated with ABT-869 at dose of 5, 10 and 20 nM for 48 h. As residual expression of survivin persists after treatment of survivin shRNA, it may provide some level of protection from a full scale apoptosis. Apoptosis was measured by Annexin V-FITC binding assay. p-values demonstrate the comparison between survivin-shRNA and control-shRNA treated group. All p-values of MV4-11-R samples are less than 0.001. All p-values of MV4-11 samples are greater than 0.05. Means for three replicated experiments; bars represent standard deviation (SD). (C) Immunoblot analysis of the survivin protein level in MV4-11-Survivin and MV4-11 vector control cells.

3.3.7. Indirubin derivative (IDR) E804 induced apoptosis through inhibition of STAT pathway and survivin and sensitized MV4-11-R to ABT-869

Next, we screened a panel of small molecule inhibitors of CDKs, SRC, BCR-ABL, and JAKs including IDR E804, Tyrene CR4, AG490, JAK3 Inhibitor II, and NU6140. We found that MV4-11-R cells are most sensitive to IDR E804, an inhibitor of SRC-

STAT3 pathway, using MTS assay (data not shown). IDR E804 treatment dose-dependently induced MV4-11-R cells to undergo apoptosis (Figure 3.5A). Western blot analysis also showed that IDR E804 inhibited the expression of p-STAT1, p-STAT3, p-STAT5 and completely blocked survivin (Figure 3.5B). It is worthy to note that IDR E804 completely inhibits survivin in the absence of complete inhibition of p-STATs, This apparently incongruous inhibition could be due to the fact that survivin expression is regulated in a cell cycle dependent manner and rapidly decline in G_1/G_0 phase and IDR E804 significantly arrested MV4-11-R cell in G_1/G_0 phase ($p<0.01$). Furthermore, cleaved PARP, a hallmark of apoptosis, was detected at concentrations of 100 nM and higher (Figure 3.5B). Notably, IDR E804 did not inhibit FLT3-ITD kinase activity (Figure 3.5B), so its cytotoxicity to MV4-11-R cells was derived specifically from targeting STAT pathway and survivin. The IC_{50} value of ABT-869 in MV4-11-R decreased from 52 to 6 nM calculated by CalcuSyn software in the presence of a sub-therapeutic concentration (2 nM) of IDR E804, suggesting a synergistic effect (Figure 3.5C, $p<0.01$). Whereas, the same combination treatment did not augmented the inhibition effect in MV4-11 parental cells as compared to ATB-869 alone (Figure 3.5C, $p>0.05$). These results are in accordance with the data obtained by shRNA study as above. In order to confirm the molecular mechanism of synergism via targeting STAT-Survivin pathway, we further tested the effect of lower doses of IDR E804 on MV4-11-R cells, IDR E804 from 2 to 20 nM inhibited the STAT activities and the expression of survivin in a dose-dependent fashion. About 23% reduction of survivin was observed at 2 nM of IDR E806 as compared to the control treatment.

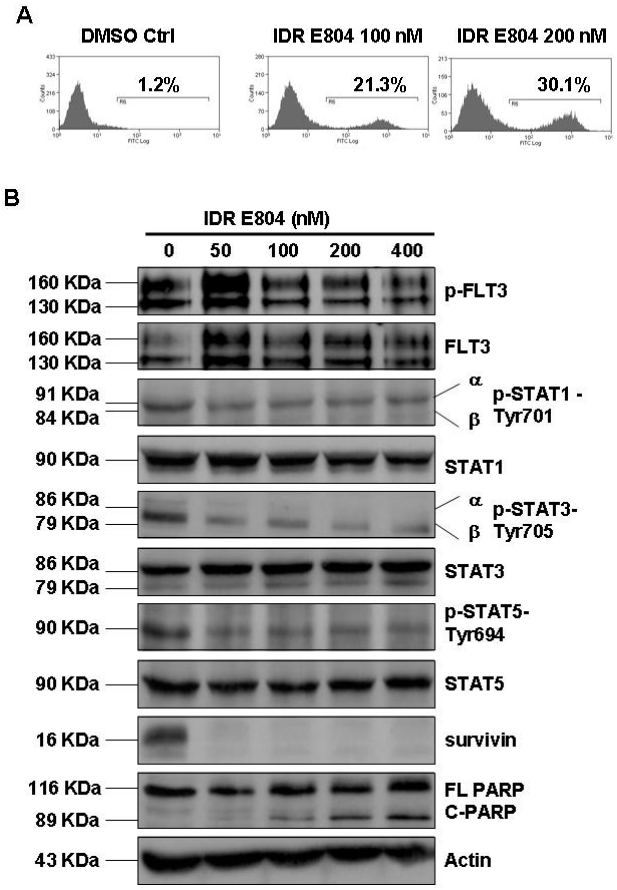
A
DMSO Ctrl
IDR E804 100 nM
IDR E804 200 nM
1.2%
21.3%
30.1%
B
IDR E804 (nM)
0
50
100
200
400
160 KDa
130 KDa
p-FLT3
FLT3
91 KDa
84 KDa
α
β
p-STAT1 - Tyr701
90 KDa
STAT1
86 KDa
79 KDa
p-STAT3- Tyr705
STAT3
p-STAT5- Tyr694
STAT5
16 KDa
survivin
116 KDa
89 KDa
FL PARP
C-PARP
43 KDa
Actin
C
OD of Control
1.2
1.0
0.8
0.6
0.4
0.2
0.0
MV4-11-R, ABT-869
MV4-11, ABT-869
MV4-11-R, IDR E804 2nM + ABT-869
MV4-11, IDR E804 2nM + ABT-869
DMSO ctrl
2 nM
4 nM
8 nM
16 nM
ABT-869

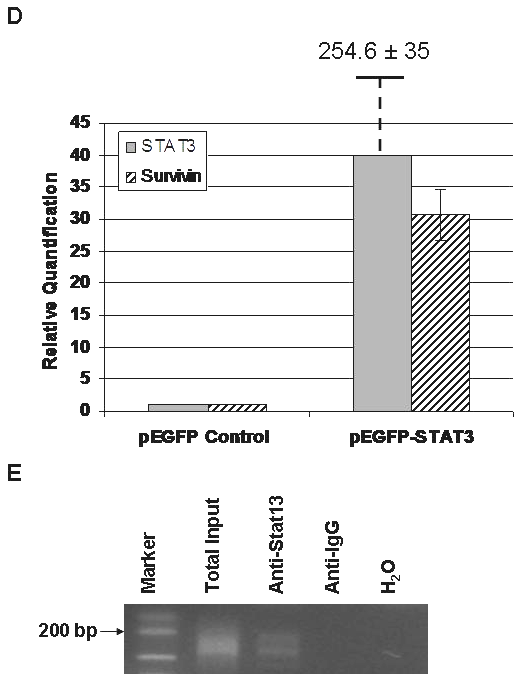

Figure 3.5. IDR E804 induced apoptosis and sensitized MV4-11-R to ABT-869. (A) Two million cells of MV4-11-R were treated with either DMSO control or IDR E804 at concentrations of 100 and 200 nM for 48h. Cells were then washed and stained with Annexin-V-FITC for apoptosis assay. The shown graphs represent 3 independent experiments. (B) MV4-11-R cells (10×10^6) were cultured with DMSO control or IDR E804 at concentrations of 50, 100, 200, 400 nM for 48 h. The IP of p-FLT3 receptor was performed as in Figure 1. Cells were washed, lysed and subjected to 10% to 12% SDS-PAGE. Western blots were detected with the indicated antibodies for the assessment of the expression level changes in STAT pathway molecules and Survivin, PARP, and cleaved PARP. Actin was used as a loading control. (C) MV4-11-R and MV4-11 cells were treated with various concentrations of ABT-869 alone or together with 2 nM IDR E804 for 48h. MTS assay was used to determine the viable cell number. Means are shown for three replicated experiments. (D) After parental MV4-11 cells were transiently transfected with pEGFP empty vector or pEGFP-STAT3 for 48h, RNA was extracted, followed by cDNA synthesis and relative quantification by RQ-PCR. The baseline expression of STAT3 and survivin in MV4-11 cells transfected with pEGFP vector was set as 1.0. The relative quantification of STAT3 in MV4-11 cells transfected with pEGFP-STAT3 was 354.6 ± 35 from 3 independent experiments. (E) ChIP assays were done using anti-STAT3 antibody or control anti-IgG antibody. PCR primers for the survivin gene promoter were applied to detect promoter fragment in immunoprecipitates. PCR controls included total sheared chromatin (total input), DNA isolated through the negative control IgG-ChIP and no DNA at all (H_2O).

3.3.8. Survivin was a direct target of STAT3

We examined whether STAT3 directly regulated survivin. In transient transfection studies with pEGFP-STAT3, we showed that forced expression of STAT3 in MV4-11 cells induced expression of survivin about 30-fold calculated by relative quantification RQ-PCR, as compared to pEGFP vector (Figure 3.5D). To test whether STAT3 could bind the survivin promoter, we performed ChIP assays in MV4-11-R cells. The amplified survivin promoter DNA was present in chromatin immunoprecipitated with an anti-STAT3 antibody (Figure 3.5E).

3.3.9. *In vivo* efficacy of IDR E804 in combination with ABT-869 for treatment of MV4-11-R mouse xenografts

Based on the *in vitro* results that IDR E804 could sensitize the resistant line to ABT-869, we tested the combination of IDR E804 and ABT-869 in a subcutaneous mouse xenograft model *in vivo*. MV4-11-R tumors in mice treated with vehicle control developed rapidly up to 3569 ± 619 mm^3 after two weeks. Growth of tumors in mice treated with a single agent (ABT-869 or IDR E804) was reduced to 2189 ± 211 mm^3 and 1588 ± 368 mm^3, respectively (Figure 3.6A). However, in the combination group, tumors size did not increase and was kept at 158 ± 16 mm^3 throughout the course of treatment. The anti-tumor effects of the combination were significantly better when compared to single agent or control (all $p<0.001$).

In addition to reducing TV by about 22-fold compared to vehicle control, combination therapy demonstrated significant biochemical effects on MV4-11-R xenografts tumor. Histological examination of tumor specimens showed that ABT-869 alone had minimal impact on the expression of survivin (Figure 3.6B, top panel) whereas IDR E804 alone triggered a modest decrease in survivin-positive cells (brown color) compared with tumors from vehicle control. However, the combination therapy

markedly inhibited the number of survivin-positive cells compared with either single agent treatment (Figure 3.6B, top panel, Figure 3.6C, left panel, all $p<0.001$). In agreement with these data, a significant decrease in expression of Ki67 (Figure 3.6B and 3.6C, middle panels) and an increase in the number of cleaved PARP-positive cells (Figure 3.6B, bottom panel, Figure 3.6C, right panel) were observed in tumor sections from ABT-869 plus IDR E804–treated mice compared to tumors from mice receiving either treatment alone. Together, these data demonstrate a potent *in vivo* anti-leukemic effect of ABT-869 in combination with IDR E804 and support the potential clinical utility of combing ABT-869 with inhibitors of the STAT signaling pathway in the treatment of TKI-resistant AML.

A

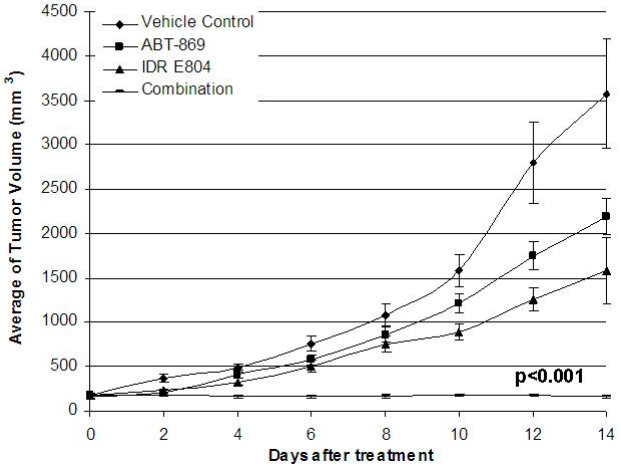
Vehicle Control
ABT-869
IDR E804
Combination
Average of Tumor Volume (mm 3)
Days after treatment
p<0.001

B

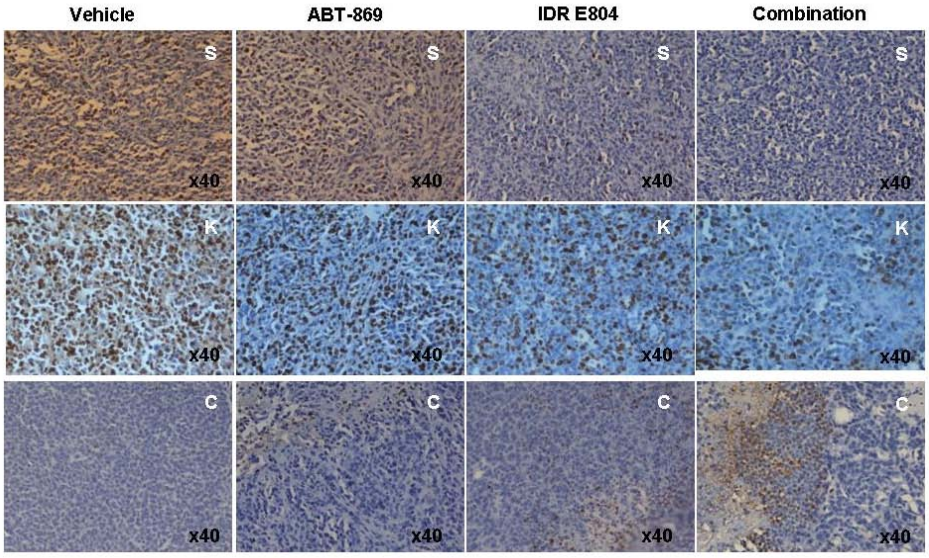
Vehicle
ABT-869
IDR E804
Combination
S
K
C
x40

C

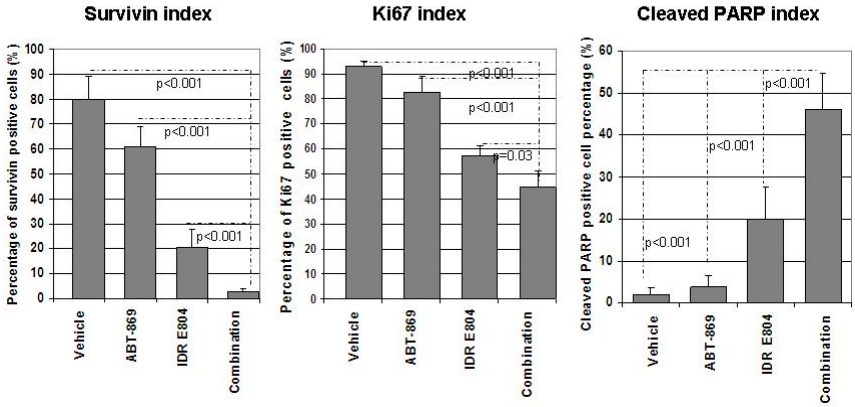
Survivin index
Ki67 index
Cleaved PARP index
Percentage of survivin positive cells (%)
Percentage of Ki67 positive cells (%)
Cleaved PARP positive cell percentage (%)
p<0.001
p=0.03
Vehicle
ABT-869
IDR E804
Combination

Figure 3.6. *In vivo* effect of combination therapy on the MV4-11-R tumor xenograft model. (A) Combination of ABT-869 with IDR E804 achieved impressive regression of tumor growth compared to either vehicle control or single treatment (ABT-869 or IDR E804) alone (all $p<0.001$). (B) Excised tumor pieces from each group were embedded in paraffin and stained with anti-survivin (S), anti-Ki67 (K) and anti-cleaved PARP (C). Photographs are representative of similar observations in 3 different mice receiving same treatment. (C) Quantitative analysis of the expressions of survivin, ki67 and cleaved PARP in IHC sections from each group shown in (B). The survivin index, ki67 index and cleaved PARP were calculated as the percentage of positive staining cells of total nucleated cells in a 400x field. A total of 10 fields for each index were counted. Bars indicate SD. Statistical comparison and associated p values are indicated by the broken lines in each photograph.

3.4. Discussion

FLT3 mutations represent one of the most common genetic lesions in AML. FLT3 inhibitors, like CEP-701, PKC412, MLN518, SU11248, or ABT-869 are in different phases of clinical development as monotherapy or in combination studies.[1,2,4,5,7,8,15] It is predictable that patients could develop resistance to RTK inhibitors after a long period of monotherapy as suggested by the clinical use of Gleevec. A number of point mutations in the KD were identified in murine Ba-F3-FLT3-ITD cells which led to resistance to these agents.[10,25] It is also found that overexpression of FLT3-ITD proteins in one resistant subline of Ba-F3-ITD lead to resistance to PKC412.[26]

However, so far, acquired point mutations are a rare event in patient samples in FLT3 inhibitor clinical trials.[12] Here, for the first time, we report the enhanced activation of STAT pathway and overexpression of survivin as a novel mechanism of resistance to ABT-869 and other FLT3 inhibitors. The resistance can be overcome by inhibition of the STAT pathway or by targeting survivin, thereby inducing MV4-11-R cells to undergo apoptosis and resensitizing them to ABT-869 *in vitro* and *in vivo*.

We first excluded the overexpression of multi-drug resistant-related efflux proteins such as MDR, MRP1, by flow cytometric analysis and LRP by Western blot analysis in our MV4-11-R1, -R2, -R3 cell lines. We also did not find point mutations in the FLT3 KD by sequencing analysis. In addition, overexpression of total FLT3 receptors was not evident in the resistant lines. These results are consistent with the findings from Piloto *et al*. where three different human leukemia cell lines and various FLT3 inhibitors were used.[13]

STAT pathways have been intensively investigated in cancer biology, because they regulate an array of fundamental cell functions such as survival, proliferation, differentiation, apoptosis and immunity.[27] Aberrant activation of STAT pathways, particularly STAT3, STAT5 and less frequency STAT1, has been found in the majority of solid tumors and hematological malignancies, including AML.[28,29] We demonstrated hypermethylation of SOCS genes correlating lower expression status and restored expression by 5-aza treatment in MV4-11-R cells, indicating the epigenetically regulated, transcriptional silencing plays an important role in the development of resistance. SOCS proteins are the part of key pathways that negatively regulate STAT signaling.[21] SOCS inhibits STAT pathways either by directly competing for binding with STAT proteins to receptor complex, or by degradation of upstream JAK kinase or competing binding with JAK protein.[30] So overactivation of STAT pathways in MV4-11-R cells results from, at least in part, decreasing expression of SOCS molecules as revealed by LDA analysis, rendering their resistance to FLT3 inhibitors. The observation that the activity of PI3K/AKT and MAPK pathways are not enhanced in the resistant lines relative to the parent MV4-11 cells further supports the importance of STAT-mediated resistance in MV4-11-R cells.

Both soluble and membrane-bound FLT3 ligand isoforms are biologically active. FLT3 ligand in conjunction with other cytokine growth factors, like granulocyte colony-stimulating factor (G-CSF), granulocyte macrophage-CSF (GM-CSF) and thrombopoietin (TPO), stimulates survival, proliferation, and differentiation of hematopoietic stem and progenitor cells (HSPC).[31] Specifically, FLT3 ligand has potent direct-acting stimulating/costimulating activities on myeloid stem/progenitor cells.[32] Compelling evidence shows that the existence of an autocrine FLT3LG/FLT3 loop promotes proliferation and prevents apoptosis of primary AML blasts and AML cell lines.[33-35] In MV4-11-R cells, upregulation of FLT3 ligand triggers a stronger autocrine reaction, thus further enhancing STAT pathway activity and survivin expression, which is supported by observations of elevated phosphorylated proteins and survivin in the parental MV4-11 cells stimulated with FLT3LG in a cell culture system.

Survivin (encoded by *BIRC5*), the smallest member of inhibitor of apoptosis protein (IAP) family,[36] has been identified as the fourth most highly expressed transcript in cancer [37] and is one of the most cancer-specific molecules. Survivin is detected in a broad spectrum of different types of tumors, but is undetectable in most terminally differentiated normal tissues,[24] except a number of normal tissues, particularly those high proliferative and self renewal rates, i.e., hematopoietic cells, neuronal stem cells, keratinocyte, and mucosal epithelial cells.[23,38] Survivin antagonizes apoptosis through stabilization of X-linked IAP (XIAP), another member of IAP family, against proteasomal degradation.[24] Overall, strong survivin expression has been associated with shorter disease-free or overall survival in the majority of patients with hematological malignancies and solid tumors.[18,24,38,39] Moreover, survivin proves to

be a direct downstream target gene in BCR-ABL positive cells.[40,41] Several studies indicate survivin plays an important role in resistance to (1) paclitaxel in ovarian cancer,[42] (2) antiandrogen therapy in prostate cancer,[43] and (3) doxorubicin in thyroid cancer.[44] Here we demonstrate that increased expression of survivin contributes to acquired resistance to a molecularly targeted therapy (a FLT3 inhibitor), expanding its role in mediating resistance to conventional chemotherapy. Survivin has been identified as a direct target of the STAT3 transcription factor in primary effusion lymphoma,[45] breast cancer[46] and endothelial cells stimulated with interleukin-11 (IL-11).[47] Now we confirm this relationship in AML, and provide further understanding that STAT3 directly binds and regulates the survivin promoter. The continuous activation of STAT3 signaling in the FLT3 inhibitor-resistant AML cells enhances the expression of survivin and grants resistance to apoptosis.

STAT pathways and survivin play a pivotal role in oncogenesis and have been validated as targets for cancer therapy.[48,49] Targeting survivin by shRNA induced apoptosis and augmented ABT-869-mediated toxicity in MV4-11-R cells. On the contrary, overexpression of survivin in MV4-11 cells leads to remarkable resistance to the panel of FLT3 inhibitors. These results are consistent with the previous finding that silencing survivin by RNA interference (RNAi) restores sensitivity to doxorubicin in resistant thyroid cancer cells.[44] IDR E804 has been shown to inhibit the SRC-STAT3 pathway and to down-regulate survivin in breast cancer cells.[50] In our study, treatment with IDR E804 prompts MV4-11-R cells to undergo apoptosis as demonstrated by an increase in Annexin-V binding assay and in the 89-KD fragment of PARP, which is responsible for DNA breakage. The inhibitory effect of IDR E804 is not only on STAT3 activity, but it also abolishes STAT1 and STAT5 activity, which could possibly reinforce its cytotoxicity to MV4-1-R cells. A sub-therapeutic

concentration of IDR E804 signifcantly resensitizes MV4-11-R cells to ABT-869 treatment. This synergism is not evident in the parental MV4-11 cells. The animal experiments provide further evidence to support the therapeutic benefit of targeting STAT pathways and survivin. The dramatically inhibition of tumor growth in mice treated with the combination therapy is correlated with almost complete disappearance of survivin expression and signifcantly increased expression of cleaved PARP, as well as a decrease in the number of Ki67-positive (an indictor of proliferation) cells in tumor specimens from the combination therapy group compared to either single agent treatment alone.

The *in vitro* co-culture resistance model mimics the clinical practice of targeted agents given on a chronic dosing schedule. it recapitulates to a certain extent the clonal heterogeneity in clinical tumors where resistant clones emerge as oligo-clonal population and eventually expand, and therefore may reflect the natural course of many cancers which later relapse after initial therapy. However, it may also signify underlying clonal heterogeneity and other potential resistance mechanism(s) are yet to be identified.

In conclusion, our results suggest a novel mechanism of resistance to the FLT3 inhibitor ABT-869. In this model depicted in Figure 3.7, upregulation of FLT3 ligand and methylation silencing of the SOCS family integrate to enhance STAT signaling activity and overexpression of survivin, in turn suppressing apoptosis and promoting survival, which leads to a resistant phenotype. Understanding the mechanism of resistance to FLT3 inhibitors could help develop new antileukemic agents or uncover compelling combinations. Our data strongly support the combination of FLT3 inhibitors with agents targeting STAT pathway or survivin such as small molecular

inhibitors or shRNA and may represent a novel strategy to minimize resistance or resensitize resistant cells to FLT3 inhibitors in AML patients with FLT3-ITD mutation.

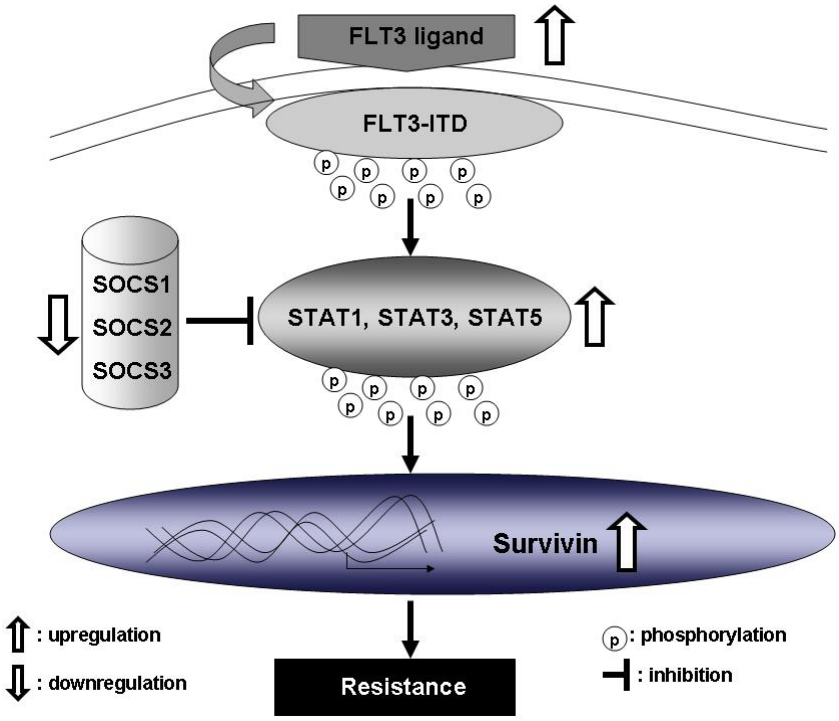

Figure 3.7. A model of enhanced STAT activation and overexpression of survivin leading to resistant phenotype in MV4-11-R cells.

3.5. References

1. Gilliland DG, Griffin JD. The roles of FLT3 in hematopoiesis and leukemia. Blood. 2002;100:1532-1542.
2. Levis M, Small D. FLT3: ITDoes matter in leukemia. Leukemia. 2003;17:1738-1752.
3. Nakao M, Yokota S, Iwai T, et al. Internal tandem duplication of the flt3 gene found in acute myeloid leukemia. Leukemia. 1996;10:1911-1918.
4. Sternberg DW, Licht JD. Therapeutic intervention in leukemias that express the activated fms-like tyrosine kinase 3 (FLT3): opportunities and challenges. Curr Opin Hematol. 2005;12:7-13.
5. Stirewalt DL, Radich JP. The role of FLT3 in haematopoietic malignancies. Nat Rev Cancer. 2003;3:650-665.

6. Frohling S, Scholl C, Levine RL, et al. Identification of driver and passenger mutations of FLT3 by high-throughput DNA sequence analysis and functional assessment of candidate alleles. Cancer Cell. 2007;12:501-513.
7. Knapper S. FLT3 inhibition in acute myeloid leukaemia. Br J Haematol. 2007;138:687-699.
8. Small D. FLT3 mutations: biology and treatment. Hematology Am Soc Hematol Educ Program. 2006:178-184.
9. Gorre ME, Mohammed M, Ellwood K, et al. Clinical resistance to STI-571 cancer therapy caused by BCR-ABL gene mutation or amplification. Science. 2001;293:876-880.
10. Cools J, Mentens N, Furet P, et al. Prediction of resistance to small molecule FLT3 inhibitors: implications for molecularly targeted therapy of acute leukemia. Cancer Res. 2004;64:6385-6389.
11. Bagrintseva K, Schwab R, Kohl TM, et al. Mutations in the tyrosine kinase domain of FLT3 define a new molecular mechanism of acquired drug resistance to PTK inhibitors in FLT3-ITD-transformed hematopoietic cells. Blood. 2004;103:2266-2275.
12. Heidel F, Solem FK, Breitenbuecher F, et al. Clinical resistance to the kinase inhibitor PKC412 in acute myeloid leukemia by mutation of Asn-676 in the FLT3 tyrosine kinase domain. Blood. 2006;107:293-300.
13. Piloto O, Wright M, Brown P, Kim KT, Levis M, Small D. Prolonged exposure to FLT3 inhibitors leads to resistance via activation of parallel signaling pathways. Blood. 2007;109:1643-1652.
14. Albert DH, Tapang P, Magoc TJ, et al. Preclinical activity of ABT-869, a multitargeted receptor tyrosine kinase inhibitor. Mol Cancer Ther. 2006;5:995-1006.
15. Zhou J, Pan M, Xie Z, et al. Synergistic antileukemic effects between ABT-869 and chemotherapy involve downregulation of cell cycle-regulated genes and c-Mos-mediated MAPK pathway. Leukemia. 2008;22:138-146.
16. Shen J, Tai YC, Zhou J, et al. Synergistic antileukemia effect of genistein and chemotherapy in mouse xenograft model and potential mechanism through MAPK signaling. Exp Hematol. 2007;35:75-83.
17. Mahotka C, Wenzel M, Springer E, Gabbert HE, Gerharz CD. Survivin-deltaEx3 and survivin-2B: two novel splice variants of the apoptosis inhibitor survivin with different antiapoptotic properties. Cancer Res. 1999;59:6097-6102.
18. Invernizzi R, Travaglino E, Lunghi M, et al. Survivin expression in acute leukemias and myelodysplastic syndromes. Leuk Lymphoma. 2004;45:2229-2237.
19. Sutherland KD, Lindeman GJ, Choong DY, et al. Differential hypermethylation of SOCS genes in ovarian and breast carcinomas. Oncogene. 2004;23:7726-7733.
20. Zhou J, Khng J, Jasinghe VJ, et al. In vivo activity of ABT-869, a multi-target kinase inhibitor, against acute myeloid leukemia with wild-type FLT3 receptor. Leuk Res. 2008;32:1091-1100.
21. Starr R, Willson TA, Viney EM, et al. A family of cytokine-inducible inhibitors of signalling. Nature. 1997;387:917-921.
22. Watanabe D, Ezoe S, Fujimoto M, et al. Suppressor of cytokine signalling-1 gene silencing in acute myeloid leukaemia and human haematopoietic cell lines. Br J Haematol. 2004;126:726-735.
23. Sampath J, Pelus LM. Alternative splice variants of survivin as potential targets in cancer. Curr Drug Discov Technol. 2007;4:174-191.
24. Altieri DC. The molecular basis and potential role of survivin in cancer diagnosis and therapy. Trends Mol Med. 2001;7:542-547.

25. Bagrintseva K, Geisenhof S, Kern R, et al. FLT3-ITD-TKD dual mutants associated with AML confer resistance to FLT3 PTK inhibitors and cytotoxic agents by overexpression of Bcl-x(L). Blood. 2005;105:3679-3685.
26. Weisberg E, Boulton C, Kelly LM, et al. Inhibition of mutant FLT3 receptors in leukemia cells by the small molecule tyrosine kinase inhibitor PKC412. Cancer Cell. 2002;1:433-443.
27. Bowman T, Garcia R, Turkson J, Jove R. STATs in oncogenesis. Oncogene. 2000;19:2474-2488.
28. Gouilleux-Gruart V, Gouilleux F, Desaint C, et al. STAT-related transcription factors are constitutively activated in peripheral blood cells from acute leukemia patients. Blood. 1996;87:1692-1697.
29. Xia Z, Baer MR, Block AW, Baumann H, Wetzler M. Expression of signal transducers and activators of transcription proteins in acute myeloid leukemia blasts. Cancer Res. 1998;58:3173-3180.
30. Wormald S, Hilton DJ. The negative regulatory roles of suppressor of cytokine signaling proteins in myeloid signaling pathways. Curr Opin Hematol. 2007;14:9-15.
31. Small D, Levenstein M, Kim E, et al. STK-1, the human homolog of Flk-2/Flt-3, is selectively expressed in CD34+ human bone marrow cells and is involved in the proliferation of early progenitor/stem cells. Proc Natl Acad Sci U S A. 1994;91:459-463.
32. Broxmeyer HE, Lu L, Cooper S, Ruggieri L, Li ZH, Lyman SD. Flt3 ligand stimulates/costimulates the growth of myeloid stem/progenitor cells. Exp Hematol. 1995;23:1121-1129.
33. Meierhoff G, Dehmel U, Gruss HJ, et al. Expression of FLT3 receptor and FLT3-ligand in human leukemia-lymphoma cell lines. Leukemia. 1995;9:1368-1372.
34. Dehmel U, Zaborski M, Meierhoff G, et al. Effects of FLT3 ligand on human leukemia cells. I. Proliferative response of myeloid leukemia cells. Leukemia. 1996;10:261-270.
35. Zheng R, Levis M, Piloto O, et al. FLT3 ligand causes autocrine signaling in acute myeloid leukemia cells. Blood. 2004;103:267-274.
36. Ambrosini G, Adida C, Altieri DC. A novel anti-apoptosis gene, survivin, expressed in cancer and lymphoma. Nat Med. 1997;3:917-921.
37. Velculescu VE, Madden SL, Zhang L, et al. Analysis of human transcriptomes. Nat Genet. 1999;23:387-388.
38. Fukuda S, Pelus LM. Survivin, a cancer target with an emerging role in normal adult tissues. Mol Cancer Ther. 2006;5:1087-1098.
39. Adida C, Recher C, Raffoux E, et al. Expression and prognostic significance of survivin in de novo acute myeloid leukaemia. Br J Haematol. 2000;111:196-203.
40. Carter BZ, Mak DH, Schober WD, et al. Regulation of survivin expression through Bcr-Abl/MAPK cascade: targeting survivin overcomes imatinib resistance and increases imatinib sensitivity in imatinib-responsive CML cells. Blood. 2006;107:1555-1563.
41. Wang Z, Sampath J, Fukuda S, Pelus LM. Disruption of the inhibitor of apoptosis protein survivin sensitizes Bcr-abl-positive cells to STI571-induced apoptosis. Cancer Res. 2005;65:8224-8232.
42. Zaffaroni N, Pennati M, Colella G, et al. Expression of the anti-apoptotic gene survivin correlates with taxol resistance in human ovarian cancer. Cell Mol Life Sci. 2002;59:1406-1412.

43. Zhang M, Latham DE, Delaney MA, Chakravarti A. Survivin mediates resistance to antiandrogen therapy in prostate cancer. Oncogene. 2005;24:2474-2482.
44. Tirro E, Consoli ML, Massimino M, et al. Altered expression of c-IAP1, survivin, and Smac contributes to chemotherapy resistance in thyroid cancer cells. Cancer Res. 2006;66:4263-4272.
45. Aoki Y, Feldman GM, Tosato G. Inhibition of STAT3 signaling induces apoptosis and decreases survivin expression in primary effusion lymphoma. Blood. 2003;101:1535-1542.
46. Gritsko T, Williams A, Turkson J, et al. Persistent activation of stat3 signaling induces survivin gene expression and confers resistance to apoptosis in human breast cancer cells. Clin Cancer Res. 2006;12:11-19.
47. Mahboubi K, Li F, Plescia J, et al. Interleukin-11 up-regulates survivin expression in endothelial cells through a signal transducer and activator of transcription-3 pathway. Lab Invest. 2001;81:327-334.
48. Altieri DC. Survivin, cancer networks and pathway-directed drug discovery. Nat Rev Cancer. 2008;8:61-70.
49. Darnell JE. Validating Stat3 in cancer therapy. Nat Med. 2005;11:595-596.
50. Nam S, Buettner R, Turkson J, et al. Indirubin derivatives inhibit Stat3 signaling and induce apoptosis in human cancer cells. Proc Natl Acad Sci U S A. 2005;102:5998-6003.

Chapter 4. The combination of HDAC Inhibitors and a FLT-3 inhibitor, ABT-869, induce lethality in acute myeloid leukemia cells with FLT3-ITD synergistically through PRL-3 downregulation

4.1. Introduction

Acute myeloid leukemia (AML) is a heterogeneous clonal disease characterized by relentless overgrowth of immature myeloid blasts. Internal tandem duplication of fms-like tyrosine kinase 3 (FLT3-ITD) mutation occurs in about 25% of AML patients and is associated with poor prognosis.[1-4] Various FLT3 inhibitors of different chemical structure are under clinical investigation for the treatment of AML patients with FLT3 mutations. In contrast to their impressive potency in cell culture system, current FLT3 inhibitors as single agent in clinical trials predominantly induce transient reduction of peripheral blasts, but not bone marrow blasts.[5] Combination with other small molecule drugs represents a promising strategy to improve therapeutic efficacy of FLT3 inhibitors in clinic.

Histone acetylation and deacetylation, controlled by the balance of histone acetyltransferase (HAT) and histone deacetylase (HDAC), play a key role in regulating gene expression by changing chromatin structure.[6,7] Small molecule HDAC inhibitors (HDACi) have proven to be a promising new class of anticancer drugs against hematological malignancies, as well as solid tumors.[8,9] Suberoylanilide hydroxamic acid (SAHA, Vorinostat) is the first HDACi that obtained US FDA approval for the treatment of relapsed or refractory cutaneous T-cell lymphoma (CTCL).[10] SAHA has been shown to alter several key genes involved in the regulation of cell cycle, apoptosis and differentiation, notably including the induction

of $p21^{WAF1}$,[11] TBP-2,[12] TGFβ receptors type I,[13] ASK1,[14] Bim,[15] and reduction of TRX,[12] nuclear factor-kappaB,[16] and c-Myc.[17]

As a potent HDACi, SAHA has also been examined in a combinatory fashion with other different class of anticancer agents in acute leukemias. Combination of SAHA with cyclin-dependent kinase (CDK) inhibitor flavopiridol results in marked apoptosis through the downregulation of short-lived pro-survival proteins XIAP and Mcl-1 in U937 leukemia cell and primary AML cells.[18] Co-exposure of 17-allylamino- 17-demethoxygeldanamycin (17-AAG), a HSP90 antagonist, with SAHA induces profound mitochondrial damage and apoptosis through the inactivation of ERK activity and a block in $p21^{WAF1}$ induction in U937, HL60 and Jurkat leukemia cells.[19] Furthermore, inactivation of Akt and activation of c-Jun N-terminal kinase (JNK) has been identified as the mechanism of synergistic antileukemic effect between 2-medroxyestradiol (2-ME) and SAHA in leukemia cell lines and primary human leukemia cells.[20] These data suggests that combination of SAHA with different types of antitumor therapies might engage distinct molecules and signaling transduction pathways.

ABT-869, a multiple receptor tyrosine kinase inhibitor, inhibits FLT3 phosphorylation and signaling and is now in active clinical cancer therapeutic development.[21] We previously reported that synergism between ABT-869 and chemotherapy results from disruption of cell cycle-regulated genes and MAPK pathway.[22] We hypothesized that combining ABT-869 with HDACi would lead to synergistic killing of AML cells with FLT3 mutations. In this study, we show that this combination have synergistic anti-leukemic activity in both conventional as well as stroma co-culture system. We further investigated the potential underlying molecular mechanisms for this

synergism. This study identified PRL-3, a metastasis-associated gene, as an important mediator of drug resistance and the suppression of PRL-3 was an important mechanism for the synergism between ABT-869 and SAHA.

4.2. Materials and Methods

4.2.1. Cell lines and primary patient samples

MV4-11 and MOLM-14 cells were cultured with RPMI1640 (Invitrogen, Carlsbad, CA) supplemented with the addition of 10% of fetal bovine serum (FBS, JRH Bioscience Inc, Lenexa, KS) at density of 2 to 10 x 10^5 cells/ml in a humid incubator with 5% CO_2 at 37ºC. Bone marrow (BM) blast cells (>90%) from newly diagnosed AML patients were obtained at National University Hospital (NUH) in Singapore with informed consent. Three samples harboring FLT3-ITD mutation were reported previously.[22] Thawed cells were cultured in EGM™-2 medium (Cambrex, Walkersville, MD) supplemented with SingleQuots® (Cambrex) growth factors, cytokines (hFGF, hEGF, Hydrocortisone, GA-1000 , VEGF, R3-IGF-1) with or in absence of drug incubation.

4.2.2. Drugs and chemicals

ABT-869 was kindly provided by Abbott Laboratories (Chicago, IL). ABT-869 was dissolved in DMSO at concentration of 10 mM as stock kept in -20ºC. SAHA was purchased from BIOMOL (Plymouth Meeting, PA). Valproic acid (VPA) and Pentamidine was supplied by Sigma-Aldrich (St. Luis, MO).

4.2.3. Cell proliferation assays

Leukemic cells were seeded in 96-well culture plates at a density of 2 × 10^4 viable cells/100 µl/well in triplicates, and were treated with ABT-869, SAHA, VPA or

combination therapy. Colorimetric CellTiter 96 AQueous One Solution Cell Proliferation Assay (MTS assay, Promega, Madison, WI) was used to determine the cytotoxicity. The absorbance of each well was recorded at 490 nm using an Ultramark® 96-well plate reader (Bio-Rad, Hercules, CA). The percentage of viable cell was reported as the mean of optical density (OD) of the treated wells divided by the mean of OD of DMSO control wells after normalization to the signal from wells without cells. IC50 was determined by MTS assay and calculated with CalcuSyn software (Biosoft, Cambridge, UK). Each experiment was triplicated.

4.2.4. Human Stromal cell coculture system

HS-5 human stromal cells were seeded at $1x10^5$ per well in a 24-well plate one day in advance. MV4-11 and MOLM-14 cells were seeded at $4 x10^5$ in a cell culture insert (Becton Dickinson Labware, Franklin Lakes, NJ) placed into the 24-well plate with HS-5 cells, followed by treatment with various concentrations of ABT-869 and SAHA alone or in combination. After incubation for 48 hours, leukemia cells were subjected to MTS assay.

4.2.5. Combination index calculation

The calculation of combination index (CI) was analysed with the CalcuSyn software. Briefly, the CI values were calculated according to the levels of growth inhibition (Fraction affected, Fa) by each agent individually and combination of ABT-869 with SAHA or VPA. CI <1 illustrates synergism, and CI >1 indicates antagonism and additivity CI = 1. Constant ratio combinations of the two drugs at 0.25x, 0.5x, 1x, 2x and 4x of their ED50 was used. Three independent studies were conducted for each combination.

4.2.6. Apoptosis assay

MV4-11 and MOLM-14 cells were cultured in the presence of either ABT-869, SAHA alone or in combination for 48 hours. Cells were washed twice with 1xPBS, stained with Annexin V/Propidium Iodide (PI, BD PharMingen, San Jose, CA), and immediately analyzed by flow cytometry.

4.2.7. Western blot analysis

Preparation of the cell lysate and immunoblotting were performed as previously described.[24] Antibodies used were as follows: anti-acetylated H3, anti-acetylated H4, anti-poly (ADP-ribose) polymerase (PARP), and anti-cleaved PARP from Cell Signalling Technology (CST, Danvers, MA); anti-Actin, anti-p21, from Santa Cruz Biotechnology (Santa Cruz, CA).

4.2.8. Microarray study

For the microarray experiments, MV4-11 and MOLM-14 cells were treated with DMSO control, ABT-869 3 nM, SAHA 6 μM and combination therapy for 24 hours. Cells were then washed in PBS and high-quality total RNA was extracted RNeasy Midi Kit, according to the manufacturer's instruction (Qiagen, Valencia, USA). RNA quantity, quality, and purity were assessed with the use of the RNA 6000 Nano assay on the Agilent 2100 Bioanalyzer (Agilent Technologies, Santa Clara CA, USA).

Gene expression profiling was performed using Affymetric U133plus2.0 gene chip (Affymetrix, Santa Clara, CA, USA) according to the manufacturer's protocol. The scanned data was processed using MicroArray Suite version 5.0 (MAS) (Affymetrix).The gene expression data was then log-transformed, median centered and analysed using the Genespring GX 7.3.1 software (Agilent Technologies). Sequential filtering was employed to select genes for subsequent analysis. First,

non-expressed probesets (assigned an absent or marginal flag by MAS) were excluded. The remaining probesets were subjected to ANOVA across the samples. The probesets with significant variation with a corrected p-value of less than 0.05 after multiple testing corrections using the Benjamini and Hochberg methods were used for subsequent comparative analysis. Three lists of genes with 2 fold or more difference in gene expression between treatment and control will be generated as follows: ABT-869 alone versus DMSO control, SAHA alone versus DMSO control and ABT-869 plus SAHA versus DMSO control. These gene lists were then analyzed using Venn Diagram to identify genes that are uniquely differentially expressed in the ABT-869 and SAHA combination. This analysis is done separately for the MV4-11 and MOLM-14 cell lines and the final gene lists are genes that are unique to the ABT-869 and SAHA combination in both cell lines.

The gene lists were also subjected to network analysis using a web-based software Metacore (Genego Inc, St Joseph, MI). Metacore contains an interactive, manually annotated database derived from publications on proteins and small molecules that allows for representation of biological functionality and integration of functional, molecular, or clinical information. Several algorithms to enable both the construction and analysis of gene networks are integrated as previously described.[24]

4.2.9. Real-time quantitative (RQ)-PCR

A number of related genes identified from microarray analysis, including PRL-3, MND1, ZNF85, S100A8, were validated by RQ-PCR. The primers were designed with PirmerQuest^{SM} (Integrated DNA Technologies, Coralville, IA, USA). The sequences of these primers were summarized in Table 1. Power SYBR® Green PCR Master Mix is used as recommendation by the manufacturer (Applied

Biosystems, Foster City, CA). β-actin was used as internal control. SDS 1.4 software (Applied Biosystems) is used to perform relative quantitation (RQ) of target genes using the comparative CT (ΔΔCT) method.

4.2.10. Construction and infection of PRL-3-expression vector

The human full-length cDNA of PRL-3 was purchased from Open Biosystems (Huntsville, AL) and inserted into *Eco*RI/*Bam*HI sites of lentivirus pLVX-puro vector (Clontech, Mountain View, CA), This pLVX-puro-PRL3 construct was validated by sequencing. Plasmid vectors were transfected into HEK 293T/17 packaging cells (ATCC) using Lentiphos^{TM} HT protocol (Clontech, PT3984-2) as recommended by the manufacturer. High-titer viral particle-containing medium were harvested 48 hr after transfection and used to infect MV4-11 cells with 10 μg/mL polybrene. Two days after infection, cells were transferred to fresh medium constituting 90% RPMI1640, 10% Tet System Approved FBS (Clontech) and 2 μg/mL puromycin (Millipore, Billerica, MA) for selection of transduced cells.

Table 4.1. The sequences of primers used in real-time PCR.

Gene	Forward Primer	Reverse Primer
PRL-3	5'-AGA AGG ATG GCA TCA CCG TTG T-3'	5'-ACT TCA TCC CGC TCT CAA TAA GCG-3'
ORC1L	5'-TTC TCG GAG ATC ACC TCA CCT TCT-3'	5'-AGCTGC AAT TCG GGT TCT CAG GAT-3'
ZNF85	5'-TAC AGA AAC CTG GTC TTC CTG GGT-3'	5'-ATA TTC TGC TCC GGC CAA AGG TCT-3'
MND1	5'-GGA GAA GAT TGC TCC CAA AGA GAA AGG C-3'	5'-TTC CGA TCC TCT CAC AGT CAA CCA-3'
LMO4	5'-GTC CCG GGA GAT CGG TTT CAC T-3'	5'-ATG GGA TCC ACC TGT GAT GAA CAA A-3'
β-Actin	5'-ATG TGG CCG AGG ACT TTG ATT-3'	5'-AGT GGG GTG GCT TTT AGG ATG-3'

4.3. Results

4.3.1. Synergistic cytotoxicity of combination of ABT-869 and SAHA in leukemia

We first determined the effect of HDACi on MV4-11 and MOLM-14 cells. Leukemia cell lines were treated with SAHA at increasing doses of 1 to 16 μM or VPA at escalating concentration of 250 μM to 4 mM for 48 hours. MTS assays were used to determine the inhibition of cell proliferation. The ED_{50} of SAHA on MV4-11 and MOLM-14 were 11 μM and 9 μM respectively as determined by CALCUSYN software. The ED_{50} of VPA on MV4-11 and MOLM-14 were 1 and 2.3 mM respectively. Then, we set about determining whether concurrent exposure of MV4-11 and MOLM-14 cells to ABT-869 and SAHA would result in enhanced cytotoxicity. As shown in Fig.4.1, the CI values at ED50, ED_{75} and ED_{90} ranged from 0.6 to 0.87, indicating synergistic effect. To confirm that the interaction was not specific to SAHA, we further examined the combination of ABT-869 with VPA in these two cell lines. Again, the CI values arrayed from 0.16 to 0.73, representing highly synergistic to synergistic interactions (Fig.4.1).

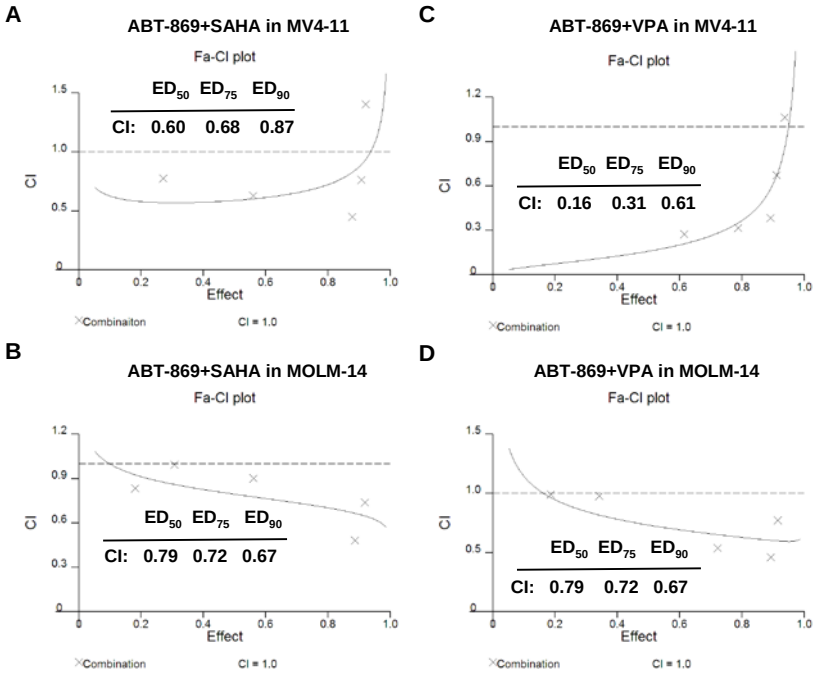

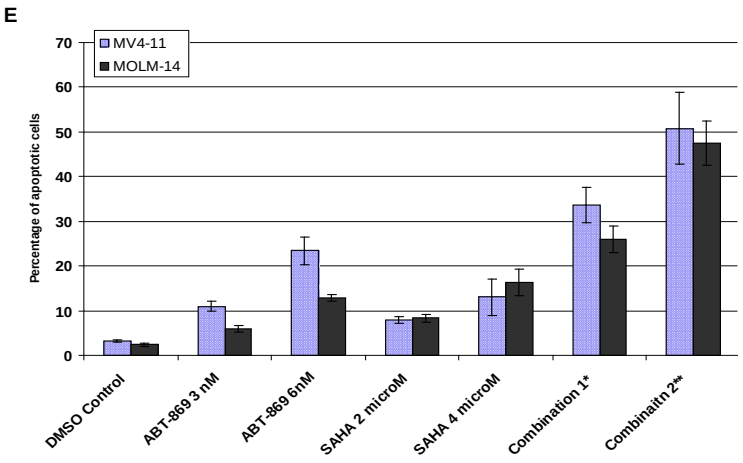

Figure 4.1. Antileukemic effect of combination of ABT-869 with SAHA or VPA on leukemia cell lines with FLT3-ITD mutations. Combination indexes (CIs) quantitatively described the interactions between ABT-869 and SAHA in MV4-11 cells (A), MOLM-14 cells (B), as well as the interactions between ABT-869 and VPA in MV4-11 cells (C), MOLM-14 cell (D). The X-axis is CI values and Y-axis is inhibitory effect by the combination of two drugs. ED stands for effect dosage. The CI values at ED_{50}, ED_{75} and ED_{90} values of two drugs were inserted into the figures. These results were generated by CalcuSyn software. Synergism is defined as the combination of two agents produces greater than expected additive effect (CI < 1), antagonism as smaller than expected additive effect (CI >1) and as additive effect (CI = 1). (E) Percentage of apoptosis induced by ABT-869 alone, SAHA alone, and combination treatment. The experiments were triplicated.

Because SAHA is more potent than VPA, we chose SAHA as a representative HDACi in the rest of the study. To determine whether the combination therapy produce synergism in induction of apoptosis, the Annexin-V/PI double staining was used to assess MV4-11 and MOLM-14 cells treated with ABT-869 and SAHA. Although exposure of MV4-11 and MOLM-14 cells to either ABT-869 or SAHA alone at indicated doses did not induce significant Annexin-V positive cells, the combination therapy stimulated a marked increase in apoptosis in both cell lines. ($p<0.01$, Fig.4.1E).

HDAC inhibitors have been shown to induce total acetylated H3, acetylated H4 and the expression of p21, a cell cycle G_1 inhibitor, in various cancer cells.[12] We therefore

assessed the effect of different treatments on these molecules in MV4-11 and MOLM-14 cells. As shown in Fig.4.2, significant upregulation of acetylated H3 and acetylated H4 protein was observed in both SAHA and combination treatment, but not in ABT-869 single treatment. As expected, markedly increased levels of p21 proteins was induced by SAHA in MV4-11 and MOLM-14 cells. It is interested to note that combination treatment did not induce p21 expression in MV4-11 cells, but stimulated a moderate increase in MOLM-14 cells. Importantly, individual drug exposure leaded to modestly cleaved PARP, in contrast, a remarkable cleaved PARP occurred in cotreatment of ABT-869 and SAHA, indicating a marked lethality as cleavage of PARP is a hallmark of apoptosis cascade.

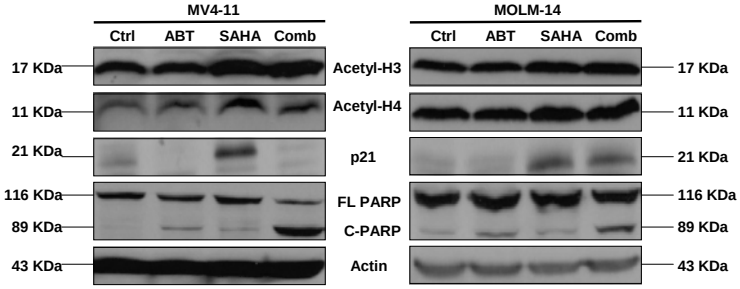

Figure 4.2. Western blot analysis of acetylation of H3, H4 and expression of p21, cleaved PARP in MV4-11 and MOLM-14 cells. Actin was used as loading control.

We tested whether the interactions in cell lines also were validated in primary human leukemia. Primary cells from 3 patient with FLT3-ITD were incubated with either ABT-869 (20, 40, 80, 160, 320 nM), or SAHA (100, 200, 400, 800, 1600 nM) alone and in combination. The CI values of these patient samples with FLT-ITD mutations are 0.50 to 0.82, indicative of synergism between the two agents on a primary AML specimen with FLT3-ITD mutation.

4.3.2. Effect of ABT-869 plus SAHA on MV4-11 and MOLM-14 and stromal cell coculture system

The bone marrow microenvironment acts as a sanctuary site for leukemia cells, by providing survival signals, secretion of growth factors, proangiogenesis factors and direct adhesion molecule interactions.[25] Therefore, bone marrow stroma-mediated effect could play a role in the less-than-expected potency of FLT3 inhibitors in clinical trials. A membrane separated coculture system was used to mimic the bone marrow microenvironment. In the presence of human HS-5 stromal cells, both MV4-11 and MOLM-14 displayed moderate a degree of resistance to ABT-869 alone, or SAHA alone as compared to conventional culture condition. However, co-treatment of MV4-11 and MOLM-14 cells with ABT-869 and SAHA in HS-5 stromal cell coculture system achieved similar cytotoxicity as that accomplished in the absence of HS-5 stromal cells (Fig.4.3A-D, $p < 0.01$).

Taken together, these results support the notion that co-expsoure of SAHA could overcome bone marrow stroma-mediated resistance to FLT3 inhibitors.

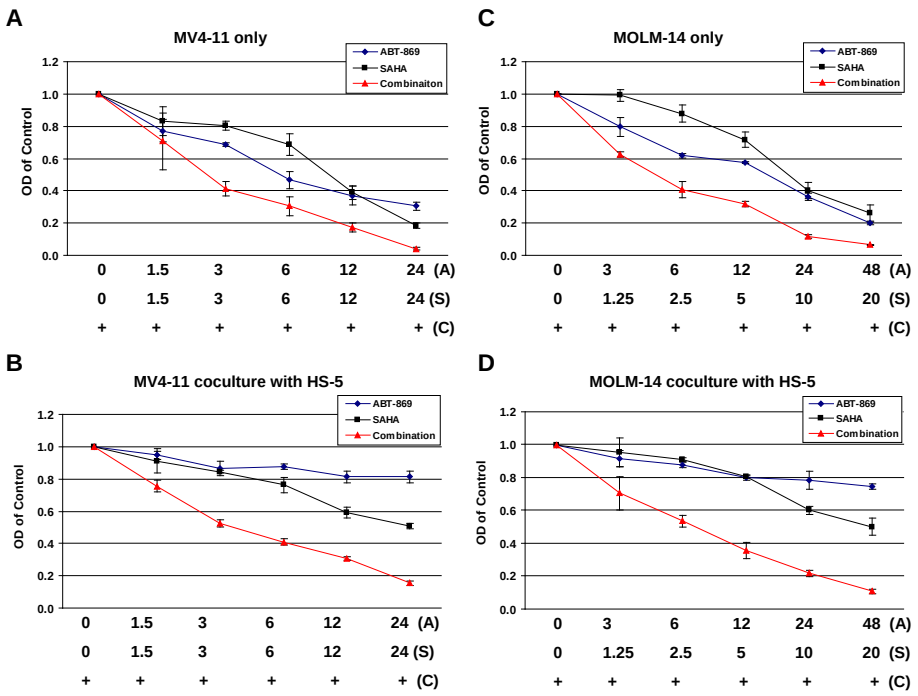

Figure 4.3. Effects of ABT-869 plus SAHA on stromal mediated resistance of MV4-11 and MOLM-14 cells. (A) Proliferation assay showing treatment of MV4-11 cells with ABT-869 and SAHA in absence of human stromal cell HS-5. (B) Proliferation assay showing treatment of MV4-11 cells with ABT-869 and SAHA in presence of human stromal cell HS-5. (C) Proliferation assay showing treatment of MOLM-14 cells with ABT-869 and SAHA in absence of human stromal cell HS-5. (D) Proliferation assay showing treatment of MOLM-14 cells with ABT-869 and SAHA in presence of human stromal cell HS-5. Data shown represents means of three independent experiments ± SD.

Taken together, these results support the notion that coexpsoure of SAHA could overcome leukemia cells acquired or bone marrow stroma-mediated resistance to FLT3 inhibitors.

4.3.3. Identifying core gene signature crucial for the synergism between ABT-869 and SAHA

To elucidate the molecular mechanism of the synergistic lethality between ABT-869 and SAHA, we compared the gene expression profiles of MV4-11 and MOLM-14 cells treated with DMSO control, ABT-869, SAHA and combination therapy using

Affymetrix microarray platform. We focused on delineating a core set of gene signature unique and common to the combination therapy in both MV4-11 and MOLM-14, which could reveal important molecular insights into the therapeutic synergy we observed. Table 4.2 summarized the core gene signature differentially induced more than two-fold by combination therapy in both cell lines. The expression changes of some of the genes including PTP4A3 (Phosphatase of regenerating liver-3, PRL-3), ORC1L, MND1, ZNF85 and LMO4 were confirmed by RQ-PCR on mRNA level (Fig.4A-E). To further validate the gene expression changes caused by combination therapy, Western blot analysis was performed for PRL-3.

When these genes were analyzed using a network analysis tool, a network connecting several protein products of these genes can be constructed through a single intermediate molecule that is not in our list. Interestingly, this network suggests that over-expression of IFI16 lead to the activation of p53 which usually will trigger PTP4A3 over-expression as a pro-survival feedback signal to p53's pro-apoptotic signal (Figure 4.5). In our case, PTP4A3 is downregulated which may lead to potentiation of pro-apoptotic signals resulting in the synergism between SAHA and ABT-869.

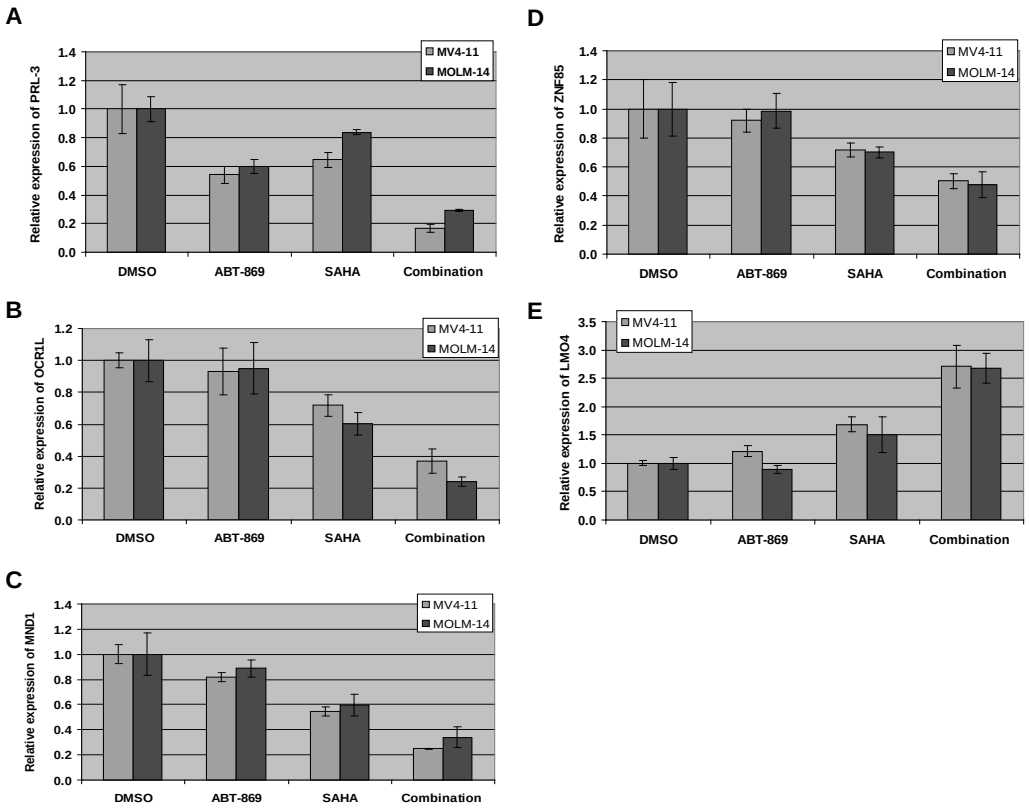

Figure 4.4. **Real-time quantitative-PCR validation of some gene changes in the core gene signature identified by microarray studies.** (A) RQ-PCR quantification of PRL-3 gene. (B) RQ-PCR quantification of OCRL1 gene. (C) RQ-PCR quantification of MND1gene. (D) RQ-PCR quantification of ZNF85 gene. (E) RQ-PCR quantification of LMO4 gene.

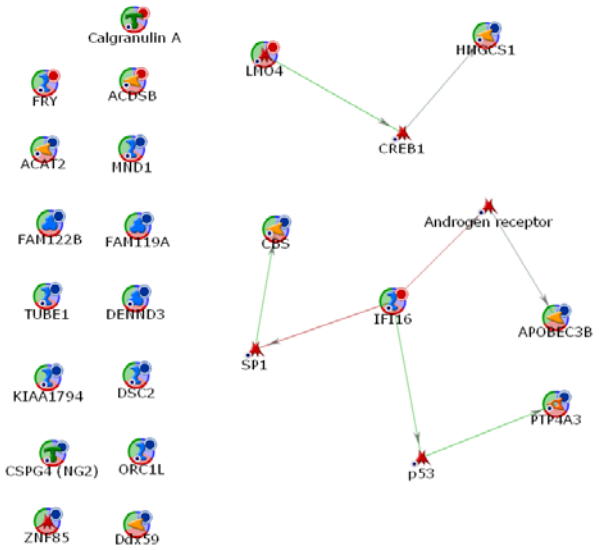

Figure 4.5. **Metacore network analysis of core gene signature which is common in combination treatment in both MV4-11 and MOLM-14 cells.** Green line arrow indicates positive stimulation and red line arrow represents inhibition.

Table 4.2. The list of core gene signature identified by Affymetrix microarray studies of MV4-11 and MOLM-14 cells treated with combination of ABT-869 and SAHA.

Probe ID	Gene Name	Description	Expression Change
1553743_at	FAM119A	family with sequence similarity 119, member A	Downregulation
212975_at	DENND3	DENN/MADD domain containing 3	Downregulation
209695_at	PTP4A3	protein tyrosine phosphatase type IVA, member 3	Downregulation
205085_at	ORC1L	origin recognition complex, subunit 1-like (yeast)	Downregulation
223700_at	MND1	meiotic nuclear divisions 1 homolog (S. cerevisiae)	Downregulation
206572_x_at	ZNF85	zinc finger protein 85	Downregulation
225362_at	FAM122B	family with sequence similarity 122B	Downregulation
209608_s_at	ACAT2	acetyl-Coenzyme A acetyltransferase 2 (acetoacetyl Coenzyme A thiolase)	Downregulation
221750_at	HMGCS1	3-hydroxy-3-methylglutaryl-Coenzyme A synthase 1 (soluble)	Downregulation
206632_s_at	APOBEC3B	apolipoprotein B mRNA editing enzyme, catalytic polypeptide-like 3B	Downregulation
213008_at	KIAA1794	KIAA1794	Downregulation
226817_at	DSC2	desmocollin 2	Downregulation
214297_at	CSPG4	Chondroitin sulfate proteoglycan 4 (melanoma-associated)	Downregulation
228385_at	DDX59	DEAD (Asp-Glu-Ala-Asp) box polypeptide 59	Downregulation
1553972_a_at	CBS	cystathionine-beta-synthase	Downregulation
226181_at	TUBE1	tubulin, epsilon 1	Downregulation
1560023_x_at	---	CDNA FLJ37333 fis, clone BRAMY2020106	Downregulation
204072_s_at	FRY	furry homolog (Drosophila)	Upregulation
209205_s_at	LMO4	LIM domain only 4	Upregulation
228315_at	---	CDNA clone IMAGE:5261213	Upregulation
206332_s_at	IFI16	interferon, gamma-inducible protein 16	Upregulation
208966_x_at	IFI16	interferon, gamma-inducible protein 16	Upregulation
226030_at	ACADSB	acyl-Coenzyme A dehydrogenase, short/branched chain	Upregulation
202917_s_at	S100A8	S100 calcium binding protein A8 (calgranulin A)	Upregulation

4.3.4. PRL-3 protected cells from apoptosis induced by ABT-869, SAHA alone or the combination therapy

PRL-3, a metastasis-associated gene, has been demonstrated to be oncogenic in several types of solid tumors. The finding that PRL-3 was significantly downreguated by combination therapy in both MV4-11 and MOLM-14 stimulated us to further explore the role of PRL-3 in synergistic cytotoxicity. We established a PRL-3 over-expressing cell line, MV4-11-pLVX-puro-PRL3 and a control cell line, MV4-11-Vector Control. Cells were treated with ABT-869, SAHA at different concentration, or their combination for 48 hr, and the growth inhibition was then examined. As shown in Fig.4.6, cells transduced with PRL-3 were more resistant not only to ABT-869, SAHA single agent, but also to the combination therapy, as compared with cells transduced with empty vector.

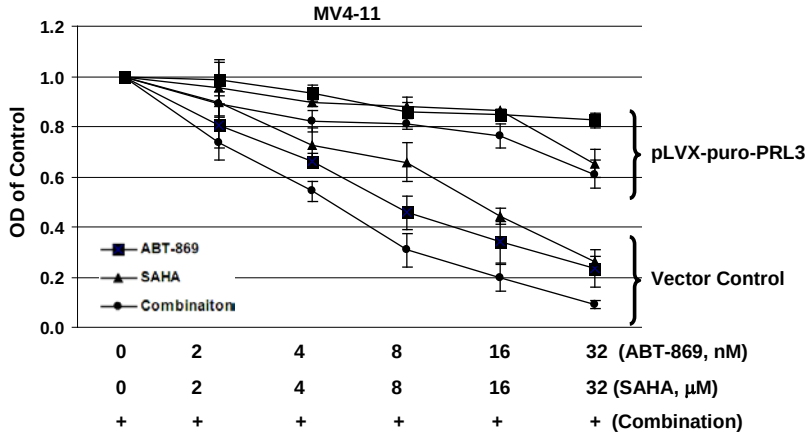

Figure 4.6. **The effect of overexpression of PRL-3 in MV4-11 cells.** MV4-11 cells were transfected with vector control or pLVX-puro-PRL3 vector. Cells were treated with either ABT-869 alone, SAHA alone or combination therapy. MTS assay was used to determine the cell proliferation in different treatments. Data shown represents means of three independent experiments ± SD.

4.3.5. Targeting PRL-3 enhanced ABT-869-mediated cytotoxicity to MV4-11 and MOLM-14

We next tested the effect of targeting PRL-3 on ABT-869-mediated cytotoxicity in MV4-11 and MOLM-14 cells. Pentamidine, an anti-protozoa drug used in clinical for leishmaniasis, has been discovered as an inhibitor of PRL phosphatases with anticancer activity.[26] Therefore, we examined the effect of Pentamidine in these two leukemia cell lines. Pentamidine dose-dependently inhibited proliferation of MV4-11 and MOLM-14 cells with both IC_{50} around 3 μM after 72 hour incubation as determined by MTS assay. To further confirm the role PRL-3 in the synergism, we evaluated the effect of targeting PRL-3 by Pentamidine in ABT-869-mediated cytotoxicity. It is noteworthy that both MV4-11 and MOLM-14 cells were showed significantly increased cytotoxicity to ABT-869 in presence of 1 μM of Pentamidine, as compared to ATB-869 treatment alone ($p < 0.001$ in both cell lines, Fig.4. 7).

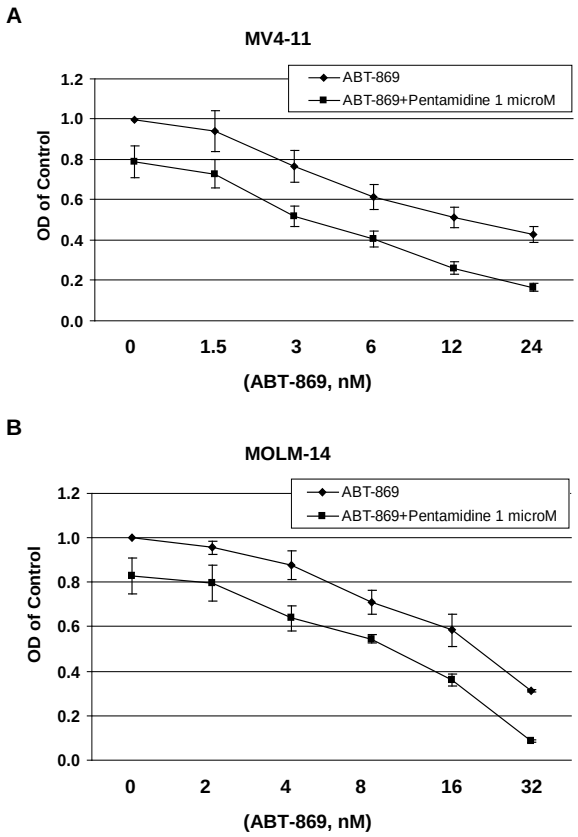

Figure 4.7. Pentamidine potentiating ABT-869-mediated cytotoxicity on MV4-11 and MOLM-14 cells. Cells were treated with ABT-869 alone or in additional of 1 μM of Pentamidine for 72 hours. MTS assay was used to determine the relative cytotoxicity of different treatments. Data shown represents means of three independent experiments ± SD.

4.3.6. Association between PRL-3 expression and FLT-ITD mutation in AML

Oncomine is a web-based cancer microarray database, including 10000+ cancer transcriptome profiles. A search of the Oncomine database (January 09) revealed that PRL-3 was significantly overexpressed in FLT3-ITD positive AML as compare in FLT3-ITD negative AML (Figure 8, study name: Valk_leukemia, 78 vs 206 cases, p-value: 1.2E-07),[28] indicating the association between PRL-3 expression and FLT-ITD mutation. Hence, it may suggest a potential role of PRL-3 in the poor prognosis of patients with FLT3-ITD mutation.

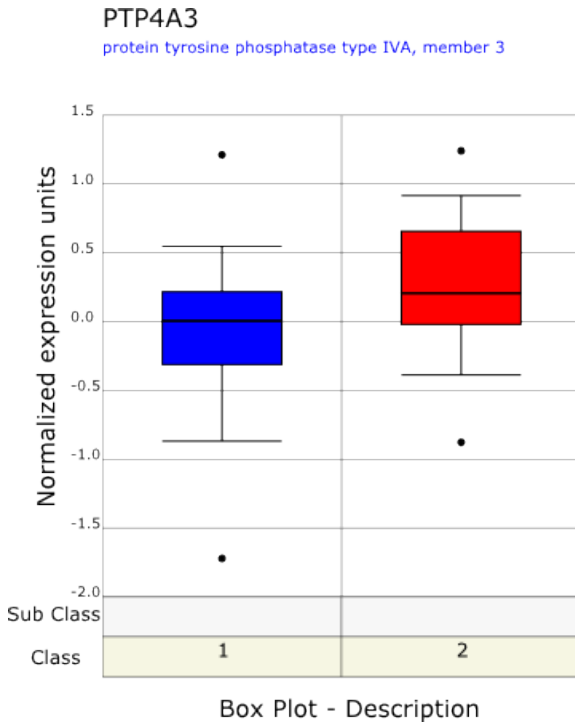

Figure 4.8. Comparison of PRL-3 expression between FLT3-ITD negative (Class 1) and FLT3-ITD positive (Class 2) AML patients. The box plot was generated by Oncomine based on the study of Valk P, *et al*. (reference 28)

4.4. Discussion

FLT3 mutations represent one of the most common genetic abnormalities in AML. More than dozen FLT3 inhibitors have been developed since the discovery of FLT3 mutations in 1996.[5,29] Although they generally lack sustainable efficacy in most clinical trials when utilised as monotherapy, several FLT3 inhibitors are now actively evaluated in combination with other therapeutic agents in preclinical and clinical trails. On the other hand, HDACi have shown anticancer effect against a broad range of solid tumors and hematological malignancies, and the first HDAC inhibitor, SAHA (Zolinza™, Merck & Co.) has been approved by the FDA for cutaneous T-cell lymphoma.[7,10] The antitumor activities of HDACi are generally ascribed to changes in

gene expression by modification of histone or non-histone protein acetylation. However, the precise molecular mechanisms of HDACi, such as SAHA, remain unclear. Herein, we demonstrate that ABT-869 and SAHA or VPA induced synergistically antileukemic effect against FLT3-ITD positive cell lines as well as primary AML patient cells. Furthermore, the combination therapies overcome stroma-mediated resistance to ABT-869 single agent. Importantly, we further identify a core gene signature, including a metastasis-associated gene PRL-3, which is responsible for the synergism.

The PRL-3 (also known as PTP4A3) gene encodes a 22-kDa tyrosine phosphatase that has been implicated in tumorigenesis and metastasis.[30,31] Saha *et al*.[32] uncovered a dramatically differential expression pattern of PRL-3 between primary and metastatic colorectal carcinomas (CRCs). This landmark study reported exceptionally higher expression of PRL-3 in liver metastatic CRCs as compared to non-metastatic CRCs and normal colon epithelium.[32] Mechanistic studies reveal that PRL-3 functions as an initiator of neoplastic angiogenesis by recruiting endothelial cells[33] and stimulates invasion and motility of tumor cells through activating Rho family of small GTPases such as RhoA and RhoC.[34] Increasing activities of Src kinase and PI3K/AKT signaling pathway via negative feedback regulation of C-terminal Src kinase (Csk) and PTEN tumor suppressor gene respectively by PRL-3 also contribute to its oncogenic role.[35-37] Recently, PRL-3 is identified as a downstream target gene of p53 and dose-dependently regulates cell-cycle progression, highlighting a fundamental role of PRL-3 in tumor development.[38] In contrast to extensive studies in solid tumors, the role of PRL-3 in hematological malignancies is less appreciated. To our knowledge, only one study reported that PRL-3 promotes human multiple myeloma (MM) cell migration and overexpression in

a subsets of MM patients assessed by gene expression profiling.[39] Herein, for the first time, we show that modulation of PRL-3 expression plays an important role in synergistically antileukemic effect of co-treatment of ABT-869 and SAHA in FLT3-ITD positive AML. Importantly, there is a close association between PRL-3 expression and FLT-ITD mutation in AML as revealed by a study of Valk P *et al*.[28] in Oncomine database. However, the potential role of PRL-3 in the FLT3-ITD positive leukemogenesis and exact mechanism(s) of mediating drug resistant remain elusive and are under further investigation in our group.

Amongst the other genes constituting the signature, there are other interesting candidates. It is well known that cell proliferation is tightly regulated and uncontrolled cell proliferation leads to development of cancer. The origin recognition complex (ORC) is a highly conserved protein complex composed of 6 subunits in eukaryotic cells and is the primary recognition protein for DNA replication.[40] In our core gene signature identified in this study, human ORC1L [ORC, subunit 1-like (yeast)] gene is significantly downregulated by combination therapy. ORC1L appears to control the cell growth and the initiation of DNA replication through E2F1 (E2F transcription factor 1)-Rb (retinoblastoma protein) network, which is essential for cell-cycle G_1/S phase transition.[41] Importantly, silencing OCR1 by RNA interference inhibits proliferation of vascular smooth muscle cells.[42] Taken together, these data support a role for the suppression of ORC1L in contributing synergism in this study.

IFI16 is a member of the HIN-200 (hematopoietic interferon-inducible nuclear antigens with 200 amino acid repeats) family of cytokines, which has been implicated in the regulation of cellular senescence-associated cell growth arrest and differentiation of myeloid progenitor cell.[43,44] Studies have indicated that increased

expression of IFI16 are associated with inhibition of colony formation and cell growth or increased apoptosis in bone and cartilage tumor cell,[45] head and neck squamous cell carcinoma,[46] prostate cancer,[47] medullary thyroid cell[48] and breast cancer cell.[49] Specifically in hematopoietic system, ectopic expression of Notch signaling induces G_0/G_1 cell-cycle arrest followed by apoptosis in human erythroleukaemic TF-1 cells, as well as normal CD34+ cord blood cells. Investigation of the mechanism reveals it is associated with upregulation of IFI-16 expression, but not modulation of other cell-cycle regulators such as p15, p16, p21, p27, CDK4 or CDK6.[50] In this regard, it may be that upregulation of IFI-16 could promote apoptosis, thereby facilitating the synergistic killing of MV4-11 and MOLM-14 cells.

Our observations provide a molecular basis for synergism of combination of ABT-869, a FLT3 inhibitor, with SAHA, a HDAC inhibitor, in FLT3-ITD positive AML cell lines and primary AML patient samples and reveal that the alteration of core gene signature including downregulation of PRL-3, OCR1L, ACAT2 and upregulation of IFI16, to name a few, contributes the potentiation. Our results also demonstrate that the cotreatment of ABT-869 and SAHA can overcome acquired resistance or stroma-mediated resistance to ABT-869 single agent raising the possibility that such combination therapies may significantly improve the therapeutic efficacy of FLT3 inhibitors in clinic.

4.5. References:

1. Gilliland DG, Griffin JD. The roles of FLT3 in hematopoiesis and leukemia. Blood. 2002;100:1532-1542.
2. Levis M, Small D. FLT3: ITDoes matter in leukemia. Leukemia. 2003;17:1738-1752.
3. Sternberg DW, Licht JD. Therapeutic intervention in leukemias that express the activated fms-like tyrosine kinase 3 (FLT3): opportunities and challenges. Curr Opin Hematol. 2005;12:7-13.

4. Stirewalt DL, Radich JP. The role of FLT3 in haematopoietic malignancies. Nat Rev Cancer. 2003;3:650-665.
5. Small D. FLT3 mutations: biology and treatment. Hematology Am Soc Hematol Educ Program. 2006:178-184.
6. Glaser KB. HDAC inhibitors: clinical update and mechanism-based potential. Biochem Pharmacol. 2007;74:659-671.
7. Marks P, Rifkind RA, Richon VM, Breslow R, Miller T, Kelly WK. Histone deacetylases and cancer: causes and therapies. Nat Rev Cancer. 2001;1:194-202.
8. Bolden JE, Peart MJ, Johnstone RW. Anticancer activities of histone deacetylase inhibitors. Nat Rev Drug Discov. 2006;5:769-784.
9. Minucci S, Pelicci PG. Histone deacetylase inhibitors and the promise of epigenetic (and more) treatments for cancer. Nat Rev Cancer. 2006;6:38-51.
10. Mann BS, Johnson JR, Cohen MH, Justice R, Pazdur R. FDA approval summary: vorinostat for treatment of advanced primary cutaneous T-cell lymphoma. Oncologist. 2007;12:1247-1252.
11. Gui CY, Ngo L, Xu WS, Richon VM, Marks PA. Histone deacetylase (HDAC) inhibitor activation of p21WAF1 involves changes in promoter-associated proteins, including HDAC1. Proc Natl Acad Sci U S A. 2004;101:1241-1246.
12. Butler LM, Zhou X, Xu WS, et al. The histone deacetylase inhibitor SAHA arrests cancer cell growth, up-regulates thioredoxin-binding protein-2, and down-regulates thioredoxin. Proc Natl Acad Sci U S A. 2002;99:11700-11705.
13. Ammanamanchi S, Brattain MG. Restoration of transforming growth factor-beta signaling through receptor RI induction by histone deacetylase activity inhibition in breast cancer cells. J Biol Chem. 2004;279:32620-32625.
14. Tan J, Zhuang L, Jiang X, Yang KK, Karuturi KM, Yu Q. Apoptosis signal-regulating kinase 1 is a direct target of E2F1 and contributes to histone deacetylase inhibitor-induced apoptosis through positive feedback regulation of E2F1 apoptotic activity. J Biol Chem. 2006;281:10508-10515.
15. Jiang X, Tsang YH, Yu Q. c-Myc overexpression sensitizes Bim-mediated Bax activation for apoptosis induced by histone deacetylase inhibitor suberoylanilide hydroxamic acid (SAHA) through regulating Bcl-2/Bcl-xL expression. Int J Biochem Cell Biol. 2007;39:1016-1025.
16. Imre G, Gekeler V, Leja A, Beckers T, Boehm M. Histone deacetylase inhibitors suppress the inducibility of nuclear factor-kappaB by tumor necrosis factor-alpha receptor-1 down-regulation. Cancer Res. 2006;66:5409-5418.
17. Xu Y, Voelter-Mahlknecht S, Mahlknecht U. The histone deacetylase inhibitor suberoylanilide hydroxamic acid down-regulates expression levels of Bcr-abl, c-Myc and HDAC3 in chronic myeloid leukemia cell lines. Int J Mol Med. 2005;15:169-172.
18. Rosato RR, Almenara JA, Kolla SS, et al. Mechanism and functional role of XIAP and Mcl-1 down-regulation in flavopiridol/vorinostat antileukemic interactions. Mol Cancer Ther. 2007;6:692-702.
19. Rahmani M, Yu C, Dai Y, et al. Coadministration of the heat shock protein 90 antagonist 17-allylamino- 17-demethoxygeldanamycin with suberoylanilide hydroxamic acid or sodium butyrate synergistically induces apoptosis in human leukemia cells. Cancer Res. 2003;63:8420-8427.
20. Gao N, Rahmani M, Shi X, Dent P, Grant S. Synergistic antileukemic interactions between 2-medroxyestradiol (2-ME) and histone deacetylase inhibitors involve Akt down-regulation and oxidative stress. Blood. 2006;107:241-249.
21. Shankar DB, Li J, Tapang P, et al. ABT-869, a multitargeted receptor tyrosine kinase inhibitor: inhibition of FLT3 phosphorylation and signaling in acute myeloid leukemia. Blood. 2007;109:3400-3408.

22. Zhou J, Pan M, Xie Z, et al. Synergistic antileukemic effects between ABT-869 and chemotherapy involve downregulation of cell cycle-regulated genes and c-Mos-mediated MAPK pathway. Leukemia. 2008;22:138-146.
23. Shen J, Tai YC, Zhou J, et al. Synergistic antileukemia effect of genistein and chemotherapy in mouse xenograft model and potential mechanism through MAPK signaling. Exp Hematol. 2007;35:75-83.
24. Nikolsky Y, Ekins S, Nikolskaya T, Bugrim A. A novel method for generation of signature networks as biomarkers from complex high throughput data. Toxicol Lett. 2005;158:20-29.
25. Zhou J, Mauerer K, Farina L, Gribben JG. The role of the tumor microenvironment in hematological malignancies and implication for therapy. Front Biosci. 2005;10:1581-1596.
26. Sands M, Kron MA, Brown RB. Pentamidine: a review. Rev Infect Dis. 1985;7:625-634.
27. Pathak MK, Dhawan D, Lindner DJ, Borden EC, Farver C, Yi T. Pentamidine is an inhibitor of PRL phosphatases with anticancer activity. Mol Cancer Ther. 2002;1:1255-1264.
28. Valk PJ, Verhaak RG, Beijen MA, et al. Prognostically useful gene-expression profiles in acute myeloid leukemia. N Engl J Med. 2004;350:1617-1628.
29. Nakao M, Yokota S, Iwai T, et al. Internal tandem duplication of the flt3 gene found in acute myeloid leukemia. Leukemia. 1996;10:1911-1918.
30. Bessette DC, Wong PC, Pallen CJ. PRL-3: a metastasis-associated phosphatase in search of a function. Cells Tissues Organs. 2007;185:232-236.
31. Stephens BJ, Han H, Gokhale V, Von Hoff DD. PRL phosphatases as potential molecular targets in cancer. Mol Cancer Ther. 2005;4:1653-1661.
32. Saha S, Bardelli A, Buckhaults P, et al. A phosphatase associated with metastasis of colorectal cancer. Science. 2001;294:1343-1346.
33. Guo K, Li J, Wang H, et al. PRL-3 initiates tumor angiogenesis by recruiting endothelial cells in vitro and in vivo. Cancer Res. 2006;66:9625-9635.
34. Fiordalisi JJ, Keller PJ, Cox AD. PRL tyrosine phosphatases regulate rho family GTPases to promote invasion and motility. Cancer Res. 2006;66:3153-3161.
35. Liang F, Liang J, Wang WQ, Sun JP, Udho E, Zhang ZY. PRL3 promotes cell invasion and proliferation by down-regulation of Csk leading to Src activation. J Biol Chem. 2007;282:5413-5419.
36. Stephens B, Han H, Hostetter G, Demeure MJ, Von Hoff DD. Small interfering RNA-mediated knockdown of PRL phosphatases results in altered Akt phosphorylation and reduced clonogenicity of pancreatic cancer cells. Mol Cancer Ther. 2008;7:202-210.
37. Wang H, Quah SY, Dong JM, Manser E, Tang JP, Zeng Q. PRL-3 down-regulates PTEN expression and signals through PI3K to promote epithelial-mesenchymal transition. Cancer Res. 2007;67:2922-2926.
38. Basak S, Jacobs SB, Krieg AJ, et al. The metastasis-associated gene Prl-3 is a p53 target involved in cell-cycle regulation. Mol Cell. 2008;30:303-314.
39. Fagerli UM, Holt RU, Holien T, et al. Overexpression and involvement in migration by the metastasis-associated phosphatase PRL-3 in human myeloma cells. Blood. 2008;111:806-815.
40. Gavin KA, Hidaka M, Stillman B. Conserved initiator proteins in eukaryotes. Science. 1995;270:1667-1671.
41. Ohtani K, DeGregori J, Leone G, Herendeen DR, Kelly TJ, Nevins JR. Expression of the HsOrc1 gene, a human ORC1 homolog, is regulated by cell proliferation via the E2F transcription factor. Mol Cell Biol. 1996;16:6977-6984.

42. Shu MQ, Qin YL, Jiang MH. RNA interference targeting ORC1 gene suppresses the proliferation of vascular smooth muscle cells in rats. Exp Mol Pathol. 2008;84:206-212.
43. Song LL, Alimirah F, Panchanathan R, Xin H, Choubey D. Expression of an IFN-inducible cellular senescence gene, IFI16, is up-regulated by p53. Mol Cancer Res. 2008;6:1732-1741.
44. Dermott JM, Gooya JM, Asefa B, Weiler SR, Smith M, Keller JR. Inhibition of growth by p205: a nuclear protein and putative tumor suppressor expressed during myeloid cell differentiation. Stem Cells. 2004;22:832-848.
45. Zhang Y, Howell RD, Alfonso DT, et al. IFI16 inhibits tumorigenicity and cell proliferation of bone and cartilage tumor cells. Front Biosci. 2007;12:4855-4863.
46. De Andrea M, Gioia D, Mondini M, et al. Effects of IFI16 overexpression on the growth and doxorubicin sensitivity of head and neck squamous cell carcinoma-derived cell lines. Head Neck. 2007;29:835-844.
47. Alimirah F, Chen J, Davis FJ, Choubey D. IFI16 in human prostate cancer. Mol Cancer Res. 2007;5:251-259.
48. Kim EJ, Park JI, Nelkin BD. IFI16 is an essential mediator of growth inhibition, but not differentiation, induced by the leukemia inhibitory factor/JAK/STAT pathway in medullary thyroid carcinoma cells. J Biol Chem. 2005;280:4913-4920.
49. Aglipay JA, Lee SW, Okada S, et al. A member of the Pyrin family, IFI16, is a novel BRCA1-associated protein involved in the p53-mediated apoptosis pathway. Oncogene. 2003;22:8931-8938.
50. Chadwick N, Fennessy C, Nostro MC, Baron M, Brady G, Buckle AM. Notch induces cell cycle arrest and apoptosis in human erythroleukaemic TF-1 cells. Blood Cells Mol Dis. 2008;41:270-277.